SACLANTCEN Conference Proceedings No. 17 Part 8

SACLANTCEN
Conference Proceedings No. 17

PART 8
SONAR MODELS

SACLANT ASW
RESEARCH CENTRE

OCEANIC ACOUSTIC MODELLING

Proceedings of a Conference held at SACLANTCEN on 8-11 September 1975

Organized by

WOLFGANG BACHMANN and ROBERT BRUCE WILLIAMS

15 OCTOBER 1975

NORTH
ATLANTIC
TREATY
ORGANIZATION

VIALE SAN BARTOLOMEO 400
I - 19026 - LA SPEZIA, ITALY

Compiled and Published by

SACLANTCEN

SACLANTCEN
CONFERENCE PROCEEDINGS NO. 17

NORTH ATLANTIC TREATY ORGANIZATION
SACLANT ASW Research Centre
Viale San Bartolomeo 400
I 19026 - La Spezia, Italy

OCEANIC ACOUSTIC MODELLING

Proceedings of a Conference held at SACLANTCEN
on 8-11 September 1975

In eight parts
Part 8: Sonar Models

Organized by
Wolfgang Bachmann and Robert Bruce Williams

15 October 1975

PAPERS PRESENTED AT CONFERENCE

Pt 1: Noise (and Introductory Matter)

1. A.W. Pryce, "Keynote address: Underwater acoustics — modelling".
2. P. Wille, "Noise sources in the ocean, Pt I".
3. M. Daintith, "Noise sources in the ocean, Pt II".
4. H. Cox, "Acoustic noise models".

Pt 2: Bubbles

5. B. Williams & L. Foster, "Gas bubbles in the sea: A review and model proposals".
6. H. Medwin, "Acoustical probing for microbubbles at sea".

Pt 3: Sea surface

7. C.R. Ward, "A spectral ocean wave model".
8. H. Schwarze, "A theoretical model for doppler spread of backscattered sound from a composite-roughness sea surface".
9. O.I. Diachok, "Effects of sea-ice ridges on sound propagation in the Arctic Ocean".
10. J. Siebert, "Low-frequency acoustic measurements in a shallow-water area with a rough sea surface".
11. P.A. Crowther, "Surface wave spectra".
12. H. Trinkaus, "Scattering and reflection of sound from the sea surface".

Pt 4: Sea bottom

13. F.M. Phelan, B. Williams & F.H. Fisher, "Highlights of bottom topography inferred from received depression and bearing angles".
14. S.R. Santaniello & F.R. Dinapoli, "Ocean-bottom reflectivity (a point of view)".
15. W.A. Kuperman & F. Ingenito, "Relative contribution of surface roughness and bottom attenuation to propagation loss in shallow water".
16. R.E. Christiensen & W.H. Geddes, "Refraction of sound in the sea floor".
17. J.A. Desanto, "Scattering from a random interface".
18. E.L. Hamilton, "Acoustic properties of the sea floor".
19. H. Bucker & H. Morris, "Reflection of sound from a layered ocean bottom".
20. B. Hurdle, K.D. Flowers & J.A. Desanto, "Acoustic scattering from rough surfaces".

Pt 5: Macro-scale phenomena

21. W. Munk, "Acoustic scintillations of acoustic waves".
22. S. Flatté, "Intensity and phase fluctuations in low-frequency acoustic transmission through internal waves".
23. T.H. Bell, Jr., J.M. Bergin, J.P. Dougan, Z.C.B. Hamilton, W.D. Morris, B.S. Okawa, E.E. Rudd & J. Witting, "Two-dimensional internal-wave spectra".
24. I.M. Blatstein, "Ocean-basin reverberation from large underwater explosions, Pt I: Source-level and propagation-loss modelling".
25. J.A. Goertner, "Ocean-basin reverberation from large underwater explosions, Pt II: Computer model for reverberation".
26. J.D. Shaffer, R.M. Fitzgerald & A.N. Guthrie, "Some effects of large-scale oceanography on acoustic propagation".
27. H.H. Essen, "Influence of internal waves on sound propagation in the SOFAR channel".
28. O.M. Johannessen, "A review of oceanic fronts".
29. R. Mellen & D.G. Browning, "Some acoustic effects of internal macrostructure".

Pt 6: Micro-scale phenomena

30. D.R. Del Balzo & W.B. Moseley, "Random temperature structure as a factor in long-range propagation".
31. J.J. McCoy, "Beam spreading and loss of spatial coherence in an inhomogeneous and fluctuating ocean".
32. R. Tait, "Internal oceanographic microstructure phenomena".
33. D. Mintzer, "Acoustic effects of internal microstructure".

Pt 7: Field calculations

34. S.N. Wolf, "Measurements of normal-mode amplitude functions in a nearly-stratified medium".
35. R.D. Graves, A. Nagl, H. Uberall, A.J. Haug & G.L. Zarur, "Range-dependent normal modes in underwater sound propagation".
36. J.A. Desanto, "Inverse wave propagation in an inhomogeneous waveguide".
37. A. Gille & D. Odero, "A solution of the wave sound equation in shallow water for real-speed profiles and solid bottom under-sediment".
38. D.J. Ramsdale, "A wave-theoretic method for estimating the effects of internal tides on acoustic wave transmission".
39. J.G. Schothorst, "Effect of ship motion on sonar detection performance".
40. C.W. Spofford & H. Garon, "Deterministic methods of sound-field computation".
41. R. Goodman, "Stochastic methods of sound-field computation".

Pt 8: Sonar models

42. B.B. Adams & G.R. Giellis, "A technique of comparative analysis of underwater-sound-transmission loss curves".
43. J.A. Desanto, "Connection between the solution of the Helmholtz and parabolic equations for sound propagation".
44. F. Dinapoli, "Computer models for underwater-sound propagation".
45. D. Wood, "Assessment techniques for computer models of sound propagation".

TABLE OF CONTENTS

Pt 8: Sonar Models

(Total number of printed pages in this document: 105)

A TECHNIQUE OF COMPARATIVE ANALYSIS OF UNDERWATER SOUND TRANSMISSION LOSS CURVES

by

B.B. Adams and G.R. Giellis
US Naval Research Laboratory
Washington D.C. 20375
U.S.A.

ABSTRACT

A procedure has been developed for the analysis of transmission loss curves in which received power is known or expressible as a linear function of range. The procedure separates each curve into a sum of three components of variability: long term trend, oscillatory, and random. Standard procedures are used to perform the separation and to make statistical comparison tests with other curves which may be companion experimental data or model predictions. Eight cases are analysed for example involving several model predictions with two high density detailed 300 n.mi shot runs. Application of the analysis procedure to transmission loss curves should provide a set of standard statistics which should facilitate quantitative statements and comparisons.

1. INTRODUCTION

1.1 BACKGROUND

A number of computer programs for intensity calculations are now widely available to scientists engaged in underwater sound studies. These programs produce curves which indicate transmission loss as a function of range, comparable to the type derived from available experimental data. Some of the more sophisticated models, such as TRIMAIN in use at NRL, can handle horizontal variations in sound speed and include bottom topography and produce four different types of intensity calculations. In research involving experimental data and development of such programs, there is a need for a procedure comparing these intensity curves in a quantitatively significant manner. The objective of the present study was to develop an analysis procedure capable of meeting this requirement.

It can be observed that acoustic intensity curves have three basic components: (1) a long-term trend, (2) oscillations about this trend and (3) residual random effects. One or more of these components may not be present to a significant degree, depending on a given physical situation. The procedure we have developed is designed to establish the existence of the components, and to isolate them for separate examination, and quantitatively estimate their contribution. An outline of the recommended procedure follows below and ends with conclusions regarding the progress to date in the development of the procedure and recommendations for further study. Appendix A is devoted to a complete description of the procedure which includes specific formulas and a discussion of underlying assumptions. The procedure has been exercised on acoustic model and experimental data, with detailed results given in Appendix B.

1.2 Outline of the Proposed Analysis Procedure

Given an intensity curve $X(r)$, the long-term trend is assumed to be of the elementary form $X_L(r) = A + B \log r$ (Fig. 1).

The coefficients A, B are determined by least squares formulas. The residuals constitute a derived curve, $X'(r)$ (Fig. 2). The subsequent tests employed depend upon the presence of significant randomness in $X'(r)$, as measured by a turning point test (M. G. Kendall [1]). If the residuals are random, the intensity curve, $X(r)$, is described by only two components, the long-term trend, $X_L(r)$, and the random residual, $X'(r)$. To compare two-component curves of this type, similarity tests based on confidence intervals for A, B and an estimate of the standard deviation for $X'(r)$ can be employed. We can also compare curves by examining the distributions of variance between the $X_L(r)$ and $X'(r)$ components. If the curve $X'(r)$ fails the test for randomness, we conclude that a third significant, oscillatory, component exists. In this case, the subsequent comparisons of trend coefficients can be made disregarding the oscillatory component with a small loss in comparison precision. Alternately, if full compliance with statistical assumptions is deemed necessary, the oscillatory component can be removed and a second regression made for refined trend parameter estimates.

In a large percentage of cases, transmission loss curves are found to possess a strong oscillatory component. We have assumed it to be of the form

$$X_o(r_K) = \sum_{j=1}^{n} a_j X'(r_{K-j}) \qquad 1.1$$

Calculation of the coefficients [aj] is discussed below in Appendix A.4. Briefly, it requires the solution of a system of equations involving the autocorrelation function for $X'(r)$. The autocorrelation function is also used to estimate the principal period of a transmission loss curve, such as the convergence zone period, and further, to calculate a zone spacing ratio, designed to compare the oscillation periods of two curves.* To show whether the autoregressive scheme is complete the residual component $X_R(r)$ is obtained as $X_R(r) = X'(r) - X_o(r)$ (Fig. 4). At this stage, a turning point test is again applied to see if $X_R(r)$ satisfies a randomness criterion. If not, refinements are necessary in the autoregressive fit procedure.

After the separation into components has been accomplished, curves for model or experimental data can be compared for the distribution of variance among these components. The comparisons are quantitative, reproducible, and contain probability thresholds, or confidence intervals all of which can be employed for systematic comparison of data sets, model sets or data/model tests.

*Fig. 3

II. Conclusions and Recommendations

A sequence of known statistical procedures have been gathered and employed on the comparative analysis of measured and calculated propagation loss data. The procedures have been deliberately kept simple to hopefully promote widespread use with a minimum of computer or calculator expense. The cases chosen for examples in Appendix B, table B-3, show the 95% confidence interval on the mean of the sets is on the order of .6 db even though a number of the model runs were purposefully flawed for illustration. This sensitivity for calibration checks, flux density estimates, hydrophone calibrations, etc. was considered surprising. Similarly the exponential decay constant 95% confidence intervals, or slopes, were of order .15 where 2 would be spherical spreading. All the cases were readily distinguishable. The distribution of variance in the tested cases shown in table B.9 also showed marked distinctions between model types as well as experimental data. The convergence zones of the chosen sample data were remarkably periodic so that in the two examples the oscillatory and long term trend were near equal in power and the final random residual variance was only 6 and 16 percent in the two cases. The model results were deliberately not tuned to the experimental data so as to better reflect what a first application of the methods would produce. As a consequence, most of model outputs contained a much larger random residual component which was suppressed only in the smoothed cases. This is similarly, in retrospect, not unexpected since the computer models are comparable to continuous wave (very narrow band) data and the experimental results have one third octave frequency domain averaging. In table B.7 we see another result where comparisons of measured and model convergence cycle lengths are listed. As shown, all the model cycle lengths exceed all the experimental lengths. The discrepancies are small, 3%, but consistent and estimated to result from velocity profile error.

In summary, the major objective has been to illustrate the surprising power of a sequence of comparatively elementary procedures and the major recommendation is to employ objective measures such as those discussed in general experimental and analytic studies.

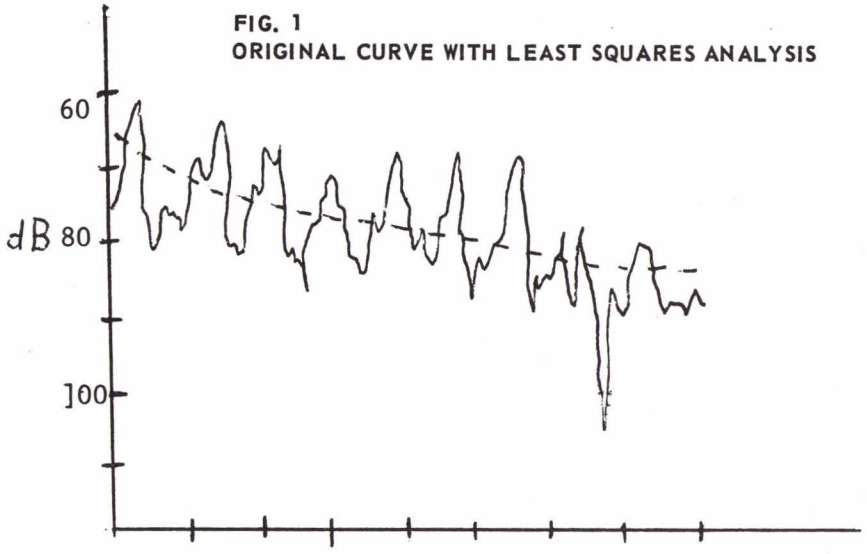

FIG. 1
ORIGINAL CURVE WITH LEAST SQUARES ANALYSIS

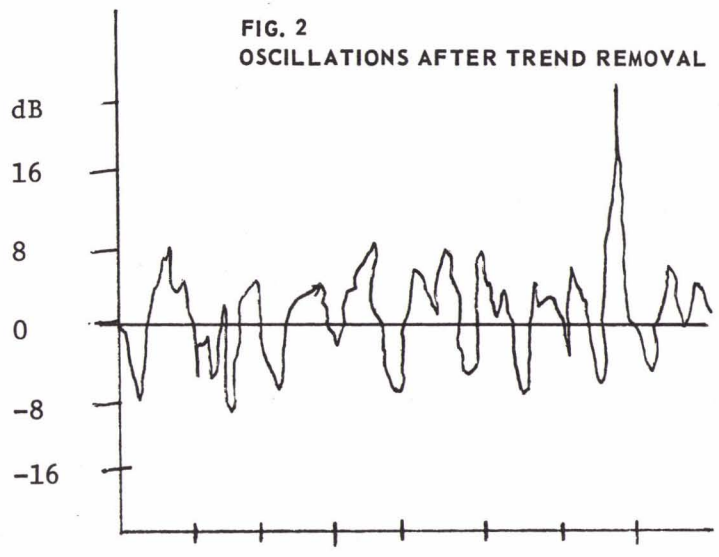

FIG. 2
OSCILLATIONS AFTER TREND REMOVAL

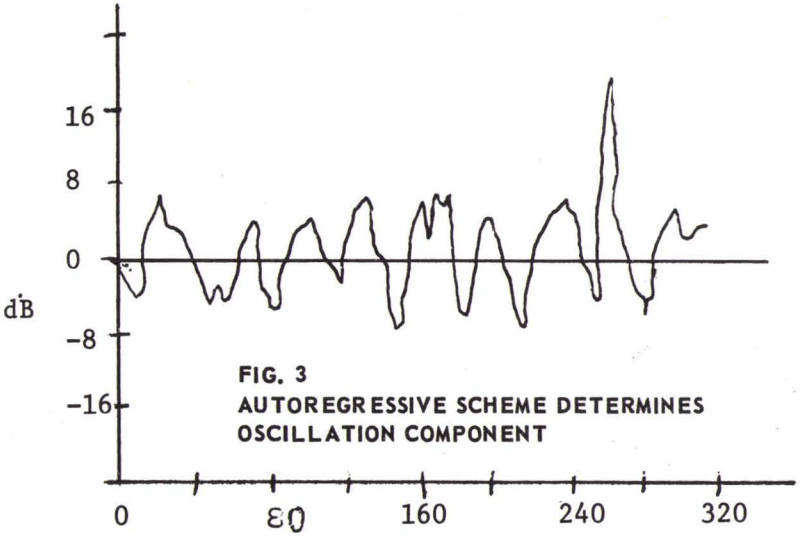

FIG. 3
AUTOREGRESSIVE SCHEME DETERMINES
OSCILLATION COMPONENT

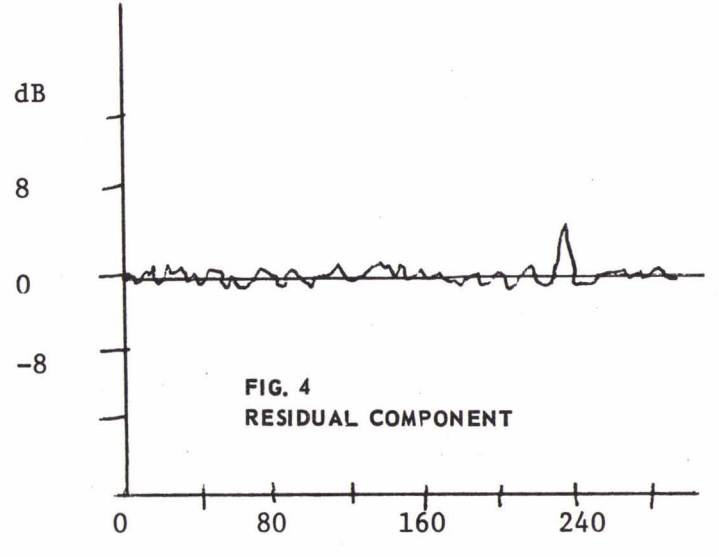

FIG. 4
RESIDUAL COMPONENT

RANGE IN NAUTICAL MILES

APPENDIX A
THE ANALYSIS PROCEDURE - A DETAILED DESCRIPTION

A.1 Computation of the long-term trend

The three fold separation of major contributing components of a transmission loss curve initially uses the form $X_L(r)=A + B \log(r)$ since over a considerable range, loss is either spherical, cylindrical, or transitional. While more complex equations can readily be devised which will fit the data and include more of the variance, they were judged to add more complexity without increasing comparison testing effectiveness appreciably.

The analysis begins with the assumption that an intensity curve $X_A(r)$ of the type depicted in Figure (1.1) can be represented in the form

$$X(r_k) = A + B \log(r_k) + X'(r_k) \qquad \text{A.1}$$

where $[r_k]$ (k=1,2,....N) is the sequence of range values. An application of standard methods, Kendall [A1], yields the following expressions for estimates of the coefficients, and the residual variance. Note the subscript, e, showing the estimate, as distinct from the true value, is shown only initially throughout the following material.

$$B_e = \frac{\sum_k \log(r_k) X(r_k) - \left[\left(\sum_k \log(r_k) \right) \left(\sum_k X(r_k)/N \right) \right]}{\sum_k (\log(r_k))^2 - \left[\left(\sum_k \log(r_k) \right)^2 / N \right]} \qquad \text{A.2}$$

$$A_e = \frac{1}{N}\left(\sum_k X(r_k) - B_e \sum_k \log(r_k)\right) \qquad \text{A.3}$$

$$S_e^2 = \frac{\sum_k \left(X(r_k) - A_e - B_e \log(r_k)\right)^2}{N-2} \qquad \text{A.4}$$

The type of test used to compare intensity curves in regards to long-term trend depends upon whether there is a significant oscillatory component in the residual curve $X'(r)$. If a test shows the residual values mutually independent, comparison tests based on the methods of linear regression analysis will apply. The tests are slightly weakened but still useful if significant oscillations are present. In special, demanding,cases the techniques of (A.4) can be used to remove the oscillating component from the trend residual. The random residual remaining may be combined with the initial trend estimate and coefficients, A.2, A.3 and A.4 redetermined. Before proceeding with the comparison tests, then, it is necessary to decide whether the trend residual is a random variable. A statistical test, a description of which follows, devised by M.G. Kendall [1] is recommended for this purpose, because of its simplicity and effectiveness.

A.2 A Test for Randomness

The turning point test is based on the statistical hypothesis that the values $\{ X'(r_k) \}$ (k=1,2,.....n) are mutually independent; thus, they could have ocurred in any order, each order being equally

likely. An observed valued $x(r_k)$ is called a turning point if

$$X(r_{k-1}) < X(r_k) \text{ and } X(r_k) > X(r_{k+1})$$

$$\text{or, if } X(r_{k-1}) > X(r_k) \text{ and } X(r_k) < X(r_{k+1}) \qquad \text{A.5}$$

Let n_T denote the number of turning points which occur in a time series of n distinct points. Assuming the above hypothesis, Kendall has shown [1,p. 22-24] that for fairly large sample sizes, n_T is approximately distributed as a normal random variable with mean

$$\mu = \frac{2}{3}(n-2) \qquad \text{A.6}$$

and standard deviation

$$\sigma = \frac{16n - 29}{90} \qquad \text{A.7}$$

The test procedure is the following: Select a confidence level α . Reduce the series by throwing out repeated values, leaving n distinct points, without changing their order of occurrence. Calculate μ and σ using Equations (A.6) and (A.7). Then the $100(1-\alpha)$ percent confidence limits for n_T are given by

$$\mu \pm \sigma Z_{\frac{\alpha}{2}} \qquad \text{A.8}$$

where $Z\alpha/2$ denotes a percentage point of the normal distribution. Count the observed number n_T of turning points for the series of distinct values. If n_T is within the interval, we accept the hypothesis and conclude that the curve has no significant oscillatory component. Therefore, $X(r)$ consists only of a long term trend and a residual, random component. This residual series may not be a purely random process, but the oscillations it exhibits are not significant at the selected confidence level to warrant description.

If n_T lies outside the confidence interval, then we reject the hypotheses, and conclude that the series $X'(r)$ has a significant oscillatory component, which should be measured separately. The probability of making this decision when in fact the hypothesis is true is α.

A.3 Trend Comparison Tests

Let us initially assume the turning point test has shown the residual curve $X'(r)$ to be random at same acceptable confidence level. By setting $z = \log(r)$ and $E(r) = X'(r)$, (A.1) can be recast in the form

$$X = A + Bz + E \qquad \text{A.9}$$

and we can apply the results of linear regression analysis (see, for example, Section 22.9 of Kendall [A1], chapter 11 of Burr [A2]) to find confidence limits for A, B and the standard error of estimate. At the 100 $(1-\alpha)$ percent confidence level, we can calculate these limits as follows:

For B, the confidence limits are $B_e \pm L_B$, where

$$L_B = \frac{t_{\frac{\alpha}{2}, N-2}\ S_e}{\left[\sum_K \left(\log(r_K) - \left(\sum_K \log(r_K)/N\right)\right)^2\right]^{\frac{1}{2}}} \qquad \text{A.10}$$

For A, the limits are $A_e \pm L_A$, where

$$L_A = t_{\frac{\alpha}{2}, N-2}\ S_e \left[\frac{\sum_K (\log(r_K))^2}{N\sum_K \left(\log(r_K) - \left(\sum_K \log(r_K)/N\right)\right)^2}\right]^{\frac{1}{2}} \qquad \text{A.11}$$

Here t $\alpha/2$, N-2 is a percentage point of the student t distribution.

For the standard deviation of the limits are

$$S_- = S_e\left[\frac{N-2}{\chi^2_{\frac{\alpha}{2},N-2}}\right]^{\frac{1}{2}} \text{ and } S_+ = S_e\left[\frac{N-2}{\chi^2_{1-\frac{\alpha}{2},N-2}}\right]^{\frac{1}{2}} \quad \text{A.12}$$

Here $\chi^2_{\mu,n}$ is a percentage point of the Chi-Square distribution.

In addition to the analytic comparisons described above, a visual comparison plays the same qualitatively useful role as in traditional data/model comparisons. One such scheme used here is to superimpose the regression equation derived from one member of a comparison pair onto the data of the other member. To guide such visual comparisons, two displaced regression curves are used, separated by four residual standard deviations of the regression data. Equation A.13 shows the equation with subscript, E, indicating experimental bounds, L, as illustrated in Figures A.1 through A.2:

$$L = A_E + B_E \log(r) \pm 2 S_E \quad \text{(A.13)}$$

With the plotted band shown on the figures we have computed an elementary overlap type measure called a Band-Fit (BF) coefficient as shown in Equation A.14,

$$BF = \frac{P_M}{P_E} \quad \text{(A.14)}$$

where the P_M is the percentage of model points (as in later illustrations) which fall within the band superimposed and defined by the experimental data. The denominator, P , is the percentage of

experimental data that is within the four sigma band (Fig. A.1, A.2).

A.4 Separation into Oscillatory and Random Residual Components

After the residual curve, $X'(r)$, has been shown non-random by the turning point test, the oscillatory component must be separated from the final random residual. An autoregressive scheme was chosen to meet this need because of its effectiveness, and the suitability of the auto covariance function. Our discussion of autoregressive processes follows that of Ref [4], where complete derivations of the equations employed can be found.

To begin with, an autoregressive process of order m, is defined as a second order uniformly sampled stationary random process $\{X(k)\}$ with zero mean, which satisfies the equation.

$$Y(k) = a_1 Y(k-1) + a_2 Y(k-2) + \ldots a_m Y(k-m) + Z(k) \qquad \text{A.15}$$

where $\{Z(k)\}$ is a purely random process. Here the coefficients $a_1, a_2, \ldots a_m$ are constant, and Eq.(A.15) must hold for all observed values $k=1,2,\ldots N$. We note that an autoregressive process consists of two parts. The first, involving the coefficients a_j is called the autoregressive scheme, and the second is called the residual process.

An autoregressive process may be generated by selecting an order m , a set of coefficients $\{a_j\}$ $(j=1,2,\ldots m)$ which satisfy a stationary condition, and a process $\{Z(k)\}$ obtained for example, from a table of independent normal deviates. Conversely, if one is given a process $\{Y(k)\}$, then one can attempt to fit an autoregressive process to $\{Y(k)\}$ in the following manner. Estimates $a_1, a_2, \ldots a_m$ of the autoregressive scheme coefficients are obtained as the solution of the system of m equations

$$c_y(1) = \hat{a}_1 c_y(0) + \hat{a}_2 c_y(-1) + \ldots \hat{a}_m c_y(1-m)$$

$$c_y(2) = \hat{a}_1 c_y(1) + \hat{a}_2 c_y(0) + \ldots \hat{a}_m c_y(2-m) \qquad \text{A.16}$$

$$c_y(m) = \hat{a}_1 c_y(m-1) + \hat{a}_2 c_y(m-2) + \ldots \hat{a}_m c_y(0)$$

where $c_y(k)$ is the sample autocovariance of the process $\{ Y(k) \}$.

$$c_y(k) = \frac{1}{N} \sum_{j=1}^{N-k} Y(j)\, Y(j+k)$$

$$(k = 0, 1, \ldots, N-1) \qquad \text{A.17}$$

We note that $c_y(0)$ will give us an estimate of the variance of $\{ Y(k) \}$. It may be shown that the variance of the residual process may be estimated by

$$S_z^2 = c_y(0) - \hat{a}_1 c_y(1) - \ldots - \hat{a}_m c_y(m) \qquad \text{A.18}$$

To compare these two variances, we will use the normalized mean square error,

$$E_0 = S_z^2 / c_y(0) \qquad \text{A.19}$$

After the coefficients $\{a_1, a_2, \ldots a_m\}$ have been calculated, the residual process is obtained by subtracting the autoregressive scheme from $\{Y(k)\}$. To check whether a valid fit has been made, the residual should be tested to determine if it is purely random. This can be done by using the turning point test described in Article (A.2).

In selecting a time series model of this type, we are carrying out a program originally suggested in a paper by Whittle [A3]. He argues that any zero mean, stationary process whose spectral density satisfies a certain condition may be represented by an autoregression of infinite order. For such a process, a reasonably accurate estimate of the residual variance may be obtained by fitting a finite autoregressive scheme of sufficiently high order. The spectral condition requires that the reciprocal of the spectrum

be expandable in a Fourier series (for all practical purposes, that the spectrum be nowhere zero), and is usually satisfied in practice.

Our analysis procedure then, is to calculate autoregressive scheme estimates for the different curves under consideration, using increasing values for m, calculating the normalized mean square error each time. Currently available computer codes (Robinson [A4] Section 2.8) enable us to do this with a minimum of time and effort. We can thus determine a value m_o for m, such that the reduction in E_o for higher order fits is insignificant in all cases.

For comparison, autoregressive fits of order m_o are then used for all curves being analyzed. Granted that this requires an excessive number of terms in some cases, it provides a basis for comparison, without essentially affecting the estimate of the residual variance.

A.5 Measurements for Oscillatory Components

Suppose now that the curve $X'(r)$ has been expressed as the sum of an oscillatory component $X_o(r)$ and a residual component $X_R(r)$. The oscillation can usually be attributed to some known physical cause such as the convergence zone effect. To study this phenomenon quantitatively, we next obtain a measure of this oscillatory component. For this, the sample autocovariance function defined by Eq. (A.6) is used. Thus, we calculate

$$c_y(k) = \frac{1}{N} \sum_{j=1}^{N-k} X_o(r_j)\, X_o(r_{j+k}) \qquad \text{A.20}$$

for k=0,1,.....N-1. A typical graph of $c_y(k)$ would resemble that of damped oscillatory motion starting at k=o, with the variance $c_y(o)$ decreasing in magnitude as k increases. In most cases the autocovariance function will be asymmetric or scalloped reflecting convergence zones, Lloyd mirror variation, or other origins most of which produce periodic but not sinusoidal variation. The principal period of the process is simply the distance between peaks of the function. To be specific, we will call this quantity the zone period, P. If we have oscillatory components for curves C_1, C_2 with zone periods P_1, P_2, then we may consider the zone spacing ratio, Z , defined by

$$Z = \frac{P_1 - P_2}{P_1} \qquad \text{A.21}$$

A positive value of z indicates that the C_2 oscillation has a shorter period than that of C_1.

A.6 Distribution of Variances

Let us briefly review the separation procedure which has been proposed for intensity curves: Starting with an initial curve X, a long-term trend X_L, is removed, leaving a residual curve X'. The residual curve is then decomposed as the sum of an oscillatory component X_o and a random residual component X_R. We will denote by V, V_L, V', V_0 and V_R the variances of the above curves. Because the component series are uncorrelated, we will have

$$V' = V_o + V_R \qquad \text{A.22}$$

and

$$V = V_L + V_o + V_R \qquad \text{A.23}$$

Thus, the fractions V_L/V, V_o/V, and V_R/V will adequately describe the distribution of the variance of the initial curve. One measure of the validity of the separation process is the extent to which Equs. (A.22) and (A.23) hold. In all of the applications of the procedure examined values very close to theoretical predictions were observed (See Appendix B.4, Table B.8).

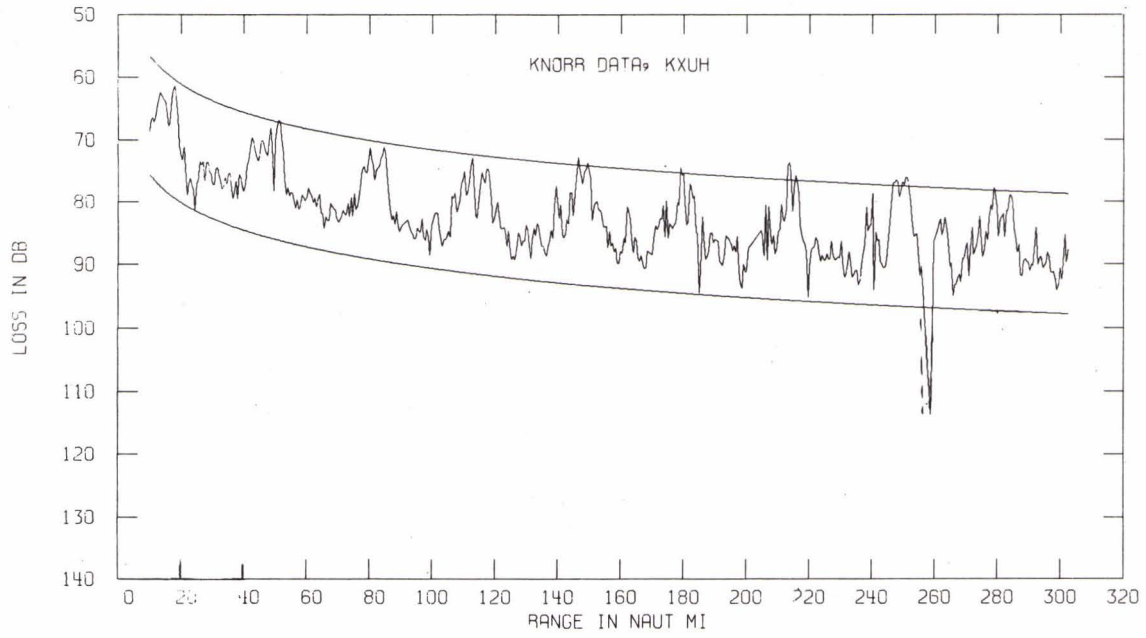

FIG. A.1 EXPERIMENTAL DATA, UPPER HYDROPHONE

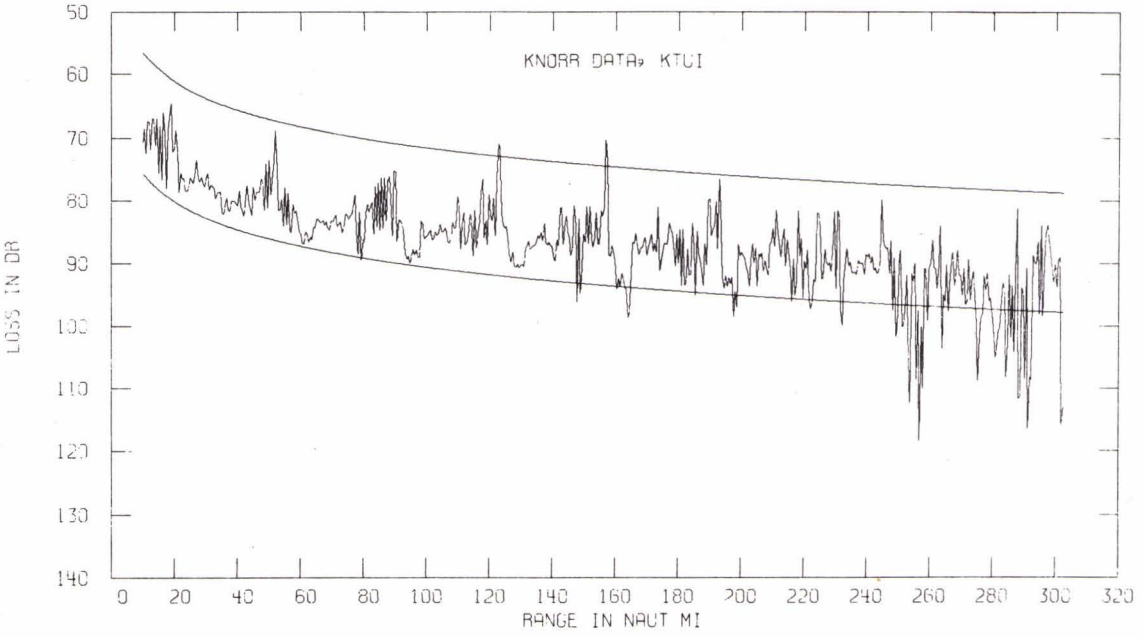

FIG. A.2 TRIMAIN MODEL UPPER HYDROPHONE

APPENDIX B

B1 Results of Comparative Analyses

In this appendix are presented results obtained from employment of the analysis procedure for a model/experimental comparison study. The objectives are to:

1. Examine and show for example the practical application of the procedure.
2. Test the resolution of the methods on two similar data sets arising from slightly different conditions.
3. Test the resolution of the method in a comparison of data vice model performance.
4. Test the resolution on model curves to distinguish algorithum differences.

The experimental data were obtained during a controlled run of the USNS MIZAR of 300 nm run directed by excellent satellite navigation. The signal sources were small explosive charges carefully timed with synchronized WWV clocks for precise range and depth control. The shot spacing was one-half nautical mile and the depth 300 ft. (91.4m). Sound speed profiles were measured at the ends and in the track center; detailed bathymetry was measured throughout the run. For acoustic model computation, the simplified profile shown in figure B1 was employed. The signals were received by hydrophones suspended from two ships, the R/V KNORR and USNS GIBBS, stationed at the beginning and end of the track, respectively. The KNORR phones were vertically separated by 150m, with the lower unit at a depth of 3386m. The same arrangement was used for the GIBBS phones, with the bottom unit at a depth of 3020m. Transmission loss curves were computed for two relatively low frequency third octave bands, separated by 50 Hz. Table B.1, shows the labeling systems used for the curves used in the present study.

Curve	Ship	Hydrophone	Frequency
KXUL	KNORR	Upper	Low
GXUH	GIBBS	Bottom	Low

Table (B.1) Experimental Intensity Curves

A series of intensity curves to be used for measured and predicted comparisons were generated largely by the computer program TRIMAIN using measured bathymetry and sound speed profiles, along with the appropriate source and receiver depths. Using incoherent (I) summation intensity calculations, three curves corresponding to the experimental runs were generated. A second (II) method using a ray weighting based upon an exponential probability distribution function in depth was used on two program runs. A third method used a Lloye Mirror (LM) correction for proximity to the surface. A listing of the resulting TRIMAIN curves used for our analysis is given in Table (B.2).

Curve	Ship	Phone	Type	Frequency
KTUI	KNORR	Upper	I	
KTUL(LM)	KNORR	Upper	I	Low
GTUI	GIBBS	Upper	I	
GTUII	GIBBS	Upper	II	

Table (B.2) TRIMAIN Model Intensity Curves

In addition, one run was made with Fast Asymptotic Coherent Transmission model (FACT) to obtain the first 250 values of the curve KXUH. The FACT Program contains a first order caustic computation but is restricted to a single sound speed profile and flat horizontal bottom. We denote the intensity curve for this case as KFUH and, for comparison, use only the first 250 values of the corresponding experimental curve, denoted as KXUH(F).

In the remaining articles of this appendix, we will discuss the results obtained as the analysis procedure was applied to the experimental and model curves listed above. We have selected two groups of curves: The first consists of KXUL, KTUI, and KTUL (LM) (Figures B.2 a,b,c); that is, an experimental curve for KNORR data, with two corresponding TRIMAIN runs, differing in the type of intensity calculations used. The second group is a similar selection, comprising the curves GXUH, GTUI, and GTUII (Figures B.3 a, b, c), based on GIBBS data.

B.2 Long-Term Trend

Following the discussion of Appendix A, the long-term trend is assumed to be of the form A + B log (r), and least squares equations A(2), A(3) are used to calculate the coefficients A, B, respectively. The residual curves remaining after trend removal are denoted with a prime (') superscript. Thus,

$$KTUI' = KTUI\ (r_k) - A - B \log\ (r_k). \qquad B.1$$

Table (B.3) lists the results of the trend estimation on several model and two experimental data suites. The significant features of this compilation are the following:

a. The mean values of the data sets are different and ordinarily would reflect systematic bias in an entire suite under comparison, a calibration error or possibly a bottom condition at a near bottomed receiver not adequately modeled. The confidence interval for this mean is included, for statistical comparison, in this grouping.

b. The regression coefficient, B, shows the estimated exponential power decay of the sets. In the first KNORR group, we see a distinctly sharper fall (larger exponent) in the two model sets. These model runs were included to show how a modeling error, ray drop out, purposely produced and plotted Figure B.2b, can produce a definite measurable difference. The effect is also reflected in the mean value difference. Next, considering the Gibbs suite, we see a case of strong smoothing (GTUII) suppressing the growth of the decay constant, B, and also increasing the model mean to near the observed set seen in GXUH. While the range smoothing has been deliberately over done for illustration it is clear that models could be brought into correspondence by this method with data and more discriminating tests for spectral content might be required for distinct numeric separation.

c. In the third set in Table B.3, we have a good comparison of the FACT model with data. A slight bottom loss adjustment would probably raise the mean and decrease the decay constant, B, to near perfect coincidence. One advantage this last set shows in model/data comparisons is how range constraint improves the quality of the match. The last curve, KTUI(F), is a TRIMAIN estimate run to the same 250 range point limit of the FACT model and quantitatively shows at lesser ranges the ray density is quite adequate, and the model improves. Generally, as might be expected, long-range predictions and comparisons prove the most difficult and are hence likely to require the techniques of this report.

d. The last two columns of Table B.3 show the original variance and the remaining or residual variance. This last column, in particular, illustrates the effects of smoothing in the GTUI/GTUII contrast. A variance comparison test, such as the F test discussed in reference A1, is ideal for quantitative smoothing comparisons or processing bandwidth comparisons.

Following a set of qualitative comparisons such as described above, let us assume that we have further noted and examined for cause the difference in mean and coefficient estimates and noted the confidence intervals on each. More detailed comparisons of two data suites require the following additional calculations:

1. Generally for curve parameter comparison, it is essential for the data to be considered as having originated from the same population. This can be tested by forming the F ratio of the residual variances of each curve pair. Approximate similarity is usually sufficient.
2. Using a pooled residual variance, a standard deviation of the difference of the regression coefficient, (decay constant) is computed.
3. A confidence interval in this difference variance is then computed using the T distribution.

While each of the above detailed steps is described in standard texts on statistics, a factor not immediately apparent is that these three steps can be quite accurately approximated as follows:

1. If the variances are near the same, assume the populations are the same.
2. Usually most experimental model comparisons will involve large numbers (50 or more) points and pooling for more accurate variance estimation is marginally useful and may be ignored.
3. The confidence coefficient for the difference in two coefficients is simply computed as the square root of the sum of the squares of the two subject coefficients.

As an example of the above procedure, Table B.3 shows Gibbs data, GXUH, residual variance is 3.8 dB. The TRIMAIN model with range averaging, GTUII, gives 3.4 dB. Let us assume these are essentially equal. The 95% confidence interval halfwidth for B is 1.1 in each case which gives combined (root of the sum of the squares) difference halfwidth of 1.6. The difference in the coefficients, however, is 4.1, that is, 13.6 - 9.5. This greatly exceeds our 95% interval and we may say the probability is less than one in twenty that the curves are the same. In this instance, the model parameters definitely need adjustment.

The simplified technique can be also used to compare the means of two groups. Using the same Gibbs data/model, GXUH/GTUII, Table B.3, we have for the 95% confidence interval on the difference in means, a root of sums squared of .6 which is not exceeded by the .3 dB difference in means. Thus, the smoothing brought the mean under control, reduced both the data variance (10.2 to 4.3), and the residual variance (9.3 to 3.4), a small amount more than required, but definitely rendered the slope unsuitable, (14.8 to 9.5).

A conclusion of this comparison is moderately clear: less smoothing and some physical factor related to mean off set probably require consideration.

In Table B.4 a tabulation of the Band Fit coefficients is shown for simple numeric comparisons as to how well the data trend band is encompassing the model estimates. This test is not of the same rigor as the regression and variance comparison test, but in conjunction with the strong visual appeal of the plots shown in Figures B.2a to B.3c is recommended for display and presentation.

CURVE DESIGNATE	MEAN M	CONF. 95% M ±	SLOPE B	CONF. 95% B ±	Std. Deviation Data,S	Resid.S_P
KXUL	90.1	.5	12.6	1.1	6.1	4.4
KTUI	96.8	.6	17.6	1.3	7.8	5.2
KTUL(LM)	98.1	.7	18.5	1.5	8.7	6.1
GXUH	95.6	.4	13.6	1.1	5.4	3.8
GTUI	101.5	.8	14.8	2.7	10.2	9.3
GTUII	95.9	.4	9.5	1.0	4.3	3.4
KXUH(F)	88.2	.8	16.3	1.8	6.2	4.1
KFUH	88.9	.8	19.2	1.6	6.5	3.6
KTUI(F)	91.3	.7	15.1	1.6	5.6	3.6

TABLE B-3

Results for long-term Trend Removal

EXP CURVE	MODEL CURVE	EXPERIMENTAL BANDWIDTH (dB)	BAND FIT (COEFF.)
KXUL	KTUI	17.6	.78
KXUL	KTUL(LM)	17.6	.62
GXUH	GTUI	15.0	.64
GXUH	GTUII	15.0	1.01
KXUH(F)	KFUH	16.5	1.00
SXUH(F)	KTUI(F)	16.5	1.03

TABLE B-4

Experimental Bandwidth and Band Fit Coefficient Results

The second phase of the trend analysis procedure requires the residual curves, X' be tested for randomness with the turning point test (see Appendix A.2). Based on the hypothesis that the curve is random, confidence limits for the number of turning points are calculated, using Eq. (A.8). Table (B.5) gives these limits, and the observed count of turning points for the six selected curves whose plots we will examine shortly.

Curve	Confidence Limits		Number of Turning Points
	Lower	Upper	
KXUL'	362	401	214
KTUI'	360	400	357
KTUL(LM)'	364	404	349
GXUH'	345	383	272
GTUI'	363	402	309
GTUII'	337	374	109

TABLE (B.5)

Test for Randomness at 95 Percent

Confidence Interval

It can be observed that in each case the number of turning points fall outside the limits. Thus, we reject the hypothesis of randomness and conclude that each of the above curves has a significant oscillatory component.

B.3 Oscillatory Residual Curve Analysis

The turning point test for randomness establishes the existence of significant oscillations in the trend residual. Each of the model and experimental residual curves which are given in figures (B.4) and (B.5), exhibit this strong oscillatory component. To begin the analysis, we may express one of the residual curves, $X'(r)$,

$$X'(r) = X_o(r) + X_R(r) \qquad \text{B.3.1}$$

Here $X_o(r)$ is the oscillatory component, and is taken to have the form of an autoregressive scheme,

$$X_o(r_k) = a_1 X'(r_k - 1) + a_2 X'(r_k - 2) + \ldots + a_m X'(r_{k-m}) \qquad \text{B.3.2}$$

The final curve, $X_R(r)$, will then be a purely random sequence.

The procedure for autoregressive scheme fitting, as discussed in reference (a 3), involves the choice of an order m, and the calculation of the coefficients $a_1, a_2, \ldots, a_m$ as the solution of a system of equations defined by the autocovariance function of the curve $X'(r)$. A FORTRAN computer code of the type devised by Robinson (A4, section 2.8) was used for this purpose. To provide a measure of completeness, the normalized mean square error, E_m, is calculated as the ratio of the residual variance to the trend variance, the program estimates E_k for all orders k less than or equal to m and calculates the coefficients $a_1, a_2, \ldots a_m$. To provide an accurate estimate of the residual variance for a variety of curve types, a large value for m is recommended. After several trials, the value m = 128 was selected as being sufficient for essentially all cases while requiring less than two minutes of machine time. In running the program for this order, the differences between values of E_m and E_{m-1} were less than .002 in all cases, indicating that the residual variance had reached a very stable level. After the autoregressive scheme fit has been made, the final residual component is tested for randomness by using Kendall's turning point test.

Table (B.6) lists the essential information obtained in the autoregressive analysis. The first column gives the normalized mean square error at m = 128. This is followed by the 95 percent confidence intervals for the turning point test, along with the observed number of turning points for each residual curve. In each case, this value falls within the confidence limits, and we can accept the hypothesis of a random residual curve. Figures (B.6) and (B.7) show the autoregressive scheme fits which were calculated as the oscillatory component of six representative curves.

Curve	Mean Sq. Error E_{128}	Confidence Intervals for Turning Points		Observed No. of Turning Points
KXUL'	.119	361	399	366
KTUI'	.606	361	403	402
KTUL(LM)'	.623	365	403	387
GXUH'	.337	359	397	364
GTUI'	.518	365	403	371
GTUII'	.018	336	373	344
	$\frac{E_{64}}{}$			
KXUH(F)	.153	150	174	159
KFUH	.093	139	162	140

Table (B.6) Separation of Zero- Mean Curves into Oscillatory and Residual Components

The autocorrelation function calculated as part of the above procedure can be readily employed to estimate the principal period of the oscillatory component. This interval is calculated from tabulation of the correlation function and is the interval between successive maxima. Usually several cycle peaks will be clearly evident and the average computed will accurately reflect the chief periodic phenomenon. In the case of all the present examples, this is the convergence zone period. This period can be used to define the zone period ratio, $ZP = (P_1 - P_2)/P_1$ to provide fractional error comparison of the curves with periodicities. Table B.7 show periods in nautical miles and the period ratios for the several model runs as compared with the two sets of experimental data.

Exp.	Curves P_1 (nm)	Model	Curves P_2 (nm)	Z_R
KXUL	33.1	KTUI	35.1	-.060
KXUL	33.1	KTUL(LM)	34.1	-.030
GXUH	32.6	GTUI	34.1	-.076
GXUH	32.6	GTUII	34.6	-.061
KXUH(F)	31.3	KFUH	36.0	-.150

Table (B.7) Zone Periods and Zone spacing ratios for oscillatory components

The above values indicate that the sample model periods are greater than the experimental. It is seen that the Lloyd's mirror calculations and Type II representations do not change the principal zonal structure, significantly, as this is a fundamental characteristic of each measured or predicted curve which is not effected even by a heavy smoothing operation.

2.1.1 Comparison of variances

At each stage of the separation process, estimates were made for the variance of the component curves, using the familiar formula,

$$V = \frac{1}{N-1} \sum_{k=1}^{N} \left(X(r_k) - \bar{X} \right)^2 \qquad \text{B.4.1}$$

Here $\overline{X}$ is the mean of the curve, and N is the number of range values. In this manner, we arrived at estimates of the variances, V for the initial curve, V_L for the long-term trend, V' for the trend residual curve, V_o for the oscillatory component, and V_R for the final residual. These values for our illustrative set of curves are listed in table (B.8)

Curve	V	V_T $(=V_L+V_o+V_R)$	V_L	V'	V_o+V_R	V_o	V_R
KXUL	37.30	37.05	17.99	19.31	19.06	16.86	2.20
KTUL(LM)	75.43	72.49	38.44	36.99	34.05	13.28	20.77
KTUI	61.53	59.31	34.76	26.76	24.55	9.41	15.14
GXUH	29.13	28.86	15.10	14.03	13.76	9.14	4.62
GTUI	103.36	101.78	17.75	85.61	84.03	40.39	43.64
GTUII	18.75	18.72	7.40	11.35	11.32	11.10	0.22
KXUH(F)	38.34	38.02	21.25	17.09	16.77	14.28	2.50
KFUH	41.56	42.35	29.54	13.01	12.81	11.56	1.25

Table (B.8) Variances for component curves

thus, if we have separated the initial curves into independent components, we should have $V' = V_o + V_R$, and $V = V_L + V_o + V_R$. In practice, the results were very close to the theoretical, with the largest discrepancy about 8 percent of the amount involved. Table (B.9) lists the proportions of the initial variance which can be attributed to each of the three components with the fractions normalized to the total for each curve.

Curve	$P_L = V_L / V_{TOT}$	$P_o = V_o / V_{TOT}$	$P_R = V_R / V_{TOT}$
KXUL	.486	.455	.059
KTUL(LM)	.530	.183	.287
KTUI	.586	.159	.255
GXUH	.523	.317	.160
GTUI	.174	.397	.427
GTUII	.395	.593	.012
KXUH(F)	.559	.376	.066
KFUH	.696	.273	.030

Table (B.9) Distribution of Variances

In summarizing the observed three part variance distribution of our sample set, a number of observations can be made:

1. An elementary point is that the variance distribution such as observed above is clearly effected by the proximity of the first point to the origin; starting at greater ranges the first term would be progressively smaller in most all cases.
2. A strong periodic component, developed from convergence zones in the present data, and not unusual in other instances, by no means can be expected to be always present. Simple bottom limited propagation would be a common case not likely to show periodic components.
3. Both the experimental data sets show a comparatively small amount of residual variance that is only approached by the FACT model operating on a restricted range of data and the smoothed TRIMAIN model on the whole range. In both model instances, extreme excursions are controlled, and this feature is found to parallel the frequency domain averaging that is a feature of typical (1/3) octave propagation data acquired with explosive charges. We would expect a measurement made with a well controlled cw

source to more closely match the random variability of model data; (excluding the ray dropout cases included here only as negative examples).

In concluding this appendix section on method application, the statement of the guiding nature of these quantitative measures must be reiterated. The three summary remarks above all show how each of the components as well as their distribution are affected by measurement techniques, range, and computational procedures. Strong conclusions can be drawn in specific cases and these can be supported with rigor and have considerable sensitivity; however the methods are not automatic and their application is supportive to the analyst who retains responsibility for their correct application and results.

References

1. M. G. Kendall, Time Series, Hafner Press, New York, 1973.

2. E. J. Hannan, Time Series Analysis, Methuen, London, 1960.

3. C. Chatfield and M. G. P. Pepper, "Time-Series Analysis: An Example from Geophysical Data", Royal Stat. Soc. J (C) 20, 217-238 (1971).

4. G. M. Jenkins and D. G. Watts, Spectral Analysis and Its Applications, Holden-Day, 1968.

A1 M. G. Kendall, The Advanced Theory of Statistics, Vol. 2, Griffin, London, 1948.

A2 I. W. Burr, Applied Statistical Methods, Academic Press, New York, 1974.

A3 P. Whittle, "Tests of Fit in Time Series", Biometrika 39, 309-319 (1952).

A4 E. A. Robinson, Multichannel Time Series Analysis with Digital Computer Programs, Holden-Day, 1967.

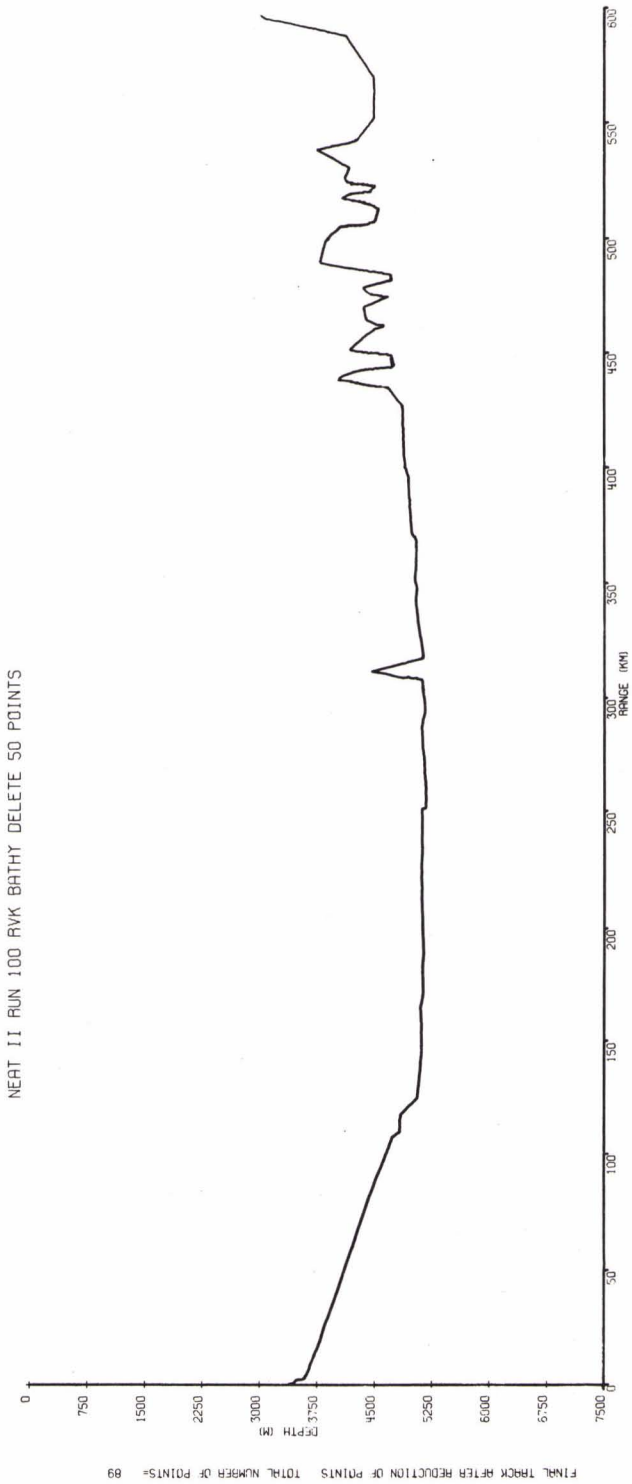
NEAT II RUN 100 AVK BATHY DELETE 50 POINTS
DEPTH (M)
0
750
1500
2250
3000
3750
4500
5250
6000
6750
7500
RANGE (KM)
0
50
100
150
200
250
300
350
400
450
500
550
600
FINAL TRACK METER REDUCTION OF POINTS TOTAL NUMBER OF POINTS= 89

FIG. B.1

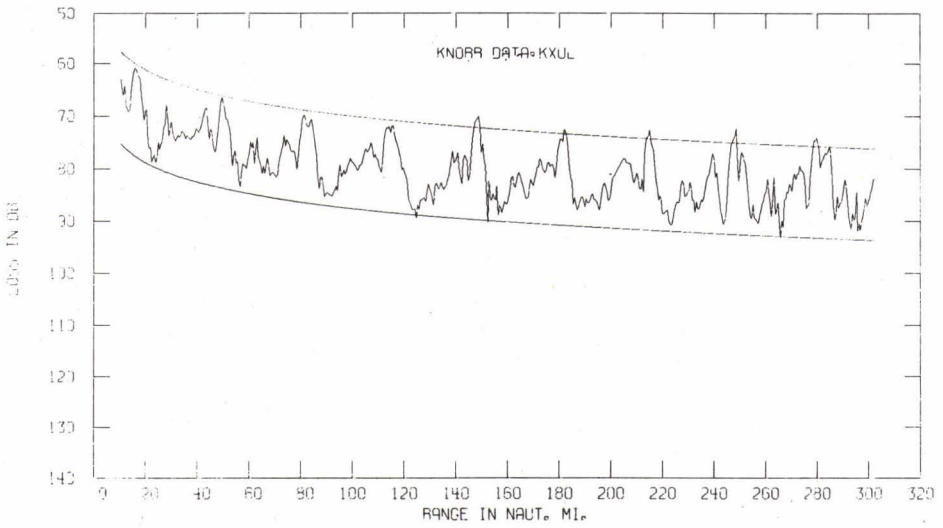

FIG. B.2a

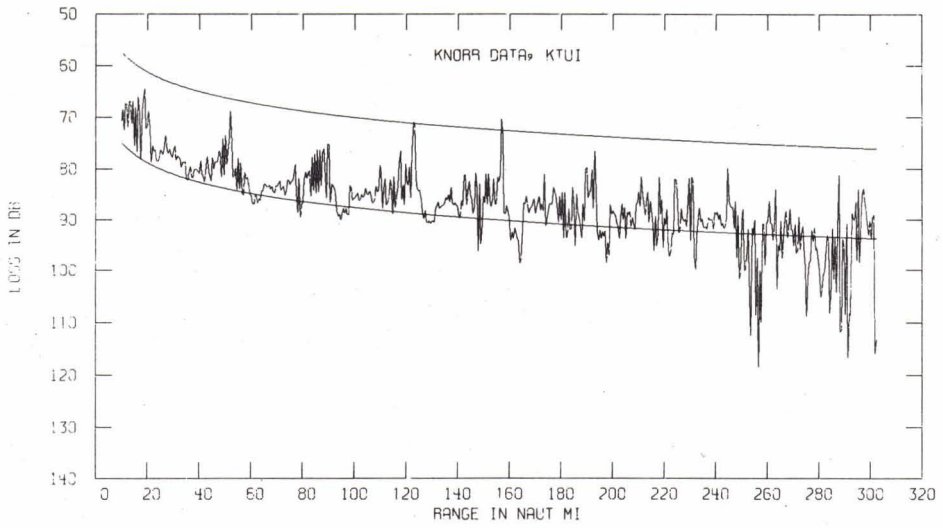

FIG. B.2b

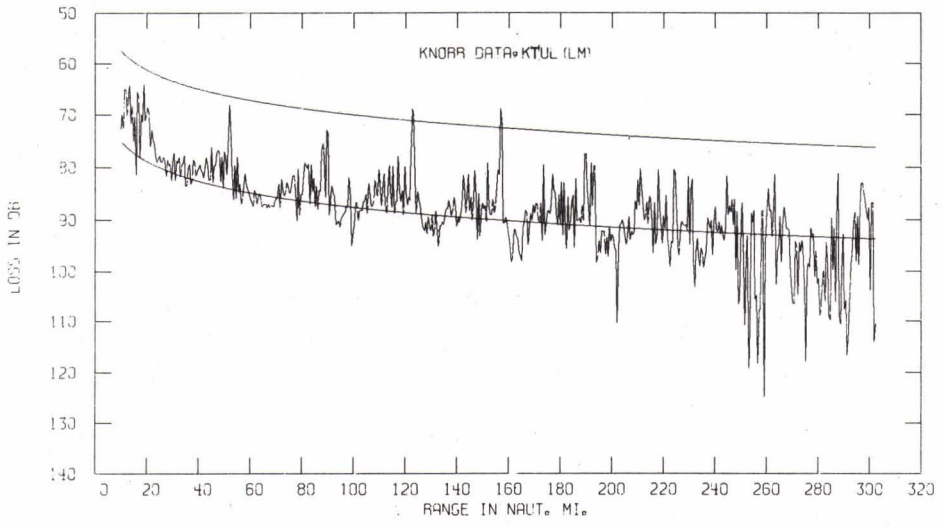

FIG. B.2c

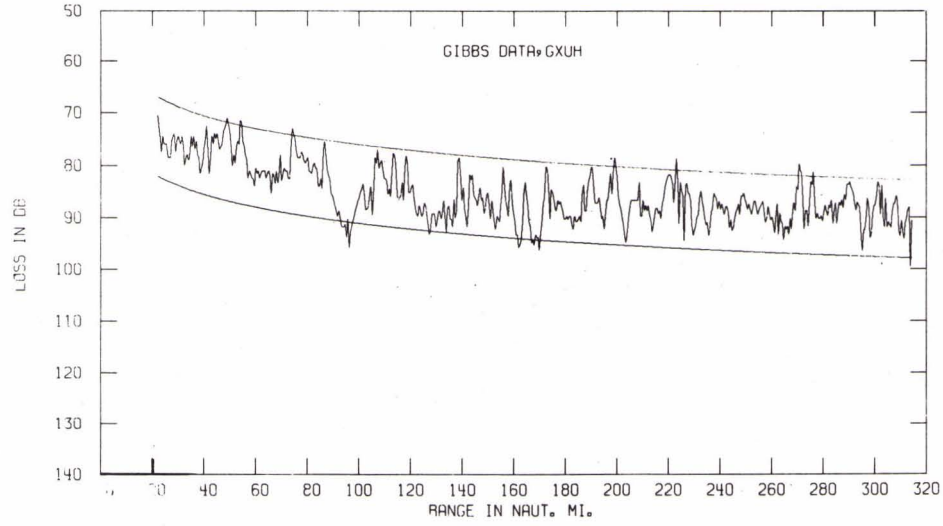

FIG. B.3a

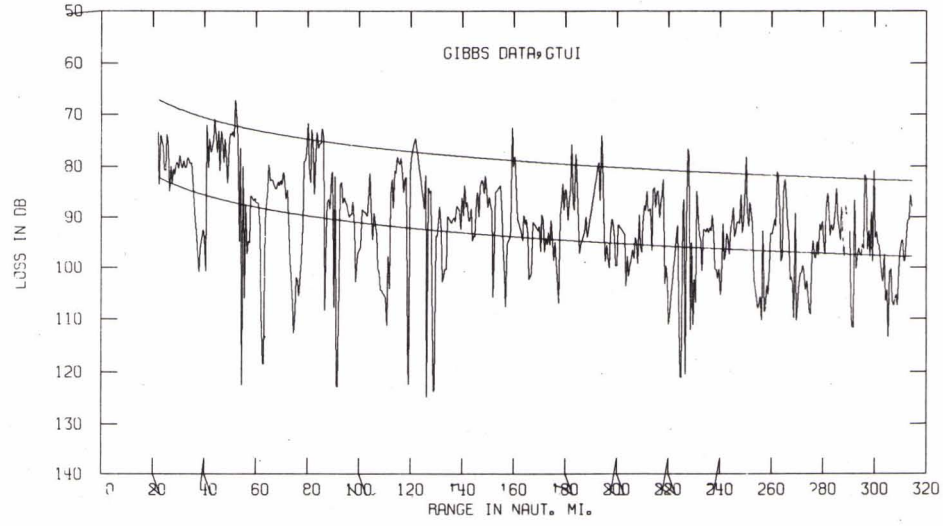

FIG. B.3b

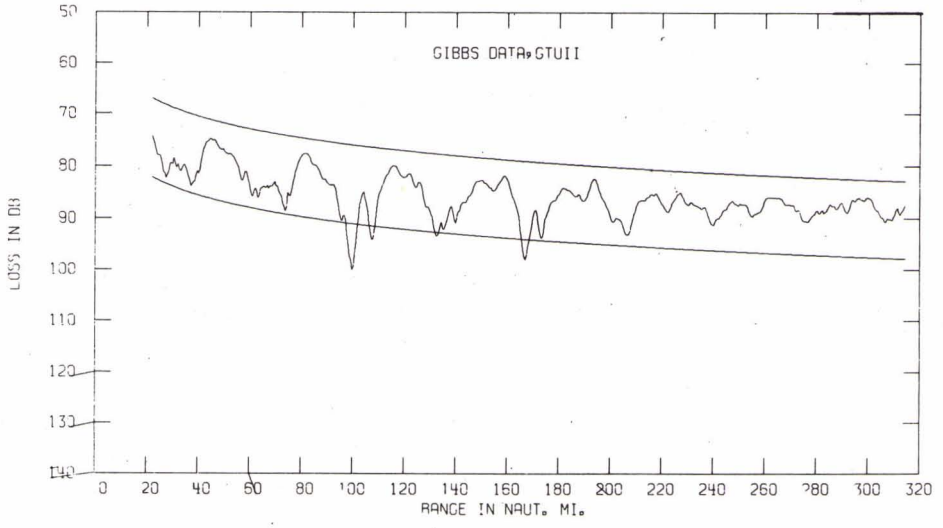

FIG. B.3c

KNORR EVENT 100 LO FREQ

FIG. B.4a KTUL'

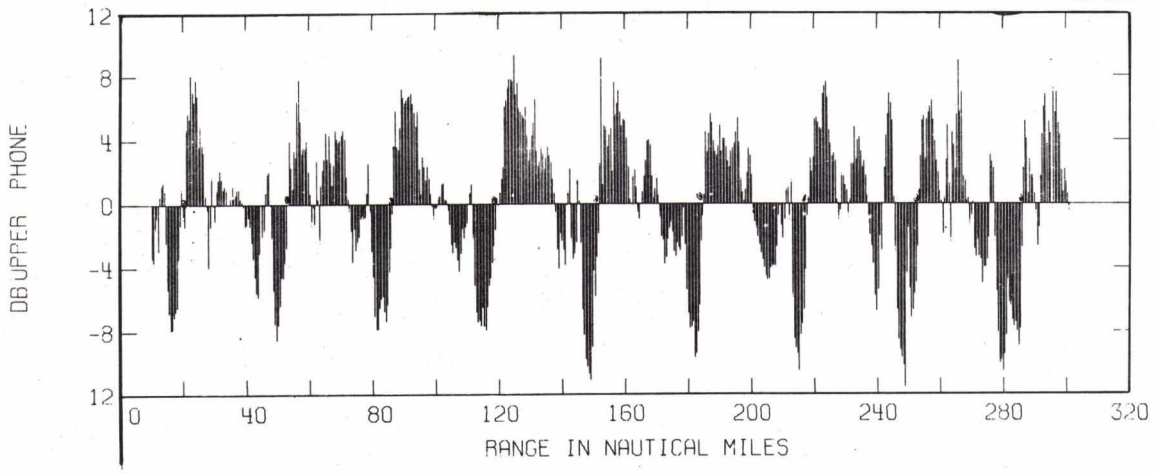

KNORR EVENT 100 HILO FREQ

FIG. B.4b KTUI'

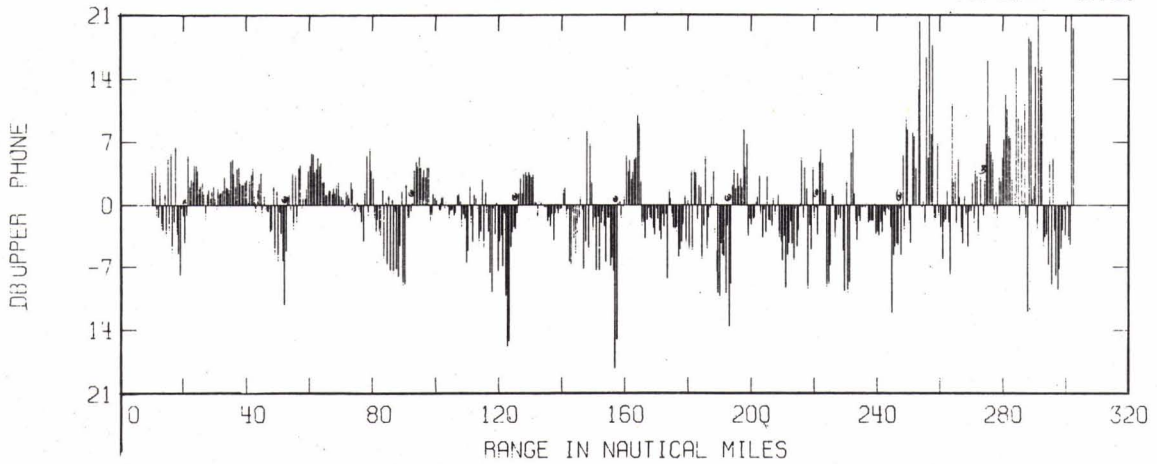

KNORR EVENT 100 LOW FREQ

FIG. B.4c KTUL (LM)'

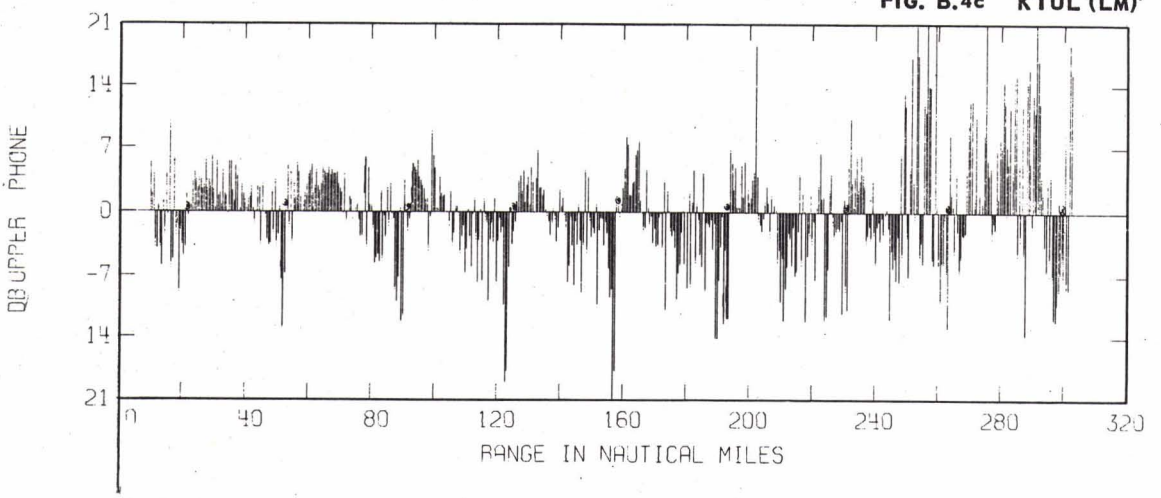

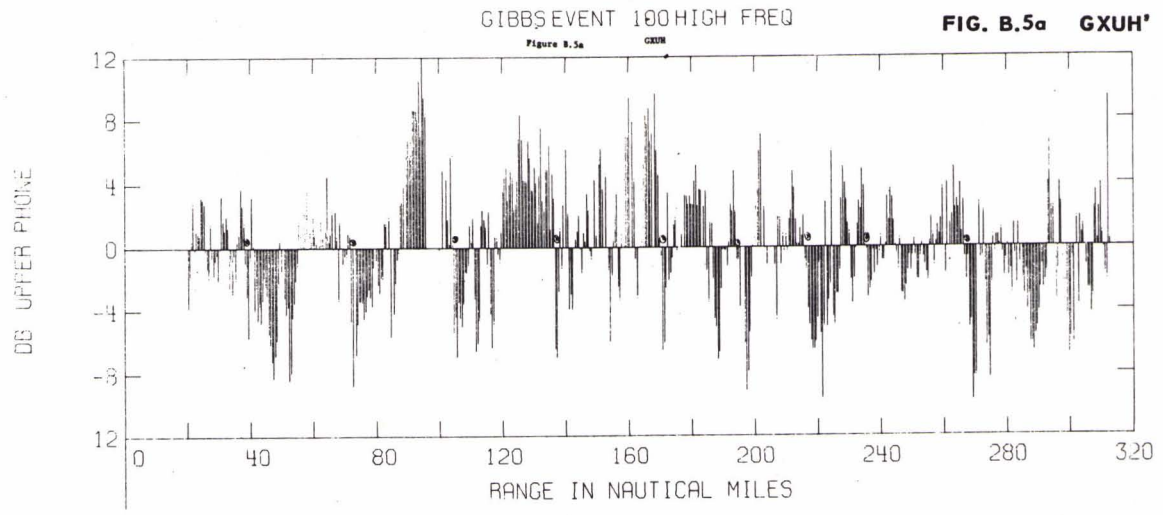

FIG. B.5a GXUH'

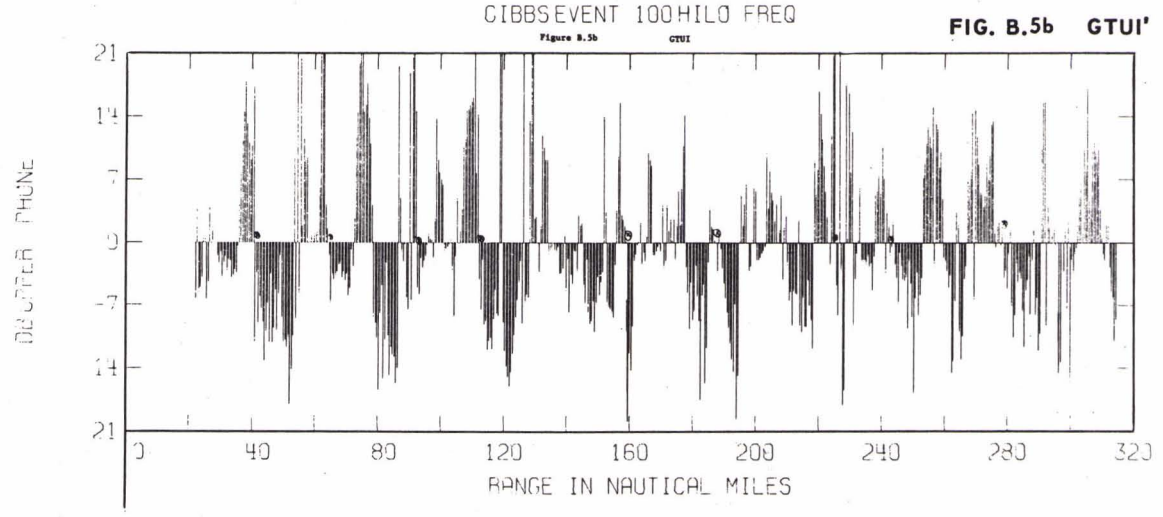

FIG. B.5b GTUI'

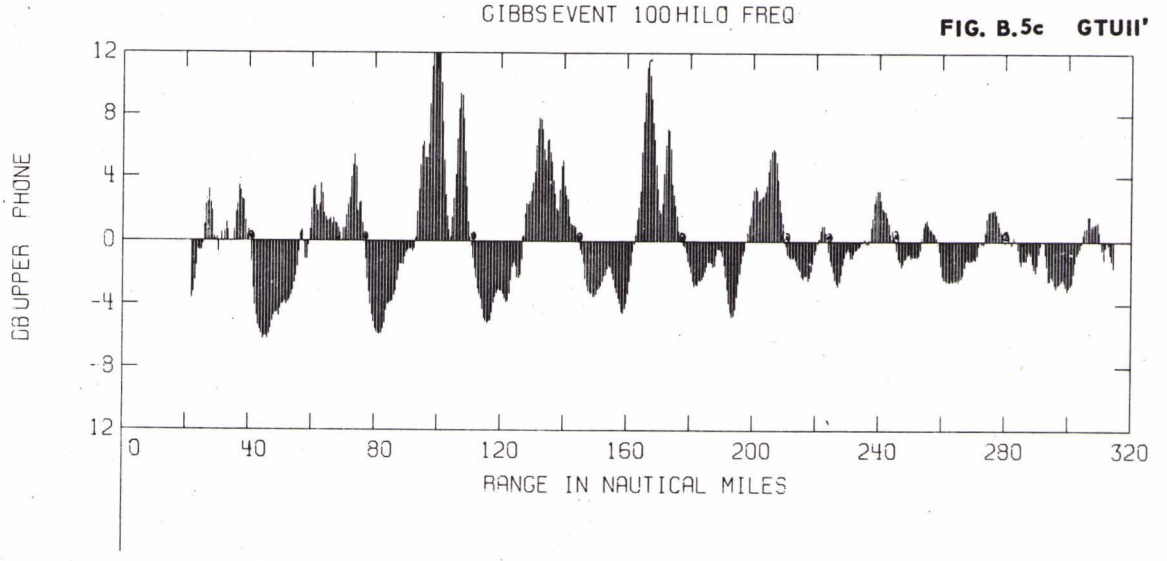

FIG. B.5c GTUII'

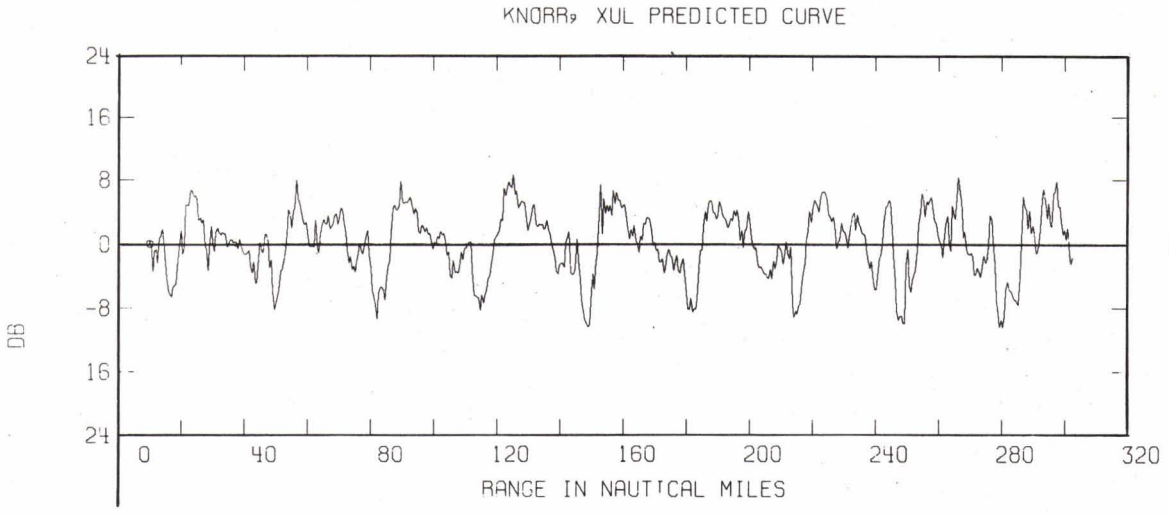

FIG. B.6a

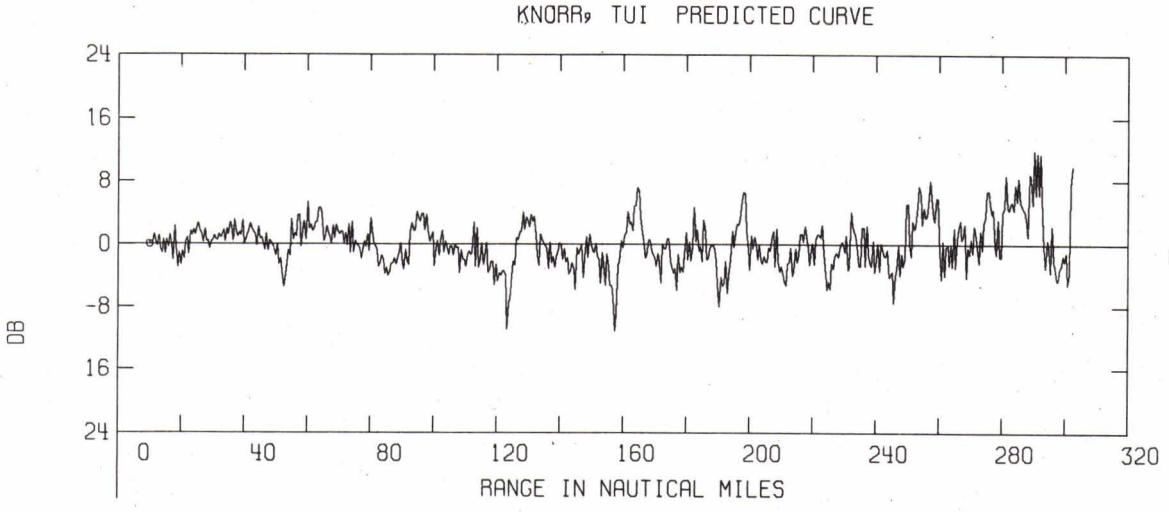

FIG. B.6b

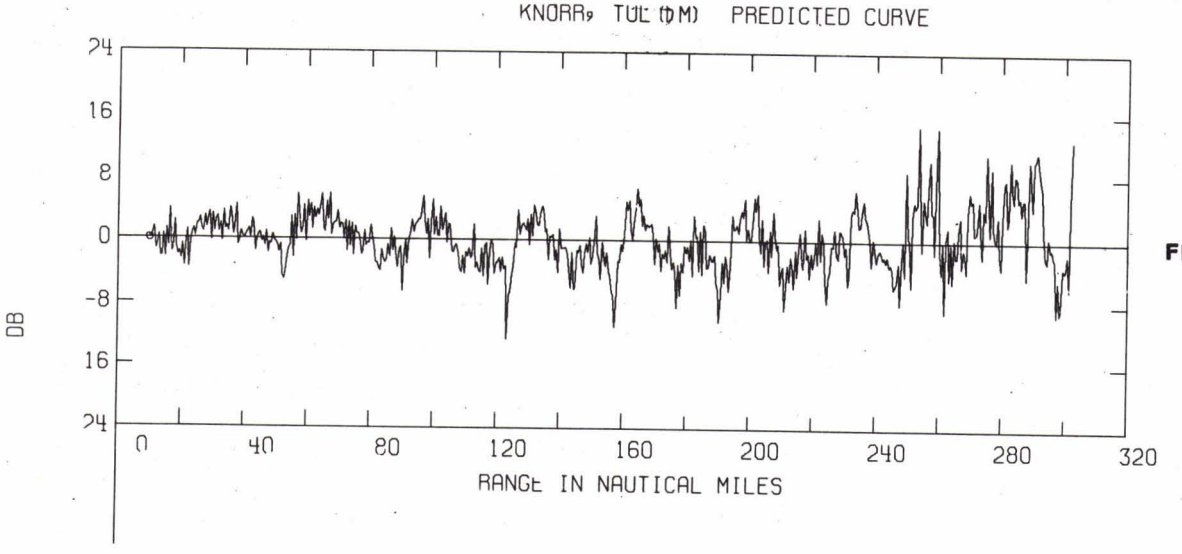

FIG. B.6c

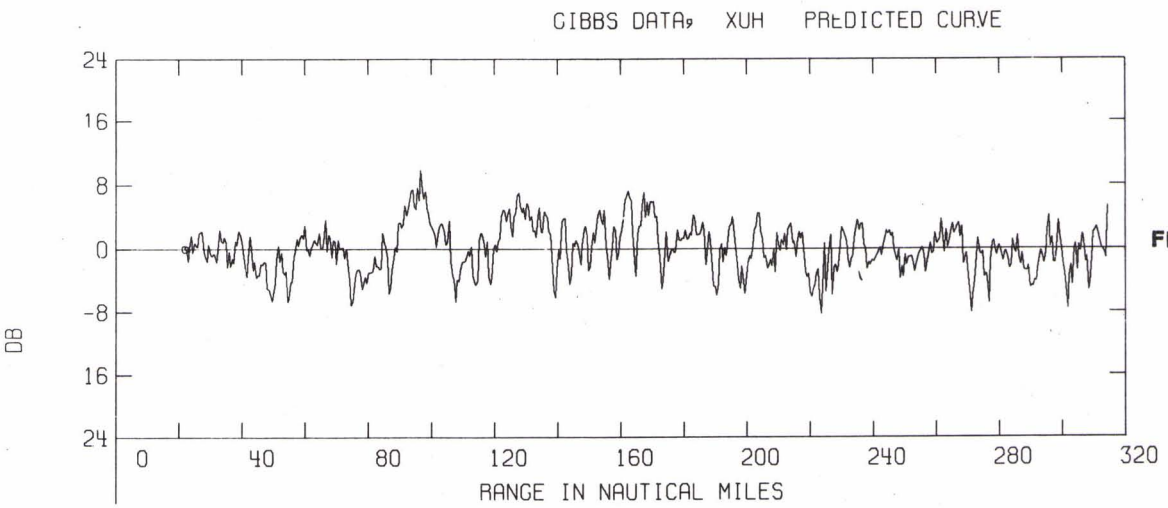

FIG. B.7a

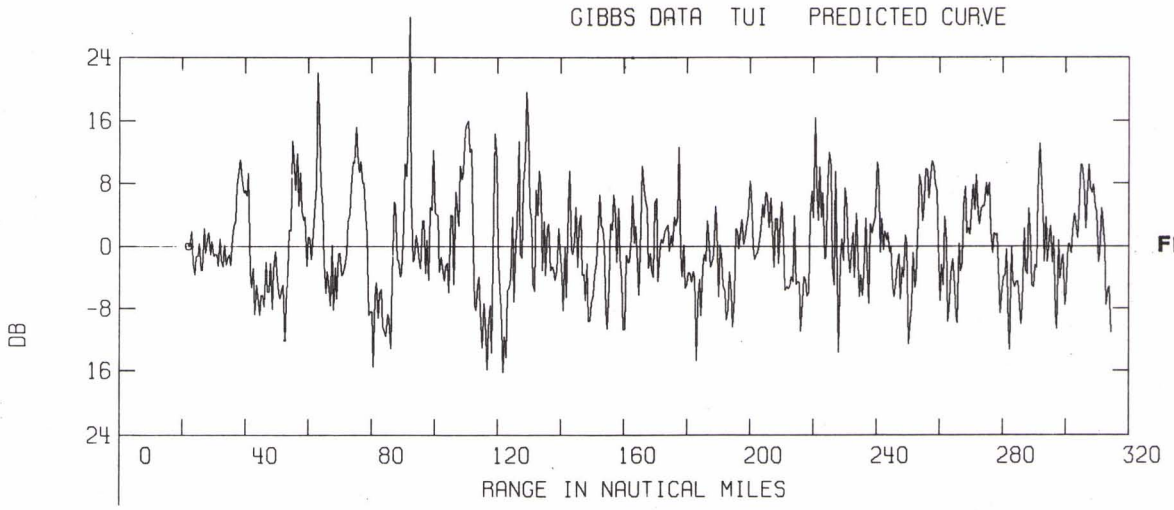

FIG. B.7b

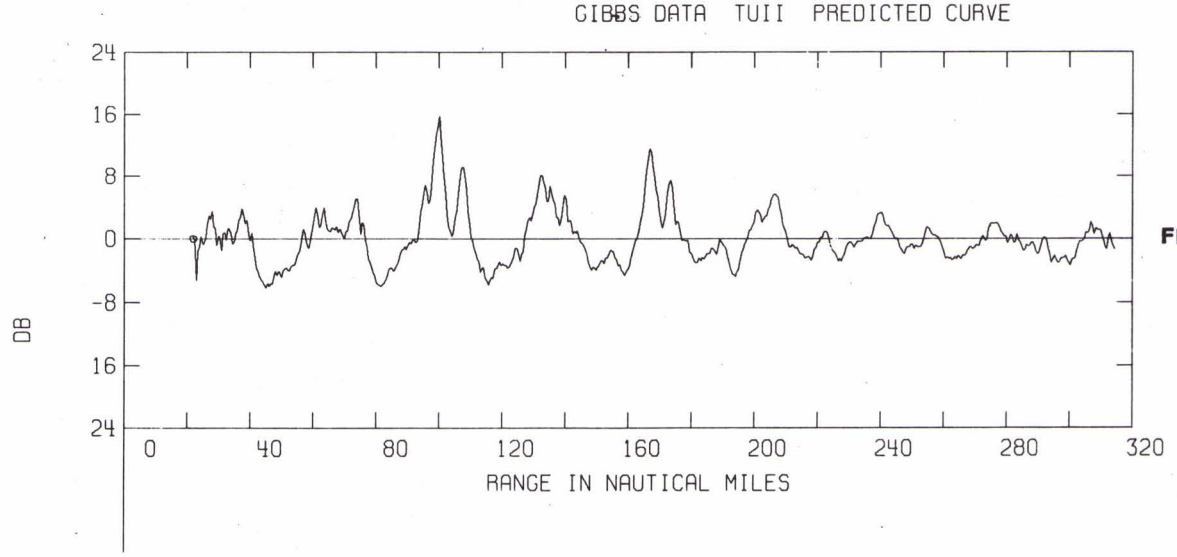

FIG. B.7c

Connection Between the Solutions of the Helmholtz and Parabolic Equations for Sound Propagation

John A DeSanto, Naval Research Laboratory,
Washington DC, and Admiralty Research Laboratory,
Teddington, England , U.K.

ABSTRACT

Using a conformal mapping technique in a rectangular waveguide, we present an exact integral relation between the solutions of the Helmholtz equation whose sound speed $c(x,y)$ varies as a function of both depth y and range x and the solutions of a parabolic equation whose sound speed varies in the mapped depth coordinate. The relation of the corresponding boundary value problems is also discussed, as well as the use of the parabolic approximation in underwater sound propagation problems. The conformal transformation interrelates the sound speeds of the two equations. Several examples are discussed. When $c(x,y) = c(y)$ is only a function of depth we get the recent result of Polyanskii. Other examples for a general conformal transformation are functions $c(x,y)$ which are sinusoidal in depth and exponentially decrease to a constant in range. Several alternative methods of using these results are also discussed.

INTRODUCTION

We wish to relate the solutions of the Helmholtz equation (an elliptic partial differential equation) to the solutions of a related parabolic partial differential equation for the problem of wave propagation in an inhomogeneous waveguide. Recently, Polyanskii[1] presented a short paper on this problem where the sound speed inhomogeneity was assumed to vary in only one direction, that of depth. A more general result is possible. In particular we present here, using a conformal mapping technique, an exact integral relation between the solution of a Helmholtz equation, ψ, whose sound speed $c(x,y)$ varies as a function of depth y and range x, and the solution of a corresponding parabolic equation, p, whose sound speed varies in the transformed depth coordinate. The method further clarifies the use of the parabolic approximation for underwater sound propagation problems.[2-4]

In Section 1 we present the notation and derive the exact integral relation between ψ and p. In Section 2 we show that, since p is separable, it is possible to derive a separable solution for ψ in the transformed coordinate, while relating the sound speeds for the elliptic and parabolic equations via the conformal map. The fact that ψ must satisfy a radiation condition yields a restriction on the available transformations. Hence ψ can be written in terms of parabolic eigenfunctions which depend on the transformed coordinates.

In Section 3 the use of the parabolic method as an approximation is studied using the integral relation and modal representation developed in Sections 1 and 2, and asymptotic properties of the Hankel function. Here, our main new conclusion is that for multi-mode propagation in cylindrical geometry the parabolic approximation can preserve at most one modal amplitude. The rest are scaled by an eigenfrequency-dependant factor. In

addition, because of the exact relation between ψ and p, a given incident field in the parabolic boundary value problem yields a different incident field in the elliptic problem.

Section 4 contains several examples, one of which is the result of Polyanskii[1]. It is possible to assume a general form for the conformal transformation compatible with the radiation condition, and a method is discussed for constructing the profile in terms of the transformation and vice versa. The examples include profiles which are sinusoidal in depth and exponentially decreasing to a constant in range.

Section 5 concludes with a discussion of several alternative methods of viewing the problem and using the results, and a summary.

1. RELATION BETWEEN ELLIPTIC AND PARABOLIC SOLUTIONS

The velocity potential $\psi(x,y)$ describing sound propagation satisfies the scalar Helmholtz equation (an elliptic partial differential equation[5])

$$\psi_{xx} + \psi_{yy} + K(x,y)\,\psi = 0 \tag{1}$$

in the waveguide region $x \geq 0$ and $0 \leq y \leq L$. Here $K(x,y) = [\omega / c(x,y)]^2$ where ω is the circular frequency of the sound and $c(x,y)$ its speed. See Fig. 1. Define the coordinate transformation

$$\xi = u(x,y)\ ,\ \eta = v(x,y) \tag{2}$$

and use the functional definition

$$\phi(\xi,\eta) = \psi(x,y). \tag{3}$$

If we assume that the transformation is conformal[6], then we can write it as ($z = x + iy$)

$$u + iv = f(z) \tag{4}$$

where u and v satisfy the Cauchy-Riemann conditions

$$u_x = v_y,\ u_y = -v_x. \tag{5}$$

Here $f(z)$ is a regular analytic function and $f'(z) \neq 0$ in the waveguide. Then ϕ satisfies the Helmholtz equation

$$\phi_{\xi\xi} + \phi_{\eta\eta} + K_2(\xi, \eta)\phi = 0 \tag{6}$$

where

$$K_2(\xi, \eta) = K(x,y)/\,|f'(z)|^2 \tag{7}$$

Next, assume the function $p(\xi,\eta)$ satisfies the parabolic partial differential equation[5]

$$\alpha p_{\xi} + p_{\eta\eta} + K_3(\eta)p = 0 \tag{8}$$

where α is a constant and K_3 is an arbitrary function of the transformed depth coordinate η. We wish to establish a relation between ϕ and p. If we assume the general form[1]

$$\phi(\xi, \eta) = C \exp[A(\xi)] \int_0^{\infty} p[g(t),\eta]\exp[B(\xi,t)]dt \tag{9}$$

where C is a constant, substitute (9) into (6) and integrate by parts using (8), then it is easy to show that (9) satisfies (6) provided we choose

$$A(\xi) = a\ \ln(\xi)\ , \tag{10}$$

$$B(\xi, t) = \beta\xi^2 t + (a - 3/2)\ln(t)\ , \tag{11}$$

$$g(t) = \alpha/4\beta t\ , \tag{12}$$

and

$$K_2(\xi, \eta) = K_3(\eta) + a(1-a)/\xi^2\ , \tag{13}$$

where β and a are constants. Here the surface terms resulting from the partial integration can be neglected.

Substituting (10), (11) and (12) into (9) and using (3) yields the integral relation

$$\psi(x,y) = C\,\xi^{a} \int_{0}^{\infty} p\left(\frac{\alpha}{4\beta t}, \eta\right) \exp(\beta\xi^{2}t)\, t^{a-3/2}\, dt \tag{14}$$

between ψ and p. For $\beta = i$ this can be viewed as a combined Mellin-Fourier-inversion transformation on the parabolic solution. Combining (7) and (13) yields the relation

$$K(x,y) = |f'(z)|^{2}\left[K_{3}(\eta) + a(1-a)/\xi^{2}\right] \tag{15}$$

between the sound speeds.

Thus we have a general exact integral relation between the elliptic and parabolic solutions given by (14), where their respective sound speeds are related using (15).

2. MODAL REPRESENTATION

The parabolic equation (8) is separable. We can write its solutions as

$$p(\xi,\eta) = \sum_{j=0}^{\infty} p_{j} N_{j}(\eta) \exp(-\lambda_{j}^{2}\,\xi/\alpha) \tag{16}$$

where the $\{p_j\}$ are constants (and can be determined from the known incident field) and where the eigenfunctions $N_j(\eta)$ satisfy, in the transformed depth coordinate, the ordinary differential equations

$$N_{j}''(\eta) + [K_{3}(\eta) - \lambda_{j}^{2}]\, N_{j}(\eta) = 0 \tag{17}$$

and boundary conditions which are discussed later.[7] The $\{\lambda_j\}$ are the discrete eigenvalues.[8] If we substitute (17) into (15) and use the integral representation[9]

$$\int_0^\infty \exp\,(it\rho^2 - \delta^2/4t)t^{-\nu-1}\,dt$$

$$= \pi i(2\rho/\delta)^\nu \exp(\pi i\nu/4)\, H_\nu^{(1)}\,(\delta\rho \exp\,(\pi i/4)) \tag{18}$$

where $H_\nu^{(1)}$ is the Hankel function of first kind and ν^{th} order, then, for $\beta = i$, ψ can be written as

$$\psi(x,y) = 0\pi i\, \xi^{1/2} \sum_{j=0}^{\infty}{}' p_j N_j(\eta)(\lambda_j/2i)^{a-1/2}\, H_{1/2-a}^{(1)}(\lambda_j\xi) \tag{19}$$

Hence (19) is a separable expansion for ψ in terms of the transformed coordinates ξ and η. In addition to satisfying boundary conditions at $x = 0$ and $y = 0$ and L, ψ must satisfy a radiation condition as $x \to \infty$ (this was the reason for the choice $\beta = i$). That is, each partial mode in (19) must behave like $\exp(ix\lambda_j)$ as $x \to \infty$. This holds if we use the asymptotic representation of the Hankel function and the requirement that as $x \to \infty$, $\xi \sim x$. This asymptotic restriction enables us to write the transformation as

$$f(z) = z + f_1(z) \tag{20}$$

where $f_1(z) \to 0$ as $z \to \infty$ in the waveguide, and, since the transformation is conformal, $f_1'(z) \neq -1$ also in the waveguide region. Unfortunately we can determine no more properties of the transformation simply and it is easiest to proceed by considering some examples. We do this in Section 4. First, however, we briefly consider the parabolic solution when it is used as an approximation.

3. PARABOLIC APPROXIMATION

For $\alpha = ik$ the parabolic solution (16) is

$$p(x,y) = p(\xi,\eta) = \sum_{j=0}^{\infty} p_j N_j(\eta) \exp(i \lambda_j^2 \xi/k) \tag{21}$$

This is used as an approximation to the asymptotic value of ψ which is, using the asymptotic representation of the Hankel function in (19)

$$\psi(x,y) \sim C(\pi i)^{1/2} \sum_{j=0}^{\infty} p_j (\lambda_j/2)^{a-1} N_j(\eta) \exp(i\lambda_j \xi) \tag{22}$$

comparison of (21) and (22) shows immediately that the parabolic approximation does <u>not</u> preserve the phase of the asymptotic elliptic solution. This is well known, as is the fact that the mode shapes <u>are</u> preserved by the approximation.[3,4] However, the question of the amplitudes of the modes is somewhat different. If $a = 1$, and the normalization constant C is chosen as $C = (\pi i)^{-1/2}$, then p preserves <u>all</u> the modal amplitudes of ψ. The case $a = 1$ is that of cartesian coordinates and is considered as Example 1 in the next section. For $a \neq 1$, all the modal amplitudes are <u>not</u> preserved by the approximation because of the λ_j factor in (22). It is possible to preserve <u>one</u> of them, say the m^{th} modal amplitude, by choosing $C = (\pi i)^{-1/2}(2/\lambda_m)^{a-1}$. Then all the remaining amplitudes will be scaled in the parabolic approximation by the factor $(\lambda_m/\lambda_j)^{a-1}$. For example, the case $a = 1/2$ is the case of cylindrical coordinates (see Ex. 2 in Sec. 4) which is most often used in sound propagation problems. Our conclusions on the preservation of the amplitude in the parabolic approximation for multi-mode propagation thus differ from the corresponding results in the literature.[10] For multi-mode propagation the parabolic approximation preserves all the amplitudes in cartesian coordinates, but can preserve at most one amplitude for cylindrical coordinates.

There is a further question having to do with the incident field. If we let $a = 1/2$ and choose cylindrical coordinates $(\xi = r, \eta = y)$, then the incident parabolic field which is known at say $r = 1$ can be used in (21) to determine the set $\{p_j\}$. Substituting $\{p_j\}$ into (19) and noting that (Ex. 2, Sec. 4) the cylindrical field in the elliptic problem is $r^{-\frac{1}{2}}\psi(r, y)$, we see that at $r = 1$, $\psi(1,y) \neq p(1,y)$. Again one point can be matched by proper choice of the constant C (which is thereby unavailable to match an asymptotic modal amplitude), but the incident fields and hence the corresponding boundary value problems are different for ψ and p. The two incident fields cannot be chosen independently.

From the exact relation (14) we thus conclude that for cylindrical coordinates the parabolic approximation in general doesn't preserve the amplitudes of the asymptotic elliptic solution, nor does it match the incident field.

4. EXAMPLES

In this section we present some examples of the exact formalism developed in Secs 1 and 2.

(Example 1)

Choose cartesian coordinates $\xi = x$ and $\eta = y$, then the transformation is $f(z) = z$. Then if $a = 1$, $\alpha = ik$, and $\beta = i$, (14), (15) and (19) yield

$$K(x,y) = K_3(y) \tag{23}$$

$$\psi(x,y) = Cx \int_0^\infty p\left(\frac{k}{4t}, y\right) \exp(ix^2 t)\, t^{-1/2}\, dt \tag{24}$$

$$= \sum_{j=0}^{\infty} P_j N_j(y) \exp(i\lambda_j x) \tag{25}$$

where $C = (\pi i)^{-1/2}$ in (25) and where we have used the definition[11]

$$H^{(1)}_{-1/2}(z) = (2/\pi z)^{1/2} \exp(iz) \tag{26}$$

This is the result of Polyanskii,[1] and by (23) only holds for sound speeds which vary in depth. Comparing (21) and (25) shows that the parabolic solution preserves all the modal amplitudes.

(Example 2)

Again choose cartesian coordinates $\xi = x$ and $\eta = y$ so that the transformation is $f(z) = z$. Let $a = 1/2$. Then (15) becomes

$$K(x,y) = K_3(y) + (4x^2)^{-1} . \tag{27}$$

If we relable $x \to r$, then the function Ψ defined by

$$\Psi(r,y) = r^{-1/2}\psi(r,y) \tag{28}$$

satisfies the Helmholtz equation in cylindrical coordinates

$$\Psi_{rr} + \frac{1}{r}\Psi_r + \Psi_{yy} + K_3(y)\Psi = 0 \tag{29}$$

Thus the term involving a in (15) is like a centrifugal barrier term in potential scattering theory.[12]

(Example 3)

More generally, choose the transformation

$$f(z) = z + f \exp(-\varepsilon z) \quad 0 < \varepsilon, f < 1 \tag{30}$$

with
$$\xi = \mathrm{Re}f(z) = x + f\cos(\varepsilon y)\exp(-\varepsilon x)$$
$$\eta = \mathrm{Im}f(z) = y - f\sin(\varepsilon y)\exp(-\varepsilon x) .$$

Further, let $a = 0$ and $K_3(\eta) = k^2$ where $k = \omega/c$ and c is an arbitrary sound speed used in the parabolic equation. Then (15) yields

$$K(x,y) = k^2\left\{1-2\varepsilon f\cos(\varepsilon y)\exp(-\varepsilon x) + (\varepsilon f)^2\exp(-2\varepsilon x)\right\}. \tag{31}$$

Since $K_3(\eta)$ is constant, the N_j eigenfunctions are by (17)

$$N_j(\eta) = D\sin(m_j\eta) + E\cos(m_j\eta) \tag{32}$$

where $m_j = (k^2 - \lambda_j^2)^{\frac{1}{2}}$. Further, assume the boundary value problem of a soft (Dirichlet) surface at $y = 0$, a hard (Neumann) bottom at $y = L$, and an arbitrary incident field at $x = 0$, i.e.,

$$\begin{aligned} \psi(x,0) &= 0 \\ \frac{\partial\psi}{\partial y}(x, L) &= 0 \\ \psi(0,y) &= \psi^{(0)}(y). \end{aligned} \tag{33}$$

and

Then since $\eta(x,0) = 0$ and $\eta(x,L) = L - f\sin(\varepsilon L)\exp(-\varepsilon x)$ the boundary conditions (33) are satisfied using (19) and (32) provided that

$$\begin{aligned} E &= 0 \\ \varepsilon &= \pi/L \\ \lambda_j &= \begin{cases} (k^2 - m_j^2)^{\frac{1}{2}} & k^2 \geq m_j^2 \\ +\, i(m_j^2 - k^2)^{\frac{1}{2}} & m_j^2 > k^2 \end{cases} \end{aligned} \tag{34}$$

and

where

$$m_j = (2j+1)\pi/2L.$$

The choice of λ_j is made to ensure that the outgoing radiation condition is fulfilled. Using (34) the parabolic boundary value problem is

$$\begin{aligned} p(\xi(x,0),0) &= 0 \\ \frac{\partial p}{\partial\eta}\,\xi(x,L),L) &= 0 \\ p(\xi,\eta)\Big|_{x=0} &= p(f\cos(\pi y/L),\ y - f\sin(\pi y/L)) = p^{(0)}(y) \end{aligned} \tag{35}$$

with $\xi(x,0)$ and $\xi(x,L)$ given by (30).

If we write (31) in terms of sound speeds using $K(x,y) = [\omega/c(x,y)]^2$ then we have

$$c(x,y)/c = \left\{ 1 - (2\pi f/L)\cos(\pi y/L)\exp(-\pi x/L) + (\pi f/L)^2 \exp(-2\pi x/L) \right\}^{-1/2}, \tag{36}$$

a one-parameter family of sound speed profiles which are sinusoidal in depth and exponentially decreasing in range. An example is given in Fig. 2.

Thus for the sound speed (36) the elliptic solution of (1), Ψ, can be expressed exactly by (14) as an integral over the solution of the simple parabolic boundary value problem (35), or as an exact modal expansion by (19) using the transformed eigenfunctions (32) (using (34)) and a set $\{p_j\}$ which can be found by point matching the incident parabolic field in (35).

(Example 4)

For a multi-parameter family of sound speeds choose the transformation

$$f(z) = z + \sum_{m=1}^{M} f_m \exp(-\varepsilon_m z) \tag{37}$$

where

$$\xi = x + \sum_{m=1}^{M} f_m \cos(\varepsilon_m y)\exp(-\varepsilon_m x)$$

and

$$\eta = y - \sum_{m=1}^{M} f_m \sin(\varepsilon_m y)\exp(-\varepsilon_m x).$$

If we again choose as in Ex. 3, $K_3(\eta) = k^2$, the eigenfunctions $N_j(\eta)$ are the same as (32) and the boundary value problem (33) is satisfied provided (34) and $\varepsilon_m = m\pi/L$ hold. The values of ξ and η at $y = 0$ and L and at $x = 0$ are found from (37). If $a = 0$, then (15) and (37) yield

$$K(x,y) = k^2\Big\{1 - 2\sum_{m=1}^{M}\varepsilon_m f_m \cos(\varepsilon_m y)\exp(-\varepsilon_m x) + \sum_{m=1}^{M}\sum_{n=1}^{M}\varepsilon_m\varepsilon_n f_m f_n \cos\left[(\varepsilon_m-\varepsilon_n)y\right]\exp\left[-(\varepsilon_m+\varepsilon_m)x\right]\Big\} \tag{38}$$

which is an M-parameter family of curves. Each additional term in the sum in (37) introduces an additional turning point in the sound speed curve. Example 3 with $M = 1$ had no turning points. For $M = 2$, (38) written in terms of sound speeds is

$$\begin{aligned} c(x,y)/c = \Big\{ & 1 + (\pi f_1/L)^2 \exp(-2\pi x/L) \\ & + (2\pi f_2/L)^2 \exp(-4\pi x/L) \\ & - (2\pi f_1/L)\big(1 - [2\pi f_2/L]\exp(-2\pi x/L)\big) \cdot \\ & \cdot\cos(\pi y/L)\exp(-\pi x/L) \\ & - (4\pi f_2/L)\cos(2\pi y/L)\exp(-2\pi x/L)\Big\}^{-\frac{1}{2}}, \end{aligned} \tag{39}$$

an example of which is plotted in Fig. 3. Note the fact that the sound speeds have one turning point. By multiplying $[c/c(x,y)]^2$ by $\cos(m\pi y/L)$ for $m = 1,2$ and then integrating over y from 0 to L it is possible to solve for f_1 and f_2 and fit them to various ranges.

Again, for the sound speed (39), Ψ is either an exact integral relation (14) or an exact modal representation (19) over terms associated with the parabolic boundary value problem defined above.

(Example 5)

Some additional examples of other transformations which can be used are, from (20)

$$f_1(z) = \sum_{m=1}^{M} g_m(z)\exp(-\varepsilon_m z) \tag{40}$$

where the $g_m(z)$ can be finite polynomials (splines), oscillatory functions, etc. Indeed f_1 can be even more general. So long as $f_1(z)$ has no singularities in the waveguide, and vanishes as $z \to \infty$ in the waveguide, it can be quite arbitrary. This admits ratios of polynomials (Padé approximants) as well as functions with more complicated singularities outside the waveguide. Some of these examples are presently being pursued.

5. SUMMARY

There are several alternative ways to view the results in this paper. Firstly, one could take as the central issue the conformal transformation. By choosing various transformations one could construct a library of available profiles including those generated using more complicated profiles in the parabolic equation, those involving centrifugal barrier terms, and those involving more complicated transformation functions. Solution of the resulting parabolic boundary value problem in the transformation distorted waveguide (as in Eqs 3 and 4) and either continuous (Eq 14) or discrete (Eq 19) quadrature yield the solution of the full elliptic problem for the various profiles. The numerical solution of the parabolic boundary value problem can be accomplished quickly by using a marching algorithm in range (although this is complicated by the distortion of the waveguide) whereas the elliptic equation requires a much more involved and time consuming numerical discretization over a closed boundary.

Secondly, one could consider the solution of the parabolic equation as central and numerically solve the simplest non-trivial parabolic boundary value problem available. This will then lead to the transformation.

Finally, the profile may be regarded as fundamental. In particular, $K(x,y)$ may be given as a discrete set of points and the conformal transformation is constructed by fitting these points. The transformation then yields the parabolic boundary value problem, etc. These three interpretations

of the ways to utilize the above results are, of course, intimately connected.

Thus we have presented an exact relation between the solution of the Helmholtz equation whose sound speed varies in both depth and range and the solution of a parabolic boundary value problem with sound speed varying in a conformally transformed depth coordinate. The relation can be expressed either as a Fourier-Mellin-inversion transformation or as a discrete modal sum. The sound speeds in both equations are themselves related via the conformal transformation. Several examples were presented, among them profiles which change sinusoidally in depth and decrease exponentially to a constant in range. When viewed as an approximation the parabolic method was found to preserve at most one of the modal amplitudes in a multi-mode propagation problem in cylindrical coordinates and, because of the exact relation between the two solutions their respective incident fields could not be independently chosen to be equal.

Footnotes

* Temporary Address

1. E. A. Polyanskii, Sov. Phys. Acoust. 20, 90 (1974)
2. See the article by F. Tappert and R. Hardin in "A Synopsis of the AESD Workshop on Acoustic-Propagation Modelling By Non-Ray Tracing Techniques", ed. by C. W. Spofford, AESD Tech. Note TN 73-05 (Nov. 1973) (Acoustic Environmental Support Detachment, Office of Naval Research, Arlington, Virginia).
3. S. T. McDaniel, J. Acoust. Soc. Am. 57, 307 (1975)
4. R. M. Fitzgerald, J. Acoust. Soc. Am. 57, 839 (1975)
5. P. R. Garabedian, "Partial Differential Equations", Wiley, New York (1964)
6. E. T. Copson, "Theory of Functions of a Complex Variable", Oxford University Press (1944), p.180
7. Usually in these problems $\alpha = ik$, where k is some average wave-number and $K_3(\eta) = k^2 K_4(\eta)$ where $K_4(\eta)$ is dimensionless. See Refs 2-4. We make these assumptions explicit later.
8. We are restricting the boundary value problem to one with a purely discrete spectrum for convenience only. Extension to a continuous spectrum is straightforward. To satisfy the radiation condition on ψ the λ_j are either positive real or positive imaginary. See Ex. 3 in Sec. 4.
9. Bateman Manuscript Project, "Tables of Integral Transforms, vol I", ed. by A. Erdelyi, McGraw-Hill, New York (1954), pg 16, no. 20 and pg 75, no. 31.
10. In Ref. 3, Eqs (11) and (12) are used as the iterative algorithms for a single mode propagating via the parabolic and elliptic equations respectively. If this single mode starts with the same aplitude for both parabolic and elliptic cases it will end up with the same amplitude. The same results are found in Ref. 4. For a single mode, as we indicated, this is always possible. But for the case of multi-mode propagation,

amplitude changes will occur. The authors of both references use in their respective multi-mode examples the fact that all the amplitudes are preserved by the approximation. They conclude this by neglecting the subtle effect the centrifugal barrier term $(4r^2)^{-1}$ has on the asymptotic amplitude (through the λ_j factor) effectively reducing their problems to cartesian coordinates where, as we indicated, all the amplitudes are preserved.

11. W. Magnus, F. Oberhettinger, "Functions of Mathematical Physics", Chelsea, New York (1949).

12. V. De Alfaro, T. Regge, "Potential Scattering", Wiley, New York (1965).

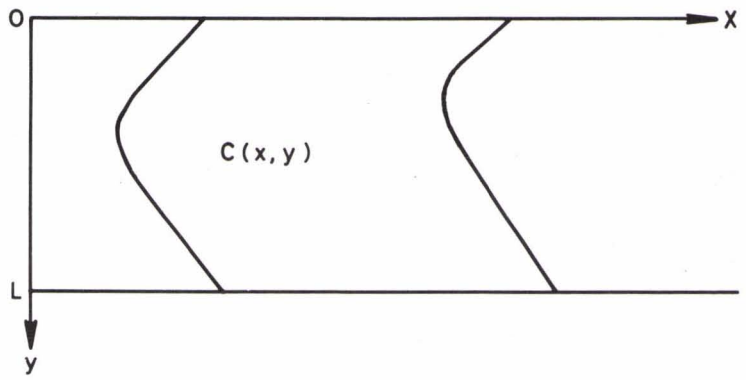

FIG. 1 THE WAVEGUIDE REGION IN WHICH WE SOLVE THE ORIGINAL ELLIPTIC (HELMHOLTZ) EQUATION FOR SOUND PROPAGATION. WE CONSTRUCT EXAMPLES OF SOLVABLE SOUND SPEEDS $c(x, y)$ DEPENDING ON BOTH RANGE x AND DEPTH y.

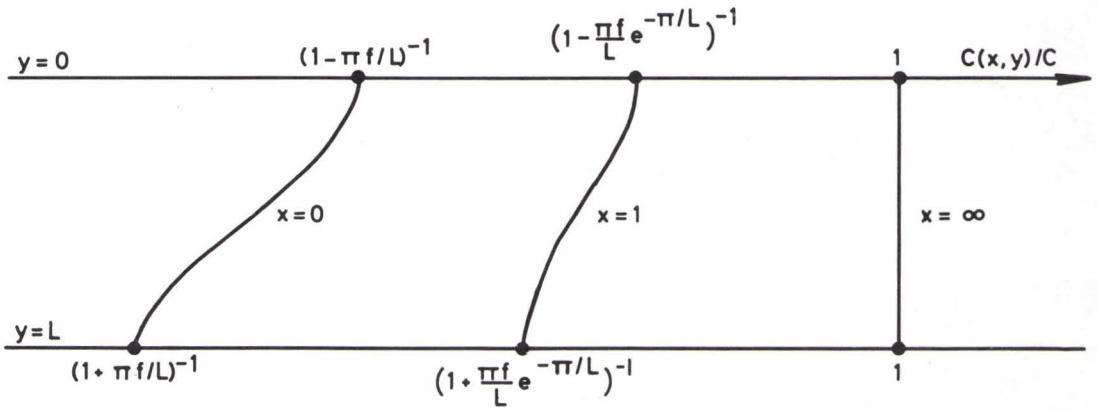

FIG. 2 AN EXAMPLE OF A 1-PARAMETER FAMILY OF SOUND SPEED PROFILES FOR WHICH THE ELLIPTIC EQUATION (1) IS EXACTLY SOLVABLE. THEY ARE SINUSOIDAL IN DEPTH, EXPONENTIALLY DECREASING IN RANGE, AND HAVE NO TURNING POINTS. THE FIGURE REFERS TO EXAMPLE 3 IN SEC. 4.

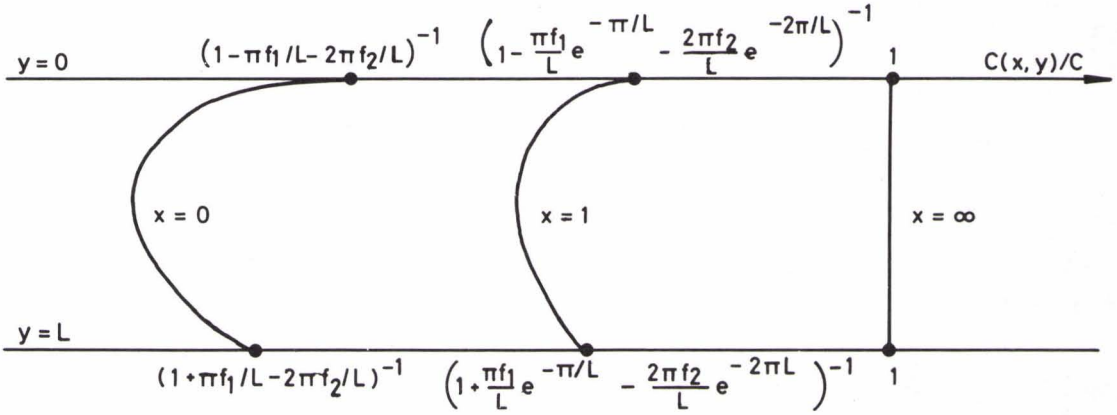

FIG. 3 AN EXAMPLE OF A 2-PARAMETER FAMILY OF SOUND SPEED PROFILES FOR WHICH THE ELLIPTIC EQUATION (1) IS EXACTLY SOLVABLE. THEY ARE SINUSOIDAL IN DEPTH, EXPONENTIALLY DECREASING IN RANGE, AND HAVE ONE TURNING POINT. THE FIGURE REFERS TO EXAMPLE 4 IN SEC. 4.

REVIEW PAPERS

COMPUTER MODELS FOR UNDERWATER SOUND PROPAGATION

F.R. DiNapoli

Naval Underwater Systems Center
New London Laboratory
New London, Connecticut 06320

ABSTRACT

The state of affairs of computer models for underwater sound propagation loss estimation is discussed from the viewpoints of two segments of the sonar community; i.e., (1) those who develop the models and are primarily concerned with the accuracy of the estimations and (2) those who use such models and view propagation loss as only one of many areas in which sub-models are required. A list of propagation models, classified according to the analytical methods used in their derivations, is presented. The features and shortcomings of each class are then discussed in broad terms. Various sonar applications for which knowledge of propagation loss is needed are briefly delineated to indicate their diversity. Also, a number of practical considerations (in addition to accuracy) are listed that influence the user's selection of a propagation loss model for a particular application. Finally, various aspects of model assessment are addressed and a method for the quantitative assessment of comparative model accuracy (now in formative stages of development) is presented. The use of this methodology is discussed through illustrative examples.

COMPUTER MODELS OF UNDERWATER SOUND PROPAGATION

During the process of writing this paper recollections of a book by the American psychologist Lawrence LeShan, entitled The Medium, Mystic, and the Physicist (the cover of which is presented in figure 1), came to mind and it seemed that this would perhaps be an appropriate subtitle for my paper. I am positive that certain segments of the sonar community look upon the developers of models for underwater sound as being the most outrageous perpetrators of mysticism ever encountered. There are still others who believe that confronting the model developer with a very straightforward question about his work evokes about the same response one would obtain from a medium if he were asked where his information comes from. Of course, the model developers believe that the situation is the reverse, i.e., in their dealings with the rest of the sonar community they feel they have somehow had a mystical experience.

Clearly, this situation has something to do with the various connotations of the term "reality." LeShan observed that serious mystics and modern theoretical physicists seem to have a common understanding of reality. To prove his point he asks the reader to determine whether statements summarizing viewpoints of reality were written by physicists or mystics. Figure 2 contains a few of those quotations with the name of the originator and the letter P or M to indicate whether he is a physicist or mystic.

After reading all of the quotations supplied by LeShan, I came to agree with his contention that there is a general consensus among mystics and physicists regarding the perception of reality. Although this point is interesting in its own right, especially in view of the diverse fields involved, I use the term

reality in this paper because it is my contention that different segments of the sonar community have (at a minimum) different interpretations of reality. This appears on the surface to be a rather obvious point. However, it is often overlooked by all concerned parties in the conduct of their daily business and a fair amount of confusion results. Perhaps not so obvious is why this fact is overlooked. I will expand on this theme as the paper develops by delineating two perceptions of reality currently popular in the U.S. It is hoped that this discussion will help the reader understand the reason for the confused state of affairs.

Up to this point I have spoken rather vaguely about various sectors of the sonar community. The remainder of the paper will deal with computer models of underwater sound and with reality in terms of the two types of sonar scientists and engineers identified in Figure 3.

To the left of the figure are those scientists and engineers who are actually engaged in the development of models. There are at least two types of models that can be discussed. The first consists of models for the individual terms in the sonar equation such as propagation loss, ambient noise, reverberation, etc., which might properly be termed sub-models. The second emphasizes sonar analysis and is concerned with combining the sub-model accounting for medium induced effects and sub-models for the system related terms in the sonar equation to form a total sonar systems model; henceforth, this will be referred to as the generic model. A distinguishing feature of this effort is that the type of funding that usually supports it is identified as research or exploratory development.

The group at the right of figure 3 might be called the model users or customers. (In some instances they may describe themselves as the reluctant model users.) It is not uncommon to find the sonar analyst previously identified also operating in this sphere. These people are usually involved in system analysis, performance prediction, and system design. The funding for their work is usually associated with advanced development and engineering. Whereas the perception of reality for the group to the left revolves around predictions or estimations, reality for the users is governed by applications. In both instances the actual understanding of reality has many aspects that are usually not precisely defined.

Since the model is common to both groups, it ostensibly emerges as the bridge connecting two historically distinct and separate groups within the sonar community. Recent experience in the U.S. suggests that although the concept appears to be sound, the bridge is far from complete (see figure 4).

One reason for this situation is that a generic model for mobile sonar systems does not currently exist. A major difficulty involved in constructing such a model is designing a computer architecture flexible enough to accommodate the different and often conflicting understandings of reality by the two groups. I will have more to say on this subject later. Finally, there is the difficult problem of assessment. Given that a generic model could be constructed and that the developer and user have reached a common understanding of what constitutes reality, the question remains as to whether the model predictions bear any resemblance to the accepted concept of reality. Toward the end of this paper I will discuss our current thinking on the subject of model assessment.

I would now like to address the subject of computer sub-models of underwater sound phenomena from the standpoint of the model developer. I should first explain that the compilation shown in figure 5 is not meant to be comprehensive but, instead indicative of the different types of propagation models existing in the U.S. sonar community classified according to the analytical methods used in their derivations. I will discuss the features and shortcomings of the models in rather general terms, according to class; to do otherwise would require examination of each model separately. Such an examination is best done by the model developer himself but, unfortunately, model documentation rarely contains statements about shortcomings. (The reason for this should become evident as we proceed.) Thus, a general approach to the subject may be the best that can be achieved at this time.

I have begun the compilation with the semi-empirical/semi-analytical class because they are significantly different from the other models on the list. A common characteristic of this class is that the models result from an attempt to fit, or explain, a rather broad base of experimental data. The perception of reality is then intimately related to the scope and quality of the experimental data set. In most cases this constitutes a rather limited outlook on underwater acoustics. The AMOS experiment, for example, consisted of approximately 100,000 data points obtained at various locations in the Atlantic, but the primary subject of investigation was surface duct propagation. The COLOSSUS II experiment was primarily intended to examine shallow water acoustics. This type of model development has, for the most part, disappeared for two reasons, one economical and one technical. The cost of conducting large scale experimental programs such as AMOS or COLOSSUS today is prohibitive. Moreover, advances in computer technology have made it possible to obtain detailed results for specific

environmental situations that appear to be more attractive to both the user and the model developer.

A summary of the main features and shortcomings of these models is provided in figure 6. Although limited in scope, they generally have the attribute that answers can be obtained in an extremely short (computer) time. For some applications this feature is of paramount importance, eclipsing even the need for accuracy. The equations involved are generally very simple expressions involving terms that have a semi-analytical flavor, such as the expression labeled $G(Z_t, Z_x)$, and terms that have an empirical flavor, such as the attenuation coefficient α .

The shortcomings stem from the intrinsic natures of the models. One expects to find a large variance between the model predictions and data from any single experimental run because the model is an attempt to summarize data obtained from many runs involving different environmental conditions. One should also expect the applicability of the models to be governed by the range of the parameters associated with the experimental data set. If one found agreement between AMOS predictions and surface duct data at 1000 Hz, it would be a fortuitous occurrence.

Another natural shortcoming is the inability to predict the detailed features of propagation loss as illustrated in figures 7 and 8. In both cases the experimental source was located at a depth of 20 ft and emitted CW pulses centered at 3.125 kHz. The receiver depth for figure 7 was 50 ft; i.e., both source and receiver were located in the surface duct. Although the AMOS prediction seems to adequately portray the mean level of the data, it gives no

indication of the rather definitive interference structure exhibited in the data. The results shown in figure 8 represent a cross-layer case with the source in the duct and the receiver well below the duct. The agreement in this case is generally quite poor even in mean level and using the AMOS results to obtain an estimate for the detection range would be judged unsatisfactory.

This is an appropriate time to mention that I have arrived at the shortcomings of this class of models (and those that will be discussed shortly) from the viewpoint that the primary interest of the sub-model developer is to produce accurate answers. If the primary interest is not accuracy, as might well be for the model user, the entries on this list would be considerably different.

The understanding of reality for the remaining classes of propagation models would appear to be the result of a compromise between what the modeler would like to achieve (namely, the ability to produce accurate answers for propagation loss) and what the state-of-the-art of mathematics and computer technology will allow him to accomplish. The basis for all of the remaining classes is not experimental data but rather the wave equation shown in figure 9. Of course, this equation and the associated boundary conditions also represent a limited scope of reality. That is, this equation represents a linearized version of the fundamental equations, which assume the transmission of energy is a purely deterministic process. Also, it is assumed that the source of energy is concentrated at a single point in space and continuously puts energy into the medium. Lastly, the sound speed profile is assumed to vary only with depth and the boundaries are taken to be horizontal and smooth. Although these assumptions appear to be restrictive, in some cases they are only the beginning

of what appears to some to be a never-ending list.

The first of these modifications involves the class of models which I have termed "ray theory with corrections" (figure 10). One may look upon this class of models as an approximate solution for the wave equation, the accuracy of which increases with increasing frequency. It is difficult, however, to state beforehand under precisely what conditions the solution will break down. The practice usually followed at the Naval Underwater Systems Center (NUSC) is to compare the results of a ray and non-ray model for the same case. If agreement is found we are then fairly confident in proceeding to obtain additional ray theory predictions. Recently, significant advancements have been made in automating corrections to the ray theory solution for known artifacts stemming from the nature of the approximate solution. This work involves correcting the solution in the vicinity of caustics. In particular, we have Keller's geometrical theory of diffraction (asymptotic ray theory), the various modified ray theories, and generalized ray theory. Each of these extensions has its own virtues and limitations. For example, the various modified ray theories attempt to make ray theory valid at caustics but each caustic correction seems to be different. The FACT model uses the non-uniform Brekhovskikh caustic correction for smooth caustics while the NISSM II program applies the uniform Ludwig correction. When these corrections are compared against wave theory results, for which caustic corrections are not required, the results are favorable in some cases but not all. In addition to the Brekhovskikh and Ludwig corrections there is the Davis extended modified ray theory and the corrections made by Levey and Felsen in terms of incomplete Airy functions.

In spite of such progress, the use of ray theory in a surface duct, in shallow water, and at low frequencies generally remains a method of dubious accuracy. Another area of concern is the use of ray theory when interaction with the sub-bottom is of significance. This is a relatively new application in underwater acoustics but an old concern for the seismic community. They have made considerable progress in extending ray theory for this application. However, as Cerveny and Ravindra point out in their book, entitled "Theory of Seismic Head Waves," the extensions are not generally applicable when interference effects become important as in thin layers of thicknesses less than, or comparable to, the wavelength.

Thus, it would seem that additional modifications will be required for future applications. It is also clear that a user is likely to have difficulty in interpreting the meaning of these mathematical expressions in terms of classical ray theory.

In spite of the inherent uncertainties concerning its validity, ray theory is widely used and in many instances preferred over other types of solutions; this is not likely to change in the near future. One reason is that the ray diagram can be easily interpreted in a gross fashion to indicate where high or low intensity regions are likely to be found. Furthermore, the ability to provide the user with information about the effects of directivity, surface loss, reverberation, and the like, seem more easily dealt with in terms of ray theory than by wave related solutions. Considerable progress has also been made in reducing the computing time needed to make ray theory predictions. In this regard, the FACT program is quite remarkable. The primary motivation behind the development of the NISSM II model was not speed but to provide the user with

predictions for boundary and volume reverberation, signal to noise ratios, and probability of detection in addition to propagation loss values. As such, it is a limited version of a generic model for surface ship sonars.

Let me now summarize the features and shortcomings of this model class (figure 11). One of the reasons for the popularity of ray theory is that the ray diagram itself is a conceptually appealing link between the mathematics involved and the final plot of propagation loss versus range, which can be appreciated by almost every segment of the sonar community.

Another important feature is the ability to routinely provide more information than merely propagation loss to a point receiver. Information about travel time, angle of arrival, reverberation and ambient noise levels, beamformer output, etc., is viewed as essential by many users. The relative speed with which modern ray theory programs provide answers is an important feature for many applications.

The major disadvantage of ray theory is that it is difficult to precisely determine when it should not be used because of invalid results. Caution should be used in applications to shallow water, surface ducts and low frequencies in general and, especially, in cases where sub-bottom interaction may be significant. The need for corrections then follows naturally and the second item results rather naturally from the first. Corrections have been implemented for two and three ray system caustic formations. However, modifications to account for such things as the lateral wave phenomenon need to be implemented.

The perception of reality for the third class of models (see figure 12) is based upon the assumption that the solution for the wave equation can be adequately represented in terms of normal mode theory. The solution is described mathematically in terms of eigenvalues where the eigenvalue spectrum is composed of possible complex, but strictly discrete, eigenvalues. Herein is the first modification this class imposes in terms of reality because the solution to the wave equation (in terms of eigenvalues) generally has both a discrete and a continuous spectrum. Proponents of this type of solution would argue that the contribution from the continuous portion of the spectrum is of nugatory significance. For some applications this is true, but it is generally not true for all mobile sonar applications. As was the case with ray theory, it is difficult to ascertain a priori the significance of the error incurred by neglecting the continuous portion of the spectrum. Therefore, when these programs are routinely run, it can only be hoped that the error will be insignificant.

There is a practical problem involving the numerical location of the discrete eigenvalues common to all general purpose normal mode programs. For some combination of water depth and frequency, the numerical scheme for determining the location of the eigenvalues in the complex wave number space will eventually break down. It is difficult to ascertain precisely when this breakdown will occur without first running the program for the specific case under consideration. Thus, there is a difficulty in determining the high frequency limit to which normal mode calculations can be confidently used.

Once these questions have been dealt with, the solution is essentially complete except for the number of modes to be included in the final summation. This decision is somewhat analogous to choosing the angular sector examined in

ray theory. Pedersen and Bartberger have examined the question of which modes are of importance for specific cases and have provided significant insight. However, a great advantage of normal mode theory is that once the significant eigenvalues have been determined, the solutions for any source and receiver combination can be easily obtained. One would like to know the total number of eigenvalues that must be located to satisfy all possible source and receiver combinations of interest. Various rules of thumb exist, e.g., Gordon suggests that the maximum mode number is approximately 1-1/2 times the frequency. Williams suggests that for shallow water the rule of thumb is H/λ, where H is the water depth and λ the wavelength.

In the final analysis, however, the procedure that is most often used is to run the program for a given number of different modes and examine the behavior of the solution as more modes are added. The same would be true in ray theory calculations when trying to determine both the angular sector of rays to be traced and the angular difference between rays. There are parameters similar to these associated with every model; they lack precise definition and make the complete automation of general purpose propagation models a very intricate and complex process. From the users' standpoint, the degree to which a model can be automated by a non-expert is an important concern.

Generally speaking normal mode programs can be broken into two sub-classes depending upon the manner in which the depth-dependent wave equation is solved. One technique is to assume that the ocean is stratified with depth and that within each stratum the sound speed varies in a predetermined fashion. In this case the solution to the depth-dependent wave equation within each stratum will be given in terms of one of the special functions of mathematical physics.

Satisfaction of the continuity of impedance condition at each interface can then be expressed in terms of equations that cascade the known impedance condition at the surface and at the last boundary to the layer in which the source is located. The dispersion equation, or the Wronskian (if Green's function terminology is preferred) results from trying to satisfy the source conditions. There are then two distinct possibilities for the source and receiver locations. Either they are located in the same layer or the receiver is located in a layer that lies below the source. The second alternative approach is to make a guess at the value for the eigenvalue and then numerically integrate the depth dependent wave equation to determine if the boundary conditions are satisfied. Problems related to the numerical convergence of the solution are encountered in both approaches.

Further modifications to the normal mode reality are sometimes made as by Kanabis, Ingenito, and others. They assume that the only significant modes are those whose associated eigenvalues are purely real. This assumption reduces both the required computing time and the applicability of the solution. The advantages and shortcomings of this class of models are summarized in figure 13.

Once one is satisfied that the continuous spectrum can be neglected and that the numerical calculations are stable and accurate, the job is essentially complete and confidence in the results is extremely high. Unlike ray theory, the intermediate steps leading to the final mode summation provide little insight except to those who have labored over normal mode theory for some time. As was the case with ray theory, it is difficult to say in advance precisely when the solution will not be applicable. Finally, information other than propagation loss is difficult to obtain and not usually provided.

I have called the fourth class of models "total field representations" because they come the closest to solving for the initial understanding of reality expressed in terms of the wave equation for an ocean having a single sound speed profile and flat bottom. An equivalent representation for this reality statement is the integral expression for the pressure field shown in figure 14.

The models of Kutschale and Stickler represent solutions obtained in terms of eigenvalues that include contributions from both the continuous and discrete portions of the spectrum. Kutschale was the first investigator to develop a general model having this capability and it should be noted that the inclusion of the continuous spectrum was viewed as a necessity for his work at very low frequencies in polar or arctic type environments. Another feature of his model is that his strata need not be perfect fluids. This was also necessary to explain propagation in the presence of an ice cover and through the sub-bottom at seismic frequencies. His assumption that the sound speed within each stratum is constant appears to be perfectly adequate at these frequencies. Stickler's model is an all fluid model for which the reciprocal of the square of the sound speed varies linearly with depth within each stratum. Since both of these programs are essentially eigenvalue solutions one should expect them to have the same shortcomings mentioned for the normal mode class, i.e., for some combination of water depth and frequency, problems of numerical accuracy and convergence will be encountered.

The Fast Field Program on the other hand is <u>not</u> an eigenvalue solution but, quite simply, a direct numerical evaluation of the field integral which makes use of the Fast Fourier Transform algorithm. In order to arrive at this point,

the single modification to reality that must be introduced (figure 15) is that the Hankel function can be adequately represented in terms of its asymptotic expansion. If this approximation is looked at in isolation, one expects to encounter difficulties at very low frequencies and very close ranges. We have examined such cases, however, and have not been able to detect any significant error. The explanation is perhaps that the approximation should not be examined in isolation but rather as it effects the integration process.

The fact that the FFP is not an eigenvalue solution is an important distinction; we believe this is the reason it provides accurate answers for any combination of frequency and water depth of interest for mobile sonar applications. We have examined the FFP solution for frequencies as low as 1 Hz to as high as 100 kHz and intermediate frequencies as well. Results for a few of the case studies conducted since 1968 that have convinced us of the general applicability of the FFP will be discussed below.

The results shown in figure 16 provide an indication of the error that can be incurred by neglecting the continuous portion of the eigenvalue spectrum. The profile was taken from the Iberian Basin in a water depth of approximately 18,000 ft. The source and receiver were located in a subsurface channel overlaying a second channel at a deeper depth; three results are shown. The line connecting the open circles with dots enclosed and labeled "ARL discrete alone" represent Stickler's results when he neglects the continuous spectrum. The line connecting the open rectangles represent his results when the contribution from the continuous spectrum is added to the normal mode summation. Finally, the line connecting the circles that are filled in are the FFP results for the total field. The neglect of the continuous spectrum results in a substantial error

for ranges less than 3 nmi. It is clear that applications exist for which the neglect of the continuous portion of the spectrum could hardly be thought of as a minor concern.

Figure 17 shows the comparison between the FFP predictions and data obtained from an active sonar system operating in the Mediterranean Sea. The agreement within the convergence zone is quite good. This is not the case, however, in the bottom bounce region before the zone. The reason for this is a lack of precise knowledge concerning the bottom loss at this location. The disagreement along the trailing edge of the zone, especially for the deeper hydrophones, is somewhat more difficult to explain. One possibility is that we are comparing the results of two dissimilar sources. The predictions are for an infinite CW omnidirectional source, whereas the experimental data source was directional and emitting LFM pulses. This line of discussion is somewhat premature because such questions are more precisely treated under the heading of assessment. However, it should be noted for future reference that the process of overplotting either predictions from various models or predictions with experimental data and arriving at a subjective conclusion regarding the agreement is a common methodology for assessing the accuracy of model predictions.

The features and shortcomings of the FFP are summarized in figure 18. The FFP is unique in that it is applicable for any combination of frequency and water depth. For this reason, various model developers have found it useful to employ the FFP as a bench mark program when they are testing new models or making improvements to older ones. Physical interpretations or the ability to gain insight are difficult with the FFP because it provides the answer for the total field. The only intermediate information that can be provided is a

plot of the absolute magnitude of the kernel of the field integral. The user very often would like to partition the total field in various ways depending on his need. This is possible with the aid of the plot of the kernel but many questions remain about exactly what interpretation should be associated with this partitioning. For this reason, and others, the ability to provide user oriented information about reverberation, ambient noise, surface loss, and the like, appears feasible but it has not been worked out.

Reality for all of the models discussed to this point consisted of an ocean having a flat bottom and a sound speed profile that did not change with range. Since this assumption pertains to the acoustics and not the actual environment of the ocean, it is often difficult to determine beforehand when the assumption will be no longer valid. The measured sound speed profiles and bottom bathymetry for an experimental track from Bermuda to the mid-Atlantic ridge are shown in the upper portion of figure 19. The acoustic data for the case of both source and receiver in the deep sound channel is at the lower left of the figure. A reasonable fit to these data is obtained using an expression that has a 10 log r dependence, implying that predictions from the previously mentioned models would provide reasonable agreement. To the right, however, are the data obtained using a near-surface source and a deep receiver. It is apparent that a single cylindrical spreading model fails to agree with the data over the entire range. The source was located in a surface duct that extended down to approximately 1500 ft near the receiver and gradually decreased in depth as the range increased. It is suspected that this is the cause for the non-cylindrical spreading loss behavior of the data.

A considerable amount of data similar to these now exists that suggests that, for some applications, the single profile, flat bottom perception of reality must be modified. In the past few years considerable progress has been made in implementing solutions that accommodate this modification. The models identified in figure 20 are based on normal mode theory, a combination of mode and ray theory, and straightforward numerical techniques. For the normal-mode approach the ocean is usually laterally sub-divided into uniform segments and the normal modes for each segment are found. There are two major points of difficulty using this approach. The first is to properly account for the coupling of energy from one segment to the next, including the possibility that some energy will travel back toward the source. The second involves the treatment of the boundary condition when the ocean bottom interface is not horizontal. In order to arrive at a solution, various approximations must be made, the validity of which is difficult to determine mathematically. One can resort to comparisons with experimental data. However, this is often not a totally satisfying process because of the lack of completeness of the associated environmental data. More directly, agreement with the data can usually be achieved if adjustments are made to model and experimental data parameters, the values of which have not been determined. Although good comparisons with experimental data are encouraging, more is often learned about the model from cases where agreement is poor. Unfortunately, these cases are very seldom widely publicized.

It is a bit early to arrive at a meaningful list of advantages and shortcomings for this class of models since development work is still in progress. Therefore, a few observations of only a general nature would be appropriate. Most of the current effort seems to be devoted to accounting

for acoustic effects caused by the range dependence in the environmental parameters of the water column. This is a natural development considering the types of data available. We believe that applications may soon be apparent for which range dependence of the sound speed and density profiles within the bottom, and the non-parallel nature of the boundaries separating different sub-bottom layers, will be more significant than the range dependence of the corresponding environmental parameters of the water column alone.

Other classes of models exist (figure 21) but time constraints prevent discussing them in detail. It is worthwhile to mention them however. For instance, there is a class of models that, in one way or another, use a combination of wave and ray theory. The mathematics involved is usually, but not always, centered around expanding the kernel for the field integral in terms of an infinite series of integrals that correspond to various types of multiple reflections. This technique dates back at least to Pekeris and Haskell.

There has also been recent interest in predicting the received pressure waveform as opposed to the usual prediction for the energy of a CW signal. General purpose programs have been developed based on both the FFP technique and normal-mode theory.

If by this time the reader is somewhat bewildered at the vast number and types of propagation models, then he is in the proper frame of mind for the remainder of this paper.

So far, the basis of reality as discussed herein has involved strictly the question of accuracy for one sub-model, namely propagation loss. To the sonar

analyst interested in developing a generic model (figure 3), this represents just one of many concerns. Thus, he may view the discussion about the relative merits of one propagation model over another as being somewhat esoteric. To provide an understanding for this attitude computer models of underwater sound from the sonar analysis viewpoint will now be discussed. In doing so, it is useful to paraphrase discussions held by the Panel On Sonar Standard Models (POSSM), which is a multi-laboratory effort founded by the Naval Sea Systems Command (NAVSEA) (Code 06H1). NAVSEA was concerned about the confusion expressed by users concerning the proliferation of models and chartered POSSM to make recommendations concerning model usage for NAVSEA programs. The membership of the panel was equally divided between those interested in developing sub-models and sonar analysts in the hope that a common reality would emerge.

The sonar analysts believed that although models for propagation loss could be found in abundance, sub-models for other terms in the sonar equation were, in some cases, nonexistent or at best represented very gross estimates. In order to provide the remainder of the panel with a glimpse of their version of reality the table shown in figure 22, listing the essential ingredients of a generic model, was constructed.

The potential applications for such a model are listed at the left. It was felt that, at a minimum, the sonar analysts needed the capability to conduct performance prediction calculations for both passive and active mobile sonars. The next higher-order use would involve engagement studies employing several platforms. Finally, they would like to conduct statistical analyses of a number of engagement or single platform studies to quantify the merits of new concepts in sonar design. To meet this goal, objective information is required

for the medium and system related quantities shown in the columns to the right. The most comprehensive sub-models listed in the fourth column pertain to the signal, noise, and reverberation fields as well as the target model. To adequately model these terms other sub-models, listed in the next column to the right, are required. This dependence continues until we arrive at the last column, entitled "Environmental or System Data."

Few would argue with the view that propagation loss is known with greater accuracy than most of the other items on the chart. Also apparent is that, although accuracy is a concern, it is not the only concern (see figure 23).

The amount of computer time required to run any sub-model is of obvious concern because of the cost involved. Similarly, if the most accurate sub-model requires more core storage than is available, the model is useless. If the sub-model is not available at a facility, additional difficulties will be associated with its implementation. In some cases this may involve time delays that cannot be tolerated. The compatibility of models from one computer to another is a concern that could also result in additional cost and time delays. There are some sub-models that can be run only by the developer and if he is not available for the duration of the study, one might decide to choose another, albeit less accurate, model. Very often it may be possible to decrease the execution time of a model without seriously effecting its accuracy. This would be difficult without extensive documentation. Finally, the sub-model may only provide propagation loss from an omnidirectional source to an omnidirectional receiver when a beamformer output is required.

Of course, these are all practical problems that can be solved with time, money, and manpower. However, they are usually at a premium. Given a multitude of candidates for any sub-model, such as propagation loss, the analyst must arrive at a decision based upon trade-offs between accuracy (and the other items on the list) in the context of the time, money, and manpower available to him.

It became obvious that it would be impossible to recommend a single standard sub-model that would meet the requirements of all potential users. It was thus decided that for each sub-model a matrix of information addressing the items shown in figure 23 be constructed. The analyst or user could then make the required trade-offs himself and select the candidate sub-model best suited for his particular application.

The assessment of accuracy is the most difficult portion of the matrix to complete. One reason for this is that there was unanimous agreement that the methodology adopted had to be significantly more objective than the old technique of graphically comparing predictions and arriving at a value judgment. To accomplish this new ground had to be broken, which was a time consuming process.

The approach currently under consideration is statistical in nature. A given data set is characterized by a sample mean and standard deviation that are functions of the independent variable (e.g., range, azimuth, and time). Two or more data sets are then compared by a variety of statistical techniques yielding quantitative measures of agreement. Although the examples to be discussed specifically deal with transmission loss versus range data, the

applicability of the comparison method is not restricted to such data.

Two approaches for finding the range dependent mean have been implemented. The first involves a moving average for which a subjective choice must be made regarding the number of points to be averaged. In the second approach, the entire record is first subdivided into segments based on the presence of predominant interference patterns. The data within each segment are then fitted with various order polynomials to minimize the mean square error. Examples illustrating this approach will be provided in the subsequent figures. All examples pertain to a profile found in the Pacific in about 18,000 ft of water having a surface duct down to 247 ft. Two source and receiver combinations (figure 24) were examined. For one the source and receiver were in the surface layer at depths of 50 ft and for the other the source and receiver were below the layer at 500 and 300 ft, respectively. Model predictions were obtained at frequencies of 50, 500 and 2000 Hz for each configuration. The frequency cases are designated 1 through 6. Experimental data were also available for the source and receiver below the layer at frequencies of 50 and 400 Hz. These have been designated as cases 7 and 8. The models examined are listed in figure 25. Raymode IV, FACT and NISSM II predictions were compared to those of the FFP.

Case 4, with source and receiver below the layer and at 50 Hz, is sufficiently representative so that most major points of interest are manifest. The FFP prediction (figure 26) begins with a Lloyd Mirror Pattern at close ranges followed by a more complex interference pattern in the first bottom bounce region (which extends to about 58 kyd). A double-peaked convergence zone extends to 75 kyd and is followed by the beginning of the second bottom-bounce interference pattern.

The entire range interval was subdivided into five segments. From right to left they are the second bottom-bounce region, then two segments within the convergence zone, a segment capturing the last major interference pattern in the bottom bounce region, and a single segment for the first 35 kyd. The smooth curve in each segment is the range dependent mean obtained using the polynomial fit. The fact that the first 35 kyd were treated as a single segment whereas it could have been subdivided into as many as 10 segments illustrates where subjectivity enters the methodology. The decision as to which features have importance should be based on the user determining which is the feature of least interest for his application. As it turned out, the choice of a single polynomial fit to the FFP for this range interval led to smaller differences between the FFP predictions and those of the other models, which show much less detail.

The polynomial fits to the FACT coherent predictions are shown in figure 27. Note that the abrupt change in the propagation loss at 86 kyd, which would appear to be an artifact, is smoothed by the polynomial fit. The feature between 40 and 50 kyd is significantly reduced in amplitude compared with the FFP value but is, nonetheless, distinguishable.

The next step in the methodology is to subtract the range-dependent mean for FACT from the range-dependent mean for the FFP. The results are provided in figure 28. The large difference at about 38 kyd is caused by the fact that the features occurring in both models just before the convergence zone are displaced from one another in range and have different amplitudes. The two peaks between 60 and 70 kyd result because the double-peaked convergence zone is more clearly defined in the FFP curve. The differences between 80 and

100 kyd are the result of the artifact in the FACT prediction that produced the abrupt increase in propagation loss.

These results serve as a quantitative measure of the difference in accuracy between the two predictions. The measure is not completely objective since, in some instances, the differences between the two means are caused by subjective decisions regarding the subdivision of the data records. In this regard it is felt that the use of a sliding average would be more appealing than subdividing and fitting with polynomials. However, a certain amount of subjectivity will always be present regardless of the technique used to find the range-dependent mean.

Although this information is considered to be a vast improvement over the purely subjective process of overplotting the two predictions, it would have more significance to the user if it could be summarized in a manner that could be easily interpreted. This is a difficult step because it involves finding a link between the realities of the model developer and user. The last set of figures represent an initial attempt at such a summary.

Since it is quite clear that the summary must be range dependent, one can find the mean and standard deviation of the difference curves in various range intervals specified by the user. For the purpose of illustration, 20 kyd intervals have been selected as shown in figure 29. The mean and standard deviation have been tabulated for all of the models considered in case 4. Thus, for the first 20 kyd, the difference between the mean of the FFP predictions and the mean of NISSM II was, on the average, 0.7 dB. Information similar to this would be available for all cases considered in the assessment (which, in

this instance, was 6).

Considering that only one profile, two source and receiver combinations, and three frequencies have been used (whereas typical user requirements would entail many more combinations) it was felt that a summary on a higher level was needed. The results shown in figure 30 represent one possible alternative.

The user should assign degrees of importance, first to the various cases and second to the different range intervals, based on the application at hand. Given these weights, which will be taken as unity for this example, the absolute value of the mean plus the standard deviation for the differences is calculated for each case in each range interval. The models are then ranked in accordance with these values. The model with the lowest value receives the rank 1, and so on. In the event that two or more models have the same sum, each is assigned an average rank.

The upper line in each box shows the rankings for cases 1, 2, and 3, respectively; the second line shows the rankings for cases 4, 5, and 6, respectively. The number in parenthesis is the sum of the rankings for the 6 cases. The final column provides the sum of the rankings over all cases and range intervals.

It is apparent that, for these cases, the FACT model employing the coherent phase addition shows the closest overall agreement with the FFP. In terms of the the total ranking provided in the last column, the FACT model using incoherent phase addition and the NISSM II model using coherent phase addition are essentially equal. The final three models (Raymode IV with coherent phase addition, Raymode IV with incoherent phase addition, and NISSM II with incoherent phase addition) show significantly less agreement with the FFP model.

When coupled with information about the other items in the matrix, data of this type should provide the user with a reasonable basis upon which to arrive at an objective selection for a sub-model.

In discussing the state of affairs of computer models for underwater sound, it has been helpful to outline the perceptions of reality of those who develop such models and those who use them. Such perceptions, unlike those of the mystic and modern theoretical physicist, are often in conflict, and a fair amount of confusion results. The ideal solution would be either that the user acquire an understanding of the detailed mathematics involved in deriving the various sub-models or that the developer acquire an appreciation for the arts of system analysis and design. A more reasonable alternative would be to establish a line of communication between the two groups so that each could learn to appreciate the realities of the other. The model, whether it be a sub-model or of the generic type, is common to both groups and could serve to bridge the gap. Before this can happen, however, an objective methodology for assessing models must be developed and tested. Some thoughts on such a methodology have been presented, but they are still in the formative stage and require additional exposure and use by both groups. Time does not permit a discussion of experimental data but there are many reasons, not the least of which is relative sparseness, why experimental data cannot be the final reality. Finally, there are perhaps some who would like to know how to avoid finding themselves in a similar predicament. I can offer no advice in this regard for it almost seems inevitable that if you have a computer of any size, you will soon have two or more models that give different answers and, most probably, none will fully represent the reality you had hoped to model. The model will always bear the same relation to reality as a shadow bears to the object that casts it.

BIBLIOGRAPHY

Bartberger, C. and L. Ackler, Normal Mode Solutions and Computer Programs for Underwater Sound Propagation, Naval Air Development Center Report NADC-72001-AE, 4 April 1973.

Blatstein, I.M., Comparisons of Normal Mode Theory, Ray Theory, and Modified Ray Theory for Arbitrary Sound Velocity Profiles Resulting in Convergence Zones, Naval Ordnance Laboratory Technical Report 74-95, 29 August 1974.

Brekhovskikh, L.M., Waves in Layered Media, Academic Press, New York, 1960.

Bucker, H.P., "Some Comments on Ray Theory with Examples from Current NUC Ray Trace Models," Geometrical Acoustics, Proceedings of SACLANTCEN Conference, 27-30, September 1971.

Bucker, H.P., "Sound Propagation in a Channel with Lossy Boundaries," J. Acoust. Soc. Am., 48, 1187-1194, 1970.

Bucker, H.P. and H.E. Morris, "Epstein Normal-Mode Model of a Surface Duct," J. Acoust. Soc. Am., 41, 1475-1478, 1967.

Chapman, C.H., "Generalized Ray Theory for an Inhomogeneous Medium," Geophys. J.R. Astr. Soc. 36, 673-704, 1974.

Davis, J.A., "Extended Modified Ray Theory Field in Bounded and Unbounded Inhomogeneous Media," J. Acoust. Soc. Am., 57, 276-286, 1975.

DiNapoli, F.R., "Fast Field Program for Multilayered Media," NUSC Technical Report 4103, 26 August 1971.

Fitzgerald, R.M., "Helmholtz Equation as an Initial Value Problem with Application to Acoustic Propagation," J. Acoust. Soc. Am., 57, 839-842, 1975.

Guthrie, K.M., "Wave Theory of SOFAR Signal Shape," J. Acoust. Soc. Am., 56, 827-836, 1974.

Haskell, N.A., "Asymptotic Approximation for the Normal Modes in Sound Channel Wave Propagation," J. Appl. Phys., 22, 157-168, 1951.

Kanabis, W.G., A Shallow Water Acoustic Model for an Ocean Stratified in Range and Depth, NUSC Technical Report 4887-1, 25 March 1975.

Kutschale, H.W., Further Investigation of the Integral Solution of the Sound Field in Multilayered Media: A Liquid-Solid Half Space with a Solid Bottom, Lamont-Doherty Geol. Obs. of Columbia University Technical Report CU-6-71, March 1972.

Leibiger, G. and D. Lee, "Application of Normal Mode Theory to Convergence Zone Propagation," Vitro Laboratory Research Memorandum VL-8512-12-0, 30 November 1968.

Levey, L. and L.B. Felsen, "On Incomplete Airy Functions and Their Application to Diffraction Problems," Radio Sci., 4, 959-969, 1969.

BIBLIOGRAPHY (Cont'd.)

Ludwig, D. "Uniform Asymptotic Expansions at a Caustic," Comm. Pure and Appl. Math., 19, 215-250, 1966.

Marsh, H.W. and M. Schulkin, Report on the Status of Project AMOS (Acoustic Meteorological and Oceanographic Survey) (1 January 1953 - 31 December 1954), NUSL Technical Report 255A, 9 May 1967.

Marsh, H.W. and M. Schulkin, "Shallow Water Transmission," J. Acoust. Soc. Am., 34, 863-864, 1962.

McDaniel, S.T., "Propagation of Normal Mode in the Parabolic Approximation," J. Acoust. Soc. Am., 57, 307-311, 1975.

Newman, A.J. and F. Ingenito, "A Normal Mode Computer Program for Calculating Sound Propagation in Shallow Water with an Arbitrary Velocity Profile," Naval Research Laboratory Technical Memorandum 2381, 1972.

Pedersen, M.A. and D.F. Gordon, "Normal-Mode and Ray Theory Applied to Underwater Acoustic Conditions of Extreme Downward Refraction," J. Acoust. Soc. Am., 51, 323-368, 1972.

Pekeris, C.L., "Ray Theory vs Normal Mode Theory in Wave Propagation Problems," Proc. Symp. Appl. Math., 2, 71-75, 1950.

Porter, R.P., "Transmission and Reception of Transient Signals in a SOFAR Channel," J. Acoust. Soc. Am., 54, 1081-1091, 1973.

Spofford, C.W., The FACT Model, Maury Center Report 109, November 1974.

Stickler, D.C., "Normal Mode Program with Both the Discrete and Branch Line Contributions," J. Acoust. Soc. Am., 57, 856-861, 1975.

Tappert, F.D., "Parabolic Equation Method in Underwater Acoustics," J. Acoust. Soc. Am., 55, 534, 1974.

Van der Pol, B. and H. Bremmer, "The Diffraction of Electromagnetic Waves from an Electrical Point Source Round a Finitely Conducting Sphere, with Application to Radio Telegraphy and the Theory of the Rainbow," Phil. Mag., 24, 825-864, November 1937.

Weinberg, H., Navy Interim Surface Ship Model (NISSM II), NUC Technical Publication 372 and NUSC Technical Report 4527, 14 November 1974.

Weinberg, H., "Application of Ray Theory to Acoustic Propagation in Horizontally Stratified Oceans," J. Acoust. Soc. Am., 58, 97-109, 1975.

Weinberg, H. and R. Burridge, "Horizontal Ray Theory for Ocean Acoustics," J. Acoust. Soc. Am., 55, 63-79, 1974.

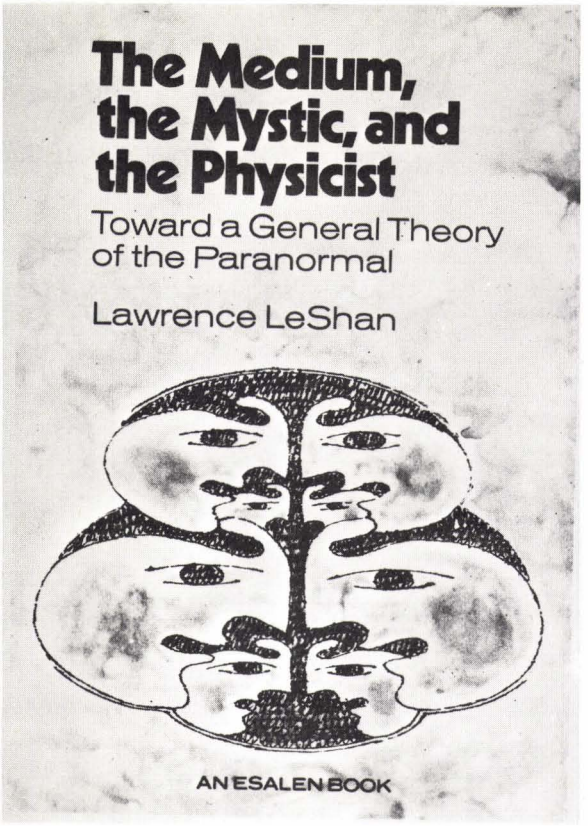

FIG. 1
COVER OF LESHAN'S BOOK

"WHEN WE THOUGHT WE WERE STUDYING THE EXTERNAL WORLD, OUR DATA WERE STILL OUR OBSERVATIONS; THE WORLD WAS AN INFERENCE FROM THEM" DINGLE (P)

"IT IS THE MIND WHICH GIVES TO THINGS THEIR QUALITY, THEIR FOUNDATION, AND THEIR BEING" DHAMMAPADA (M)

"PURE LOGICAL THINKING CANNOT YIELD US ANY KNOWLEDGE OF THE EMPIRICAL WORLD, ALL KNOWLEDGE OF REALITY STARTS FROM EXPERIENCE AND ENDS IN IT. PROPOSITIONS ARRIVED AT BY PURELY LOGICAL MEANS ARE COMPLETELY EMPTY OF REALITY" EINSTEIN (P)

" . . . MAN IS THE MEETING POINT OF VARIOUS STAGES OF REALITY" EUCKEN (M)

"AS FAR AS THE LAWS OF MATHEMATICS REFER TO REALITY, THEY ARE NOT CERTAIN; AND AS FAR AS THEY ARE CERTAIN, THEY DO NOT REFER TO REALITY" EINSTEIN (P)

FIG. 2
SIMILAR VIEWPOINTS ON REALITY

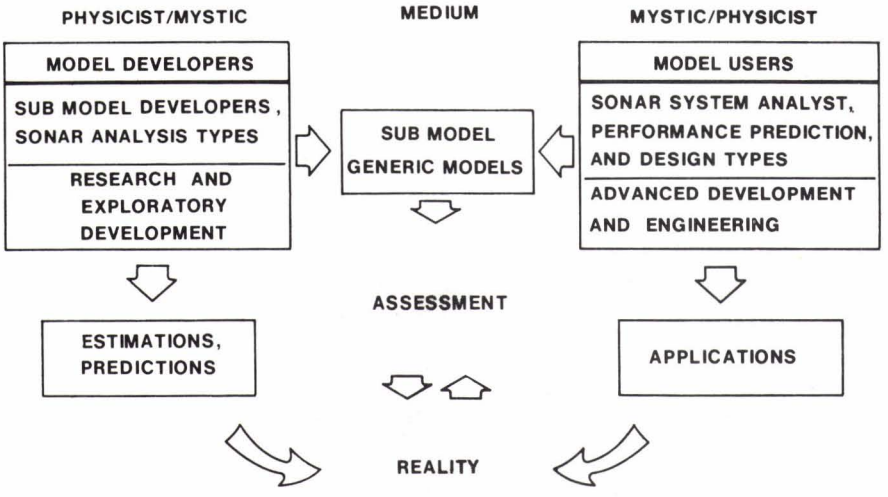

FIG. 3
TWO APPROACHES TO SONAR

CONCEPT

- GENERIC MODEL CAN BE THE BRIDGE BETWEEN THE DEVELOPER AND USER

PROBLEMS

- GENERIC MODEL FOR MOBILE SONAR SYSTEMS DOES NOT EXIST
- DEVELOPERS AND USERS HAVE DIFFERENT PERCEPTIONS OF REALITY
- ASSESSMENT METHODOLOGY IN PRIMITIVE STAGE

FIG. 4 CONCEPT AND PROBLEMS

A. SEMI - EMPIRICAL / SEMI-ANALYTICAL
   1.) AMOS
   2.) COLOSSUS

B. RAY THEORY WITH CORRECTIONS

C. NORMAL MODE THEORY

D. TOTAL FIELD MODELS

E. RANGE DEPENDENT MODELS

F. GENERALIZED/RAY MODELS

G. TIME DOMAIN (WAVE FORM PREDICTION) MODELS

H. EXACT SOLUTIONS

FIG. 5 FIRST CLASS OF PROPAGATION MODELS

FEATURES:

- EQUATIONS ARE SIMPLE, MINIMAL EXECUTION TIME REQUIRED

$$H = 20 \log (1000\, R/R0) + \alpha R + (r/r_1)\, G(Z_t, Z_x)$$

$$G(Z_t, Z_x) = \begin{cases} .1 \times 10^{2.3(Z_t - Z_x)} (f/25)^{1/3}, & Z_t - Z_x < 1 \\ 20\,(f/25)^{1/3}, & Z_t - Z_x \geq 1 \end{cases}$$

SHORT COMINGS:

- LARGE VARIANCE
- VALIDITY GOVERNED BY DATA BASE
- UNABLE TO PREDICT FINE STRUCTURE OF PROPAGATION LOSS

FIG. 6 SEMI-EMPIRICAL/SEMI-ANALYTICAL CLASS

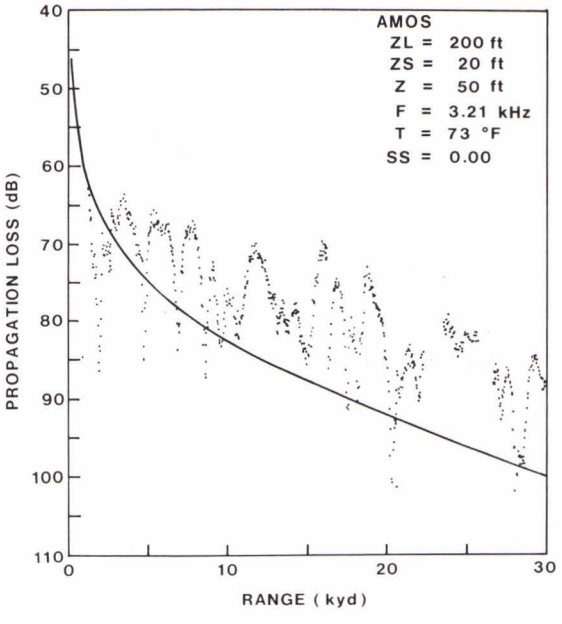

FIG. 7
PROPAGATION LOSS VERSUS RANGE
(RECEIVER DEPTH 50 ft)

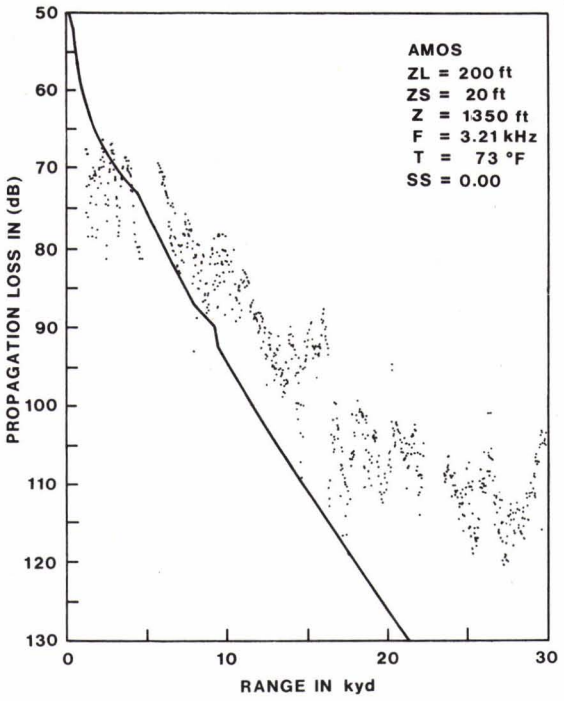

FIG. 8
PROPAGATION LOSS VERSUS RANGE
(RECEIVER DEPTH 1350 ft)

TIME INDEPENDENT WAVE EQUATION

$$\nabla^2 \psi + k^2 \psi = - \delta (z - z_0) \frac{\delta (\rho)}{\rho}$$

+ BOUNDARY CONDITIONS (FLAT BOTTOM, SINGLE SSP)

FIG. 9
REALITY FOR THE SUB-MODEL DEVELOPER

A. SEMI - EMPIRICAL / SEMI - ANALYTICAL

B. RAY THEORY WITH CORRECTIONS
   1. FACT
   2. NISSM II

C. NORMAL MODE THEORY

D. TOTAL FIELD MODELS

E. RANGE DEPENDENT MODELS

F. GENERALIZED RAY MODELS

G. TIME DOMAIN (WAVE FORM PREDICTION) MODELS

H. EXACT SOLUTIONS

FIG. 10
SECOND CLASS OF PROPAGATION MODELS

FEATURES:

RAY DIAGRAM EASILY INTERPRETED

ADDITIONAL USER ORIENTATED INFORMATION AVAILABLE

SIGNIFICANT REDUCTION IN EXECUTION TIME AND STORAGE REQUIREMENTS

SHORT COMINGS:

LIMITS OF APPLICABILITY DIFFICULT TO DETERMINE

ADDITIONAL CORRECTIONS ARE REQUIRED

FIG. 11 SUMMARY OF RAY THEORY WITH CORRECTIONS

A. SEMi - EMPIRICAL / SEMI - ANALYTICAL

B. RAY THEORY WITH CORRECTIONS

C. NORMAL MODE THEORY

1. GORDON, PEDERSEN
2. BARTBERGER
3. BUCKER, MORRIS
4. BLATSTEIN

} SPECIAL FUNCTIONS OF MATHEMATION PHYSICS

$$\frac{d^2\beta}{dz^2} + (k^2(z) - \xi^2)\beta = 0$$

5. KANABIS, INGENITO } NUMERICAL INTEGRATION

D. TOTAL FIELD MODELS

E. RANGE DEPENDENT MODELS

F. GENERALIZED RAY MODELS

G. TIME DOMAIN (WAVE FORM PREDICTION) MODELS

H. EXACT SOLUTIONS

FIG. 12 THIRD CLASS OF PROPAGATION MODELS

FEATURES

CONFIDENCE IN THE RESULTS

SOLUTION FOR ANY SOURCE AND RECEIVER DEPTH COMBINATION IS OBTAINED AT LITTLE EXTRA EXPENSE.

SHORT COMINGS:

PHYSICAL INTERPRETATION DIFFICULT

LIMITS OF APPLICABILITY DIFFICULT TO ASCERTAIN PRECISELY

ADDITIONAL USER-ORIENTED INFORMATION DIFFICULT TO OBTAIN

FIG. 13 NORMAL MODE THEORY

A. SEMI - EMPIRICAL / SEMI - ANALYTICAL

B. RAY THEORY WITH CORRECTIONS

C. NORMAL MODE THEORY

D. TOTAL FIELD MODELS

1. KUTSCHALE
2. STICKLER

EIGENVALUE SOLUTION
(MODES PLUS BRANCH CUT)

$$\psi(z,r) = \int_{-\infty}^{\infty} G(z, z_0, \xi)\, H_0^{(1)}(\xi r)\, \xi\, d\xi$$

3. FAST FIELD PROGRAM (FFP)
4. KUTSCHALE VERSION OF FFP

NON EIGENVALUE SOLUTION

E. RANGE DEPENDENT MODELS

F. GENERALIZED RAY MODELS

G. TIME DOMAIN (WAVE FORM PREDICTION) MODELS

H. EXACT SOLUTIONS

FIG. 14 FOURTH CLASS OF PROPAGATION MODELS

$$H_0^{(1)}(\xi r) \cong e^{i\xi r} / \sqrt{\xi r}\,, \quad (\xi r) >> 1$$

$$\psi(z,r) \cong \frac{1}{\sqrt{r}} \int_{-\infty}^{\infty} G(z_1\, z_0, \xi)\, \xi^{1/2}\, e^{i\xi r}\, d\xi$$

FIG. 15 ONE MODIFICATION TO REALITY

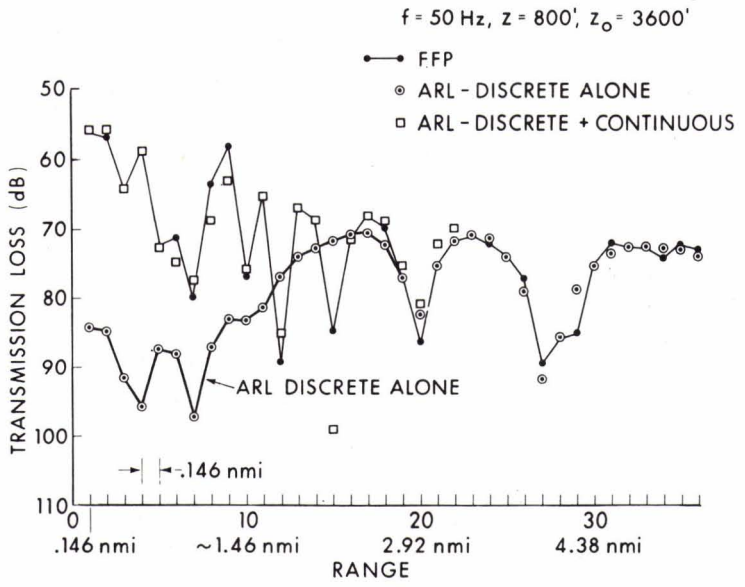

FIG. 16 GENERAL APPLICABILITY OF THE FFP

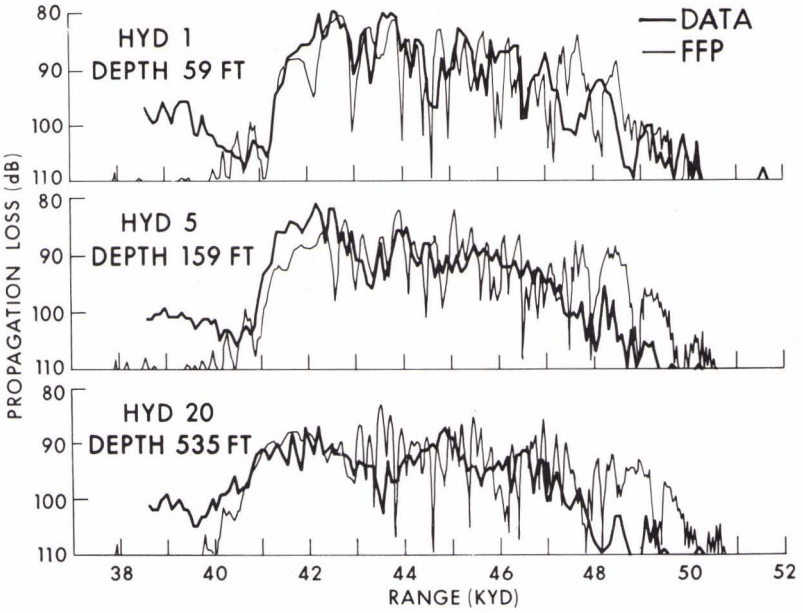

FIG. 17
COMPARISON OF FFP PREDICTIONS AND ACTIVE SONAR SYSTEM DATA

FIG. 18
TOTAL FIELD MODELS (FFP)

FEATURES:

- APPLICABLE FOR ANY FREQUENCY / WATER DEPTH COMBINATION
- IS USED AS A BENCHMARK PROGRAM

SHORT COMINGS:

- PHYSICAL INTERPRETATION DIFFICULT
- ADDITIONAL USER-ORIENTED INFORMATION DIFFICULT TO OBTAIN

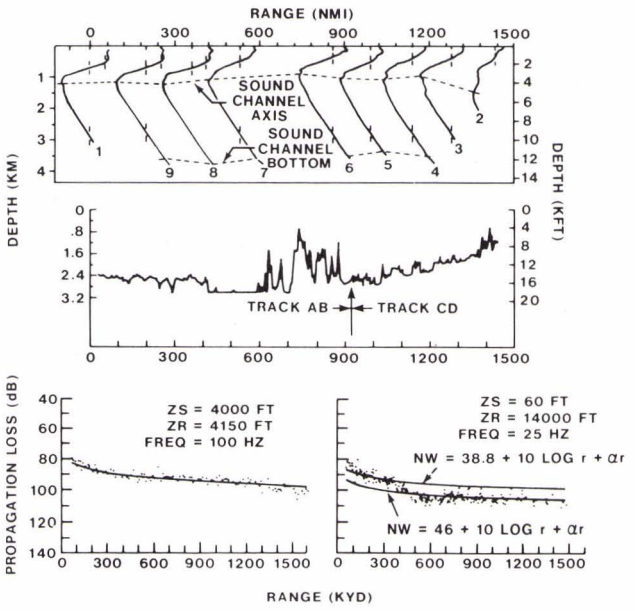

FIG. 19
ACOUSTIC DATA FOR SOURCE AND RECEIVER

A. SEMI EMPIRICAL / SEMI - ANALYTICAL

B. RAY THEORY WITH CORRECTIONS

C. NORMAL MODE THEORY

D. TOTAL FIELD MODELS

E. RANGE DEPENDENT MODELS
   1. KANABIS NORMAL MODE
   2. WEINBERG 3 D NORMAL MODE
   3. PARABOLIC EQUATION MODEL

F. GENERALIZED RAY MODELS

G. TIME DOMAIN (WAVE FORM PREDICTION) MODELS

H. EXACT SOLUTIONS

FIG. 20
FIFTH CLASS OF PROPAGATION MODELS

A. SEMI EMPIRICAL / SEMI - ANALYTICAL

B. RAY THEORY WITH CORRECTIONS

C. NORMAL MODE THEORY

D. TOTAL FIELD MODELS

E. RANGE DEPENDENT MODELS

F. GENERALIZED RAY MODELS
   1. RAY MODE
   2. RAY WAVE
   3. WEINBERG

G. TIME DOMAIN (WAVE FORM PREDICTION) MODELS
   1. TIME DOMAIN FFP
   2. TIME DOMAIN NORMAL MODES (PORTER, GUTHRIE)

H. EXACT SOLUTIONS

FIG. 21
SIXTH CLASS OF PROPAGATION MODELS

← MODEL APPLICATIONS →			→ DEPENDENCE →				
STATISTICAL	ENGAGEMENT	PERFORMANCE PREDICTION	MAJOR MODELS	MAJOR COMPONENTS	MINOR COMPONENTS	SUB COMPONENTS	ENVIRONMENTAL OR SYSTEM DATA
ENGAGEMENT STATISTICS	MULTI-PLATFORM	PASSIVE	SIGNAL	XMIT ARRAY RESPONSE	BOTTOM STRUCTURE	POWER AMPLIFIER	XMIT WAVEFORM
MODEL ASSESSMENT		ESTIMATION	NOISE	RECEIVE ARRAY RESPONSE	SURFACE LOSS	WAVE HEIGHT	HYDROPHONE LOCATION
CONCEPT COMPARISON		ACTIVE	REVERBERA-TION	PROP. LOSS	ATTENUATION	BOTTOM ROUGHNESS	XDUCR LOCATION
		TRACKING	TARGET	TARGET STRENGTH	BAFFLE	VELOCITY PROFILE	SEA STATE
		RANGING		RADIATED NOISE	WINDOW	VOLUME SCATTERING PROFILE	WIND SPEED
				SEA NOISE	BOTTOM SCAT. STR.	FILTER CORRELATOR	BOTTOM SLOPE
				SHIPPING NOISE	XMIT BEAM PATTERN	AVERAGER	SHIPPING DISTRIBUTIONS
				BIO. NOISE	RECEIVE BEAM PATTERN	NORMALIZER	TEMPERATURE PROFILE
				SELF NOISE	SIGNAL PROC.	SPECTRUM ANAL.	SALINITY PROFILE
				BOTTOM REVERB.	DATA PROC.		BOTTOM SCATTERING CONST.
				SURFACE REVERB.	INFO. PROC.		SURFACE SCATTERING CONST.
				VOLUME REVERB.	DISPLAY		
				PASSIVE PROC.			
				ESTIM. PROC.			
				ACTIVE PROC.			
				TRACKER			
				RANGE PROC.			
				CLASSIFIER			
				TMA			

FIG. 22 ESSENTIAL INGREDIENTS OF GENERIC MODEL

A. ASSESSMENT OF ACCURACY

B. RUNNING TIME

C. AMOUNT OF COMPUTER MEMORY REQUIRED

D. EASE OF IMPLEMENTATION

E. COMPLEXITY OF PROGRAM EXECUTION

F. EASE OF EFFECTING SLIGHT ALTERATIONS TO THE PROGRAM

G. AVAILABLE ANCILLARY INFORMATION

FIG. 23
FACTORS INFLUENCING MODEL SELECTION

FIG. 24
TWO SOURCE AND RECEIVER COMBINATIONS

CASE NUMBER	FREQUENCY (Hz)	SOURCE DEPTH (ft)	RECEIVER DEPTH (ft)
1	50	50	50
2	500	50	50
3	2000	50	50
4	50	500	300
5	500	500	300
6	2000	500	300
7	50	500	300
8	400	500	300

CASES 1–6: FAST FIELD PROGRAM (FFP) WITH

- **RAYMODE IV**
- **FACT**
- **NISSM II**

CASES 7,8: PARKA DATA WITH

- **FFP**
- **RAYMODE IV**

FIG. 25
CASES 1 THROUGH 6

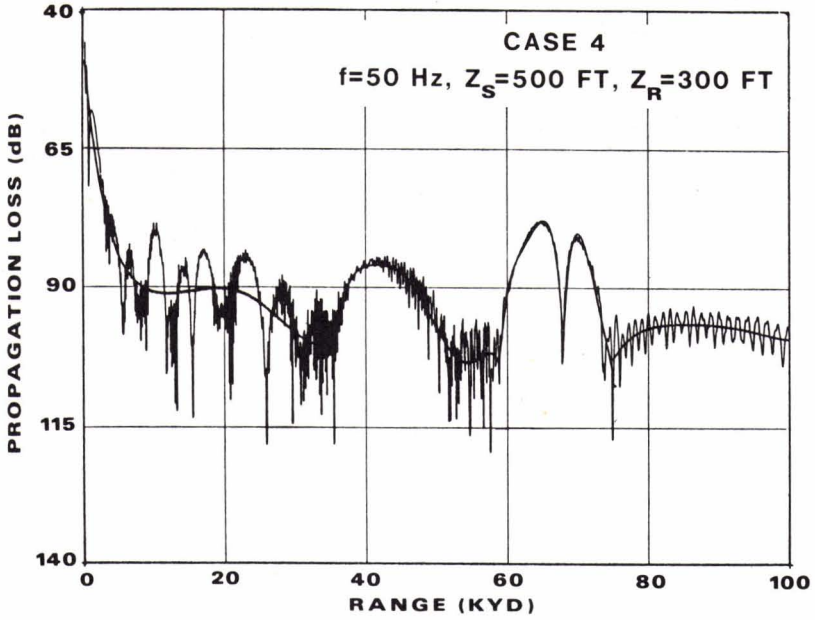

FIG. 26
FFP PROPAGATION LOSS

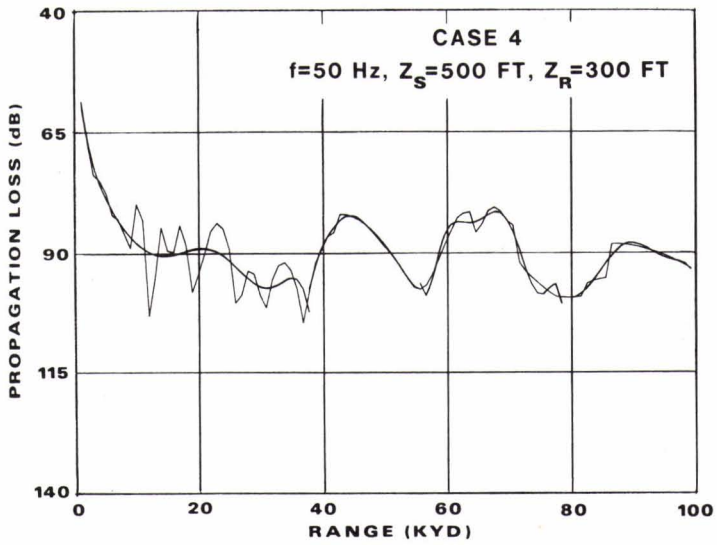

FIG 27
FACT COHERENT PROPAGATION LOSS

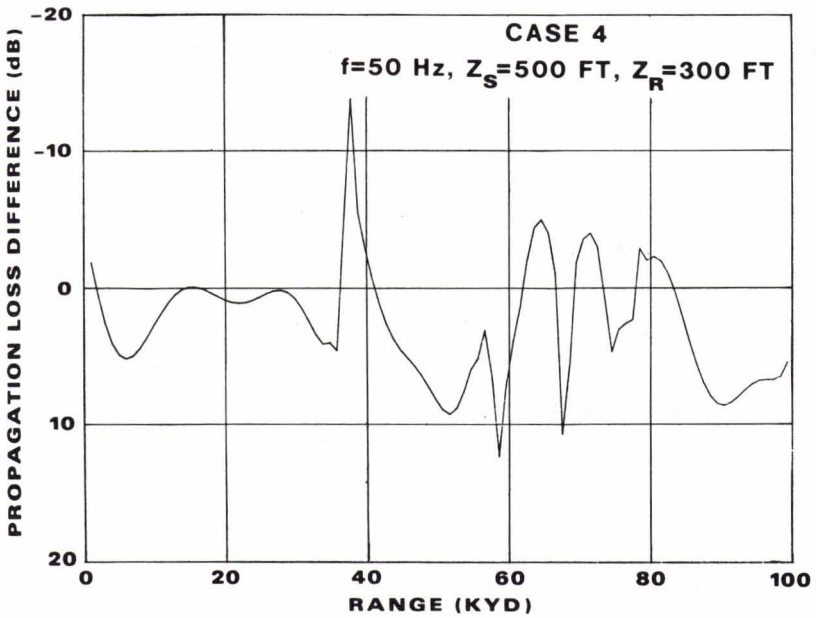

FIG. 28
FFP POLYNOMIAL MINUS FACT COHERENT POLYNOMIAL

CASE 4

RANGE INTERVAL (Kyd)	0-20		20-40		40-60		60-80		80-100		0-100	
MEAN AND STANDARD DEVIATION (dB)	μ	σ	μ	σ	μ	σ	μ	σ	μ	σ	μ	σ
FFP POLYNOMIAL MINUS RAYMODE COHERENT POLYNOMIAL	3.1	4.0	-4.3	3.7	0.3	8.2	1.0	8.3	-3.6	2.5	-7.0	6.4
FFP POLYNOMIAL MINUS RAYMODE INCOHERENT VALUES	4.0	1.9	1.1	4.4	3.1	8.9	2.8	5.7	-2.3	1.3	1.7	5.6
FFP POLYNOMIAL MINUS FACT COHERENT POLYNOMIAL	1.8	2.1	0.0	4.1	5.9	3.0	0.1	4.1	5.0	3.6	2.6	4.2
FFP POLYNOMIAL MINUS FACT INCOHERENT VALUES	3.7	2.2	4.2	4.2	6.2	6.2	0.5	4.8	1.4	3.3	3.2	4.7
FFP POLYNOMIAL MINUS NISSM COHERENT POLYNOMIAL	0.7	1.4	-0.1	1.8	-2.4	4.0	-6.9	10.3	-2.0	3.3	-2.2	5.9
FFP POLYNOMIAL MINUS NISSM INCOHERENT VALUES	3.3	1.6	3.6	4.3	5.1	7.0	-3.2	6.9	-1.0	4.3	1.5	6.0

FIG. 29 COMPARISON OF PROPAGATION LOSS MODELS WITH THE FFP

RANGE INTERVAL	0-20	20-40	40-60	60-80	80-100	TOTAL
RAYMODE COHERENT	4 4 3 6 5 2 (24)	6 3 4 5 5 6 (29)	5 5 4 2 6 6 (28)	3½ 2 3½ 4 1 1 (15)	5 1 6 5 6 6 (29)	125
RAYMODE INCOHERENT	6 3 1 4½ 6 6 (26½)	5 4 3 3 4 1 (20)	6 4 3 4 5 4 (26)	6 1 3½ 3 5 4 (22½)	6 2 5 1 5 5 (24)	119
FACT COHERENT	1 2 2 2 4 3 (14)	2 2 1½ 2 6 5 (18½)	1 2 2 3 3 3 (14)	1 3½ 2 1 2 2 (11½)	2 5 2 6 2 2½ (19½)	77½
FACT INCOHERENT	2 1 4 4½ 3 5 (19½)	3½ 1 1½ 6 3 4 (19)	4 1 1 6 4 5 (21)	5 5 1 2 3 3 (19)	4 3 1 2 4 4 (18)	96½
NISSM COHERENT	3 5 5 1 1 1 (16)	1 6 5 1 1 3 (17)	2 6 5 1 2 1 (17)	2 3½ 5 6 6 6 (28½)	1 6 3 3½ 1 2½ (17)	95½
NISSM INCOHERENT	5 6 6 3 2 4 (26)	3½ 5 6 4 2 2 (22½)	3 3 6 5 1 2 (20)	3½ 6 6 5 4 5 (29½)	3 4 4 3½ 3 1 (18½)	116½

FIG. 30 RELATIVE STANDING OF EACH MODEL ON THE BASIS OF $|\mu| + \sigma$ FOR CASES 1–6

ASSESSMENT TECHNIQUES FOR COMPUTER MODELS OF SOUND PROPAGATION

by

David H. Wood
SACLANT ASW Research Centre
La Spezia, Italy

ABSTRACT

Computer models of sound propagation have exactly three drawbacks: the model only approximates reality, the computer program only approximates the model, and the cost approximates infinity. The only way to assess these shortcomings is to compare the computer model's performance against data: experimental data, synthetic data, and financial data. Examples of these comparisons will be featured. Comparison with theoretical examples within the scope of the computer model is the best way to assess the relation between the model and the computer program. Financial data on cost of speed, accuracy, size, and special features is spotty, but a few examples will be shown.

Computer models of sound propagation have three drawbacks: the model only approximates reality, the computer program only approximates the model, and the cost and computer requirements approximate infinity. The only way to assess these shortcomings is to compare the computer program's performance against data: experimental data, synthetic data, and financial data.

Experimental Data is the final test of the model's relation to reality and an abundance of it could measure the other shortcomings by statistical methods. Unfortunately, there are too few experiments and fewer still with dependable, accurate data.

Synthetic Data poses the most rigorous test of the programming of the computer model. As in the last paper, by numerical simulation of an ocean experiment, synthetic data can suggest that the model reflects reality. Two sources of synthetic data are computer models and theoretical examples. Comparison with theoretical models throughout the area of their overlapping capabilities, whether realistic or not, promotes confidence in the programming of both models. Comparison with theoretical examples is the best way to assess the relation between the model and the computer program. This includes comparison with special models, which are simplified and accurate but otherwise impractical, these models being specifically developed for this purpose.

Financial Data on the cost of speed, accuracy, size and special features is scarce, probably because we don't yet have even one dependable model.

Let me show you (Fig. 1) some of the interrelated concepts that we have to work with. Here we have a red disc representing reality, partially overlaid with a blue disc representing the wave equation. If I had heard Di Napoli's talk before, I would have made the red disk much, much larger. Now I place a yellow disc representing the model. Notice that part of it lies outside the wave equation. Models sometimes have unrealistic features such as speeds given by complex numbers. In the orange region, we have, for example, absorption, a reality not modelled by the wave equation. In the green area, we note that many models can deal with unrealistic extreme changes in speed. In the purple area, we note that most models have layering and can only approximate the very smooth sound-speed profiles that may be found in the ocean. In the blue area, we might find zero frequency; in the red area, non-linear effects. Let me overlay on this diagram the computer program in question. I have deliberately made its representation a little spotty. Little, because it cannot fully realize the model; and spotty, because the capabilities of the

program are seldom known -- even to its author. Authors of computer models write reports about them. In the reports we see the models validated: they are compared with experimental data or with other large, general-purpose, sound-propagation computer models. Do they agree? No! Of course we would be shocked to see experimental data points fall exactly on the computed curves. On the other hand, I am shocked to see the two models' curves fail to lie exactly over each other. I think that the most we can conclude from these comparisons is that the models do not contain programming errors that have a gross effect in the test case shown. Now, I say this is not validation. I say that validation has to proceed in two separate and distinct phases: first, we have to be assured that the program truly represents the model; second, we want to see that the program approximates reality.

Reading these reports, we are expected to assume that all programming errors have been eliminated — the authors don't say. It is considered quite impolite to intimate that a particular program might contain errors. However, if the authors have gone to all the work of testing their programs as thoroughly as I am about to suggest, I am surprised that they don't say so.

In the last paper, Di Napoli told us that in a typical realistic case the models typically differed from FFP be more than 5 dB. He concludes that the models cannot produce accurate results in this test case. I don't necessarily agree. I think that Di Napoli's comparisons are probably a statistical demonstration that these models contain programming errors. I feel that before models are compared, we have to be sure that each model is correctly programmed. Let me outline the three distinct types of computer programs that I think are required to obtain the desired modelling of reality.

First, we need a type of program, I call an Archer. Typically, this

Small Program (ARCHER)
Accurate
Simple
Unrealistic
Slow

is based on a class of theoretical examples. Its main attribute is accuracy, but simplicity of programming is important, too. It will usually not be restricted to realistic conditions, but that doesn't matter. It is not to be used to model reality, it is to be used to detect programming error in the next class of computer model. Therefore, it is more important that it has capabilities in common with the next model than that it has features in common with reality. Its least important feature is speed. It is to be tested against theory and against other Archer-type programs, when they have an application in common.

The second type of program, I call a Weightlifter. Its main

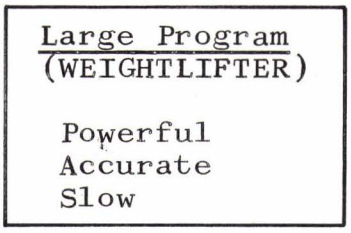

attribute is power. It is to cover as much of the abstract model as possible, including unrealistic cases, which often exaggerate the effect of previously undetected errors. It is accurate because this helps debug the program by comparing it to Archer-type models; and because it will be used to check that the third class of model retains sufficient accuracy for applications (which is not much). Speed is not expected because it is incompatible with the other requirements. This is a program that accurately mimics the abstract model. As such, it is suitable for comparison with any synthetic data or experimental data.

The third class of program, I call a Sprinter. Speed and perhaps

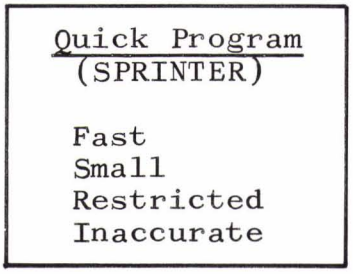

size are all-important. If restricting the program to realistic problems will make it faster or smaller, fine. We are happy to sacrifice quite a lot of accuracy, too, if that will help. This program is to be evolved from a weightlifter. It will be free of the errors that were eliminated earlier. It is to be compared to its weightlifter version to verify that it has not lost too much accuracy in realistic cases. And now, finally, it is tested against experimental data.

My thesis, then, is that we need three distinct types of programs. Certainly, if we want fast, realistic programs, we will have to have powerful programs and accurate programs. All three types should be equally documented and distributed. One model developer I know publishes weightlifter programs, but never has anything to say about his archer programs. As a matter of fact, I have one that I cherish that I got out of his wastepaper basket. At the very least, any organization that is interested in evaluating sound propagation models ought to have a collection of all three types. At SACLANTCEN we are creating a super computer model, SOLMAR, that includes many models of all three types under a common user-oriented input-output language. I believe that is an important step towards the day when we can have meaningful comparisons between models.

I want to show you a few examples, but let me apologize in advance. I show the results of these three models not because they are good examples of the three types of programs I spoke of. They are only rough approximations of an Archer model, a Weightlifter model, and a Sprinter model. However, they are models that are running at SACLANTCEN, and illustrate typical results in comparison of models.

Figure 2 shows the geometry of the example: a uniform layer of water over a plane, rigid bottom. I will show four comparisons, using four frequencies. Everything else is held constant: only the frequency changes.

1) At a radian frequency of 160 (Fig. 3), an Archer-type model, based on the exact solution of the wave equation given by Brekhovskikh, generates the monotonic curve for random phase addition and the humped curve for coherent phase addition. A Weightlifter-type model, a normal mode program by F. Jensen of SACLANTCEN, gives a curve for the coherent field indistinguishable from Brekhovskikh. The FACT model, a Sprinter-type model, gives the same result for both coherent and incoherent phase additions, some 3 or 4 dB below Brekhovskikh's random phase curve.

2) At a radian frequency of 800 (Fig. 4), we obtain the same type of results.

3) At a radian frequency of 2130 (Fig. 5), the coherent field is much more intense than the random phase approximation. Jensen's mode program no longer agrees exactly with Brekhovskikh. The FACT model again gives the same result for the coherent and random phase fields.

4) At a radian frequency of 2131 (Fig. 6) -- recall the last example was at 2130 -- the coherent field has dropped down much closer to the random phase approximation. Jensen's normal mode model again agrees with Brekhovskikh. The FACT prediction is unchanged.

So even in these simplest examples, we see that the comparisons are puzzling enough to demonstrate the need for maintaining three distinct types of computer models: accurate Archer models, powerful Weightlifter models, and fast Sprinter models.

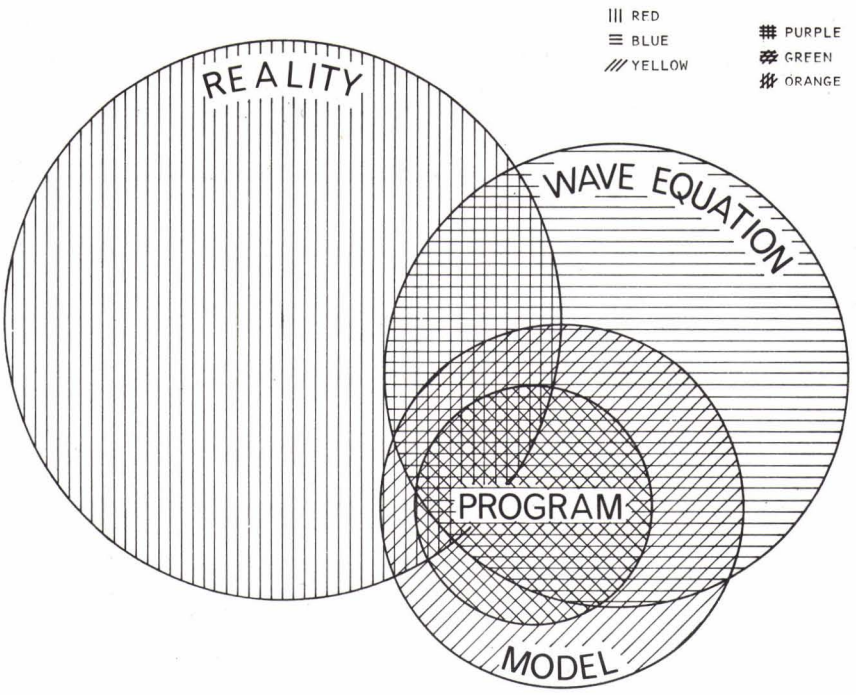

FIG. 1

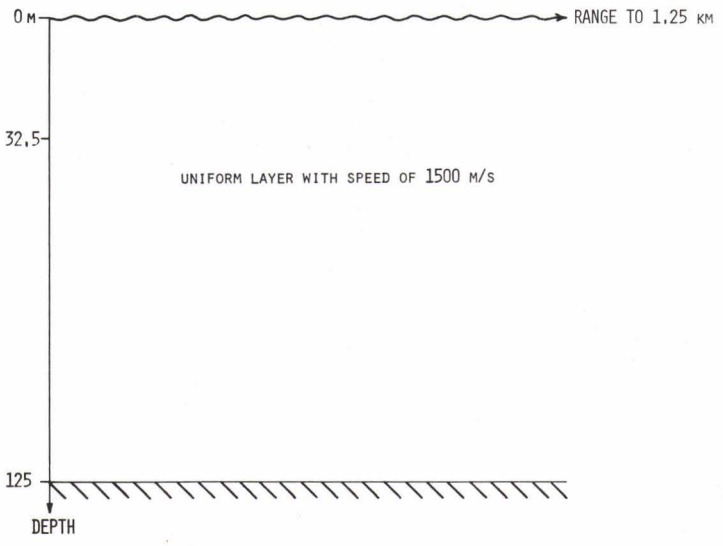

FIG. 2

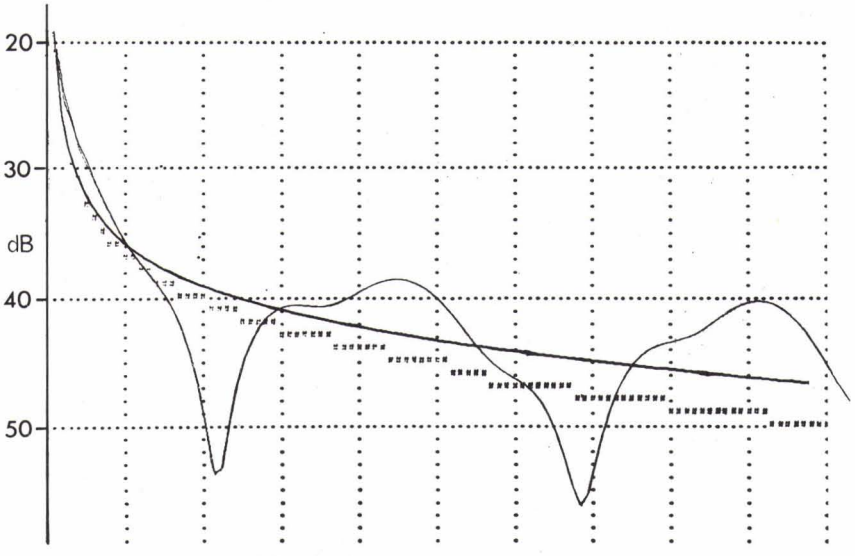

FIG. 3

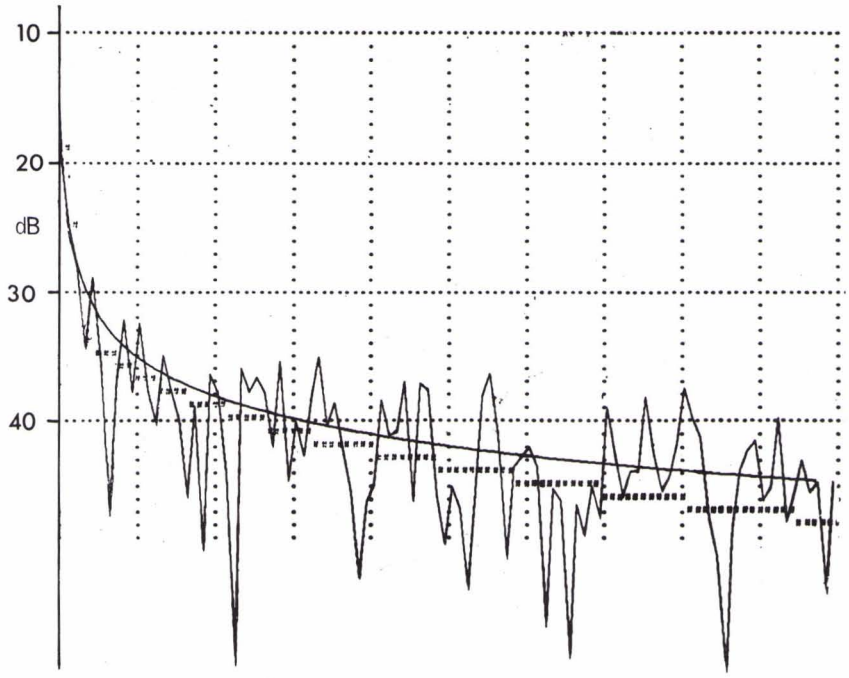

FIG. 4

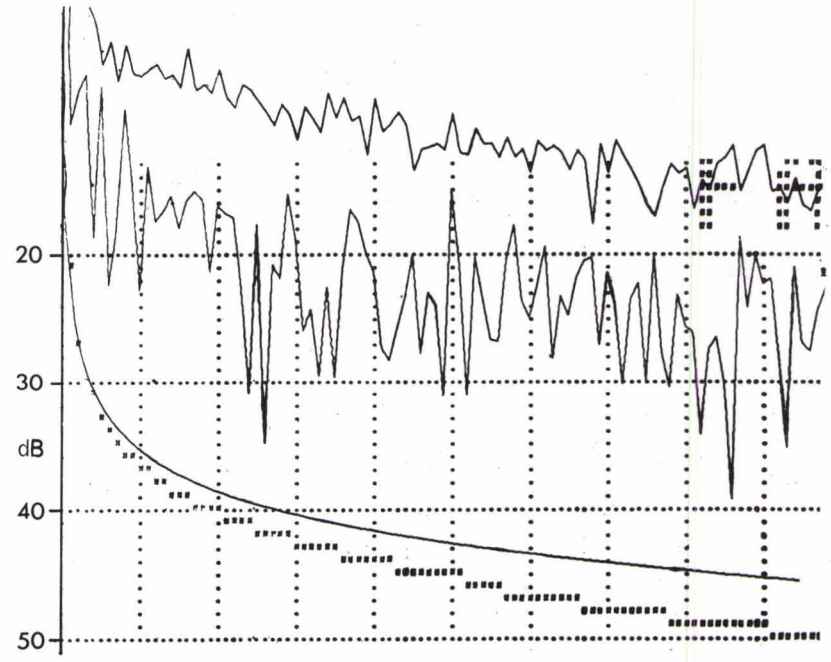

FIG. 5

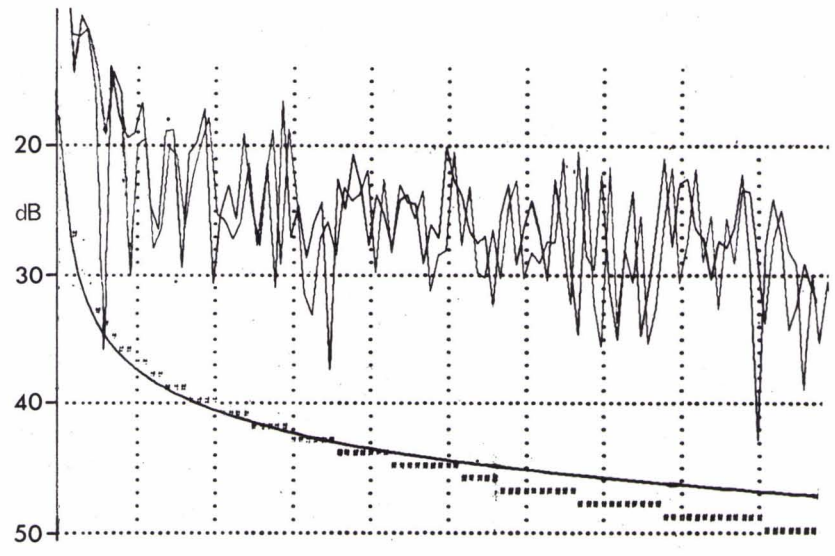

FIG. 6

DISCUSSION

DISCUSSION ON SESSION 8

Reported by D. Wood

Flatté: People often ask why we can't compare [the parabolic equation model] to exact solutions of the wave equation to check programming.

Wood: That's nonsense.

Flatté: That's nonsense, that's outside of the validity of the model.

Wood: Should be tested against exact solutions of the parabolic partial differential equation.

Mintzer: Why shouldn't we test against closed-form solutions of the elliptic equation?

Wood: You are asking a different question.

Mintzer: But what it is you are presenting.

Wood: But you see, we are asking two questions: First, is the program correctly programmed? So we see, "Can it solve a parabolic equation?" And then we ask....

Flatté: That leads us into a whole different area. [Wood compared] .... propagation loss of the normal mode solution and an exact solution, wherever that came from, but the exact wiggles didn't agree at all, you said that's bad agreement; but that depends on what question you want to ask. Perhaps I don't care what the exact propagation loss is at 27.3 km. The fact one program gave that propagation loss at 27.3 km and one gave it at 27.2 km is not of interest to my question at all. For example, my question may be "What happens when you put a fluctuation, a time varying fluctuation, on that system, what happens to each one of those points?" It may agree quite well with all those programs where detailed deterministic values are displaced by small amounts. We have to be careful which question you are asking when you assess the program.

Williams: Fred, [Di Napoli], do you want to respond to that?

Di Napoli: Yes, I'd agree perfectly with Stan [Flatté]. And that's precisely what led us to try to find some range-dependent mean for comparison of models; and work with that. Not totally satisfied with that either. For applications, it seems to be better way to do it than a point-to-point comparison between models which....

Flatté: But if you compare range-dependent mean, you will wash out whatever fluctuations might be imposed by some time varying system on both models. You will not get a comparison if you are interested, for example, in fluctuation.

Williams: I want to disagree completely with both of you. (Laughter). I think, if there is a bug in the program that you ought to detect it, find it, and correct it. I think that bugs in programs can have — not show up for a couple of years — I've had that kind of problems. Once you detect it — I hope we are not at the stage when we have these programs, we know there's bugs in there, and don't care whether there's bugs or not. I really think what we ought to stay with building perfectly the program.

Flatté: Well, I disagree with you. I really disagree, because we can never get all the bugs out of a program that's really very large; you never verify that you've gotten all the bugs out of the program.

Williams: That's different than....

Flatté: .... what their effect are on the questions .... what the answers are you're going to get to the questions you're asking.

Williams: All I'm saying is that once you detect a bug it seems like you'd want to get it out. You don't know the ramifications of a bug.

Flatté: .... spend a year detecting all possible bugs which have nothing to do with the questions you are asking.

Williams: Well, how do you know that?

Flatté: That's a different assessment technique. Depends on the question.

Blatstein: I think it is an iterative process. I think Dave [Wood] is reacting to a normal inclination to display models on top of each other. I react to what he says by saying, "Inevitably, if you are going back to laying models on top of each other, you'd better be pretty sure that one or the other is right." Our experience with ray-tracing models is that we get them from somebody else; we have 6 months getting it going on our computer; then another 6 months finding bugs by running profiles that we have run before. Yet every time I give it to somebody else, first profile they run, bombs. And it shouldn't ! It is just that when you get what you call a.... program, it's general enough so that it's invariably going to have bugs. Its just that a program is a limited being .... it can be covering only a finite set of conditions. Phinagle's law says

that the next person you give it to is going to give it a set of conditions it wasn't designed for. You can check it with exact solutions -- and think you have to -- but then you are interested in realistic cases, and that's where you really compromise the model -- to get it running in realistic cases. We haven't reached the point where we can give somebody the model and with it a guarantee certificate, you know, "Double your money back if this bombs", because that's unrealistic. Dave [Wood], to a certain extent I have the same objection you do: you're always told how good the model is: not how bad it is. Then when it doesn't run, you're shocked: and you shouldn't be.

Wood: So this little discussion can be summarized by saying that the program will undoubtedly have bugs, but Stan [Flatté] feels that maybe you can statistically demonstrate that it's unimportant to get them all out. Certainly I have to agree with him: I could never get out all the bugs of a general-purpose computer model. I think that we have to say that on the other hand, we ought to try to get all that we possibly can out. As Bruce [Williams] says: because we never know when suddenly there will be a physical circumstance that will make the effect of a bug noticeable for the first time.

Williams: Just like exercising a computer. There are diagnostics for a computer; and certainly they don't exercise everything. But I think maybe what we're getting to is a general approach to make assessments rather than just trying different profiles and see where they fail.

Cox: Propagation loss, per se, is only one question I might want to ask. There might be many properties that are more important to me. I don't know that question I'll ask tomorrow. I could write down twenty questions I might want to ask someday; and if someone could tell me "If you really want to ask that question, you ought to go to this model." .... care about propagation loss, you do it on the back of an envelope, don't bother with a computer.... It seems to me that what we have missing is a discussion of the utility of the various models and the features that we think are best modelled .... one model does this, another does that. If I'm interested in the convergence-zone width, I might be very interested in the characteristics of convergence-zone models. What model is best for that particular parameter? It seems to me just the mean or .... doesn't give me an answer. Nor does comparing to the Fast Field Program given an answer. Thus, [if] I say that the Fast Field Program is our best program, then I don't need an answer to the other question; I'll just use that .... I'm interested in what's the best program

Di Napoli: .... as far as the broad features, that's why we went to a sort of range-dependent mean. As to the fine scale fluctuation, that can be affected by how you put it on the computer. I don't think that anyone should believe that; certainly not on a point-to-point basis. And it is questionable whether if you treated that deterministic prediction in some sort of a statistical fashion whether those statistics would have any relationship to the real world. I think that question is open .... I'd like to know about all this fluctuation that we've heard about: "What part of the curve does it really affect?" Does it affect the broad features like the convergence zone significantly .... or is it affecting the fine fluctuation?

Wood: Can I ask a question? Fred [Di Napoli], when I read your manuscript, I felt there was a calibration missing. I know you wouldn't go to sea without calibrating your hydrophones. Did you look at some special case with all of these models to verify that they all gave the same result?

Di Napoli: I didn't have time, and I did not present it in the written manuscript .... this profile has experimental data associated with it. I didn't say anything about experimental data. But that's just not a benchmark if you are interested in this fine-grain prediction. If you are interested in broad features this is perhaps in some cases useful.

Wood: Let me ask this then: Did you ever look at any profile where the models agreeded extremely well?

Di Napoli: Yes....

Wood: One profile that all the models agreeded on?

Di Napoli: Yes, we did.

Wood: What profile was it?

Di Napoli: We picked a Mediterranean summer profile. We had data to go along with it — at 35 kHz — by .... at Woods Hole. And I think that most of the models that I mentioned, if you put in the proper input information, you will get what most systems people — users —. I'm talking about certain users — would be sure to say was excellent agreement.

Wood: How close?

Di Napoli: For them it doesn't have to be that close.

Wood: For me it does. (Laughter). You see, I'm talking about computer programs now. I'm not talking about systems applications.

Di Napoli: I don't disagree with that, Dave, I think that we're both saying the same thing: that first you have to specify what sort of accuracy you're interested in.

Wood: One dB means zero significant figures in agreement. You don't compute the field with a model in dB, you compute the field and then take its logarithm and multiply by 10. You compute the field. Now I except one significant figure from all the models for some profile.

Di Napoli: I really don't understand your point.

Flatté: I'd like to make a comment on the question of fine structure. All of us have seen propagation-loss diagrams coming out of various models — normal mode, parabolic equation, or whatever — in which the propagation loss looks like practically a black band from wiggles going up and down on it. Now that is a physical effect; it is really there. It is there, very understandably, from the multipath interference phenomenon. If you are questioning whether the peak of each one of those sharp spikes is occurred in exactly the right place, I agree with you. I don't expect any program to get that. But if you're questioning whether the separation between those spikes is uncertain, then I would disagree with you. That's just given by rays that are coming together at a certain angle to get the multipath interference, a very well-understood phenomenon that our computer programs are perfectly capable of calculating.

Di Napoli: Do you believe it? As representative of a real world?

Flatté: Yes, I do, in terms of the variability in a local reion: In terms of a propagated intensity pattern in a local region. Another program may have that shifted a little bit, may have it stained a little bit, but not significantly for the conclusion you want a draw.

Di Napoli: Yes, but, say you have two programs, you're saying they're shifted; but I'm saying in the real world, if you believe the programs .... fine scale .... real world .... what evidence do you have.

Flatté: Well, the evidence I have is — we can't go into all the mathematical derivations of these things — but as I said, you've got the ray's propagation system, you've got rays that cross, producing this interference pattern.

Blatstein: I think what he's saying, is the accuracy of your input sufficient?.... the program that you're going to know that your output is going to match reality. I don't see how you can say that since you have inaccuracy inherent in the model and it's inherent in the data.

(Several people speak at once)

McCoy: ....he's going to test the computer. Sometimes it makes sense to go to a controlled environment to test .... we're not so worried about whether the controlled environment is reality.... Dr Wood .... seem to say if you want to test a computer program, the first step is to test it under very, very controlled .... pass that test, go on to ....

Williams: I think that's the point.

Blatstein: The only problem with that, I think, is — now I agree with it, I think most people do, ... but when you do that, the implication is that you have the bugs out .... that exact case.

Wood: Every time I purpose a new exact case to a computer program, I detect another bug.

(Inaudiable exchange between Cox and Di Napoli occasionally interrupted by laughter).

Flatté: ....the question was how you test .... Let me give you an example of how we tested, numerically, to give you a feeling for why it's not something you can hope .... associated with numerical error. Some of you have seen Fred Tappert's picture of what the parabolic equation contours of intensity look like as functions of range and depth know that they are extremely complicated and give you intensity contour maps which look like this (draws several small, crowded irregular closed curves on blackboard) where these scales — I'm talking about 1 dB contours — occur every 10 metres, 100 metres, in a system which we're propagating for a 100 kilometres. Now, how do you decide whether that stuff is valid or not: If you've seen the pictures, you've seen in fact the contours come together to give you the caustics where they're supposed to be, the convergence zones where they're supposed to be. To be more accurate, suppose you do the following — something I have done with my program. This is given with a certain sound speed profile. If you take — actually this isn't all the information, this is the intensity and you also have phase — now take a vertical section through this system. At each of these points you have the amplitude and phase, given by this complicated structure. Now you form a beam, using that vertical array as a beamformer, and look in different directions, before you look at the result, you go back to the beginning, where your source was in this case, and you follow by Snell's Law — it's a completely different theory, very simple — .... you follow Snell's Law through the system and find out exactly where a ray is coming in. You then look at your beamformer and you find a ray exactly there. Now, I find that a very convincing test on the fine structure of....

Di Napoli: ....Do you <u>believe</u>? That means that if you actually went out and made a measurement and compared the measurement against your prediction, would you believe the fine structure?....

Williams: Isn't there a lot of data with enough source motion moving back and forth through this fine structure to be able to have time fluctuations just because of very small source motions? And can't we really, if we believe this fine structure, can't we really throw away an awful lot of data?

(Inaudiable)

Di Napoli: ....Now what they call the fine structure are the fluctuations .... the broad features .... and the mean value. Now there's a CW prediction .... it also has fine structure. I'm saying we don't believe that fine structures necessarily right.

Unidentified: Is that shot data?

Di Napoli: No, that's LFM pulse.

Flatté: You have to be very careful when you say you don't believe the fine structure. You have to say what aspect of it you don't believe. You mean you don't believe it is there at all? ....reality is continuous, smooth, like the white curve?

Di Napoli: No, I guess what I'm saying is that if you could somehow statistically describe the .... of the model and the .... of the data .... then I don't necessarily believe that the two would be close. I don't see <u>evidence</u> .... I don't see experimental data of that type.

(Inaudiable question)

Di Napoli: No, this is not a smoothing function. All we've done is make predictions in range .... to change the input ....

(Many people speak at once)

INITIAL DISTRIBUTION

	Copies
MINISTRIES OF DEFENCE	
MOD Belgium	1
DND Canada	10
CHOD Denmark	8
MOD France	8
MOD Germany	15
MOD Greece	11
MOD Italy	10
MOD Netherlands	12
CHOD Norway	10
MOD Portugal	5
MOD Turkey	5
MOD U.K.	16
SECDEF U.S.	60
NATO AUTHORITIES	
Defence Planning Committee	3
NAMILCOM	2
SACLANT	10
SACLANTREPEUR	1
CINCWESTLANT/COMOCEANLANT	1
COMIBERLANT	1
CINCEASTLANT	1
COMSUBACLANT	1
COMCANLANT	1
COMMAIREASTLANT	1
COMNORLANT	1
SACEUR	2
CINCNORTH	1
CINCSOUTH	1
COMNAVSOUTH	1
COMSTRIKFORSOUTH	1
COMEDCENT	1
COMSUBMED	1
COMMARAIRMED	1
CINCHAN	1

	Copies
SCNR FOR SACLANTCEN	
SCNR Belgium	1
SCNR Canada	1
SCNR Denmark	1
SCNR Germany	1
SCNR Greece	1
SCNR Italy	1
SCNR Netherlands	1
SCNR Norway	1
SCNR Portugal	1
SCNR Turkey	1
SCNR U.K.	1
SCNR U.S.	2
NATIONAL LIAISON OFFICERS	
NLO Denmark	1
NLO Italy	1
NLO U.K.	1
NLO U.S.	1
NLR TO SACLANT	
NLR Belgium	1
NLR Canada	1
NLR Germany	1
NLR Greece	1
NLR Italy	1
NLR Norway	1
NLR Portugal	1
NLR Turkey	1
ESRO/ELDO Doc. Service	1
ATTENDEES	110